This is the peer-reviewed, final accepted version for American Mineralogist, published by the Mineralogical Society of America.
The published version is subject to change. Cite as Authors (Year) Title. American Mineralogist, in press.
DOI: https://doi.org/10.2138/am-2026-10296. https://msaweb.org/

An updated and expanded *Type* classification scheme for diamonds based on FTIR spectroscopic data

REVISION #1

Running Title: *Type Classification of Diamonds*

Word count (body text): 15,718

Formatted for *American Mineralogist (SC50)*

Maxwell C. Day[1]*, Francesca Innocenzi[1], D. Graham Pearson[2], Thomas Stachel[2], Simon C. Kohn[3], Michael C. Jollands[4], Ingrid Chinn[5], Tiago Jalowitzki[6], Mattia La Fortezza[1], Fabrizio Nestola[1], Mark E. Newton[7], Davide Novella[1], Steven B. Shirey[8], Karen V. Smit[9], Laura Speich[10], Suzette Timmerman[11], Evan M. Smith[4], Nils B. Gies[11], and Martha G. Pamato[1]

[1] Dipartimento di Geoscienze, Università degli Studi di Padova, Via Gradenigo 6, 35131 Padova, Italy.

[2] Department of Earth and Atmospheric Sciences, University of Alberta, 116 St & 85 Ave, Edmonton, AB, T6G 2R3, Canada.

[3] School of Earth Sciences, University of Bristol, Wills Memorial Building, Queens Road, Bristol BS8 1RJ, United Kingdom.

[4] Gemological Institute of America (GIA), 50 W 47th St., New York, NY, 10036, U.S.A.

[5] De Beers Group Services, 144 Oxford Rd, Rosebank, 2196, Johannesburg, South Africa.

[6] Universidade de Brasília, Instituto de Geociencias, Programa de Pos-graduaçao em Geologia, Brazil.

[7] Department of Physics, University of Warwick, Coventry, CV4 7AL, United Kingdom.

[8] Earth and Planets Laboratory, Carnegie Institution for Science, 5241 Broad Branch Rd. NW, Washington, DC 20015, U.S.A.

[9] School of Geosciences, University of the Witwatersrand, 1 Jan Smuts Ave., 2001, Braamfontein, Johannesburg, South Africa.

[10] De Beers Group, Belmont Road, Maidenhead, SL6 6JW, United Kingdom.

[11] Institute of Geological Sciences, University of Bern, Baltzerstrasse 1+3, 3012 Bern, Switzerland.

***Corresponding Author:** Maxwell C. Day (maxwell.day@unipd.it)

Keywords: Diamond, FTIR Spectroscopy, Type Classification, Nitrogen, Defects

Always consult and cite the final published document. See https://msaweb.org/ or GeoScienceWorld

This is the peer-reviewed, final accepted version for American Mineralogist, published by the Mineralogical Society of America.
The published version is subject to change. Cite as Authors (Year) Title. American Mineralogist, in press.
DOI: https://doi.org/10.2138/am-2026-10296. https://msaweb.org/

Abstract

The *Type* classification of diamond is based on the presence or absence of nitrogen (N) and boron and the aggregation state of N-defects determined via Fourier transform infrared (FTIR) spectroscopy. Our understanding of different N-defects in natural, synthetic and treated diamond has expanded considerably since the historical *Type* classification was proposed ~100 years ago. Consequently, important geological and gemological information is not included in the *Type* classification scheme. Moreover, there is no systematic approach to expressing the fraction of the major N-defects in the *Type* classification scheme. To address these issues, and standardize the classification of diamonds across different disciplines, we propose an updated *Type* classification scheme for diamonds based on FTIR spectroscopic data.

The updated scheme includes four *Tiers* allowing classification at varying levels of detail depending on spectrum quality and/or the amount of information the user wishes to extract. This tiered scheme allows basic classification of diamonds using Tiers 1-3 and, as an optional step, more detailed classification using Tier 4. By differentiating the *instrumental detection limit* and *practical quantitation limit* of N-defects, rigorous criteria for *Type I* and *Type II* diamonds, and new *Type Ib* (e.g., *Type IbX and IbY*) and *Type Ia* subgroups (e.g., *Type IaA′* and *IaB′*), are established. Additional Tier 4 subgroups describe, platelets, CO_2 inclusions, amber centers, and synthetic and treated diamonds (*Type Ib–Ia* diamonds with ***C***-, ***A***- and ***B***-centers). A detailed description of these features and other types of point- and extended-defects observed in natural and synthetic diamond is given. Examples are provided demonstrating how the new scheme is used to classify diamonds such that useful geological and gemological information can be extracted from each *Type* designation. The effect of sample thickness, signal saturation in the two- and one-phonon regions, and spectral quality/resolution on the accuracy of calculated N-defect

Always consult and cite the final published document. See https://msaweb.org/ or GeoScienceWorld

This is the peer-reviewed, final accepted version for American Mineralogist, published by the Mineralogical Society of America.
The published version is subject to change. Cite as Authors (Year) Title. American Mineralogist, in press.
DOI: https://doi.org/10.2138/am-2026-10296. https://msaweb.org/

concentrations is evaluated. Moreover, issues assigning a specific *Type* to zoned diamonds based on individual FTIR spectra are discussed.

Keywords: Diamond, Type classification, point-defect, nitrogen defect, ***C***-, ***A***- and ***B***-centers, FTIR spectroscopy.

Always consult and cite the final published document. See https://msaweb.org/ or GeoScienceWorld

This is the peer-reviewed, final accepted version for American Mineralogist, published by the Mineralogical Society of America.
The published version is subject to change. Cite as Authors (Year) Title. American Mineralogist, in press.
DOI: https://doi.org/10.2138/am-2026-10296. https://msaweb.org/

Introduction

Point defects in diamond contain a wealth of extractable information about how, and from what types of media, diamonds form, in Earth's mantle and in factories and laboratories. Point defects also reveal how diamonds react to external forces (i.e., variable pressure – P – temperature – T – oxygen fugacity – fO_2 –, and irradiation) during post-growth treatment or mantle residence. The most common type of extrinsic point defects in diamond (i.e., those related to impurities in the crystal structure) involves substitutional nitrogen (N), routinely detected in the majority of natural (95–98%, Harlow 1998) diamonds using various spectroscopic techniques, typically Fourier transform infrared (FTIR) spectroscopy. Nitrogen is also observed in some types of synthetic high-pressure high-temperature (HPHT) treated, irradiated and chemical vapor deposition (CVD) diamonds. Consequently, spectroscopic analysis of different N-bearing point defects has become a standard and reliable tool in the study of diamond and has served as the basis for classifying diamonds since the pioneering works of Robertson et al. (Robertson et al. 1934, 1936) almost a century ago.

From a gemological perspective, the *Type* classification scheme for diamonds (e.g., Breeding and Shigley 2009), has been used as a framework in which a given *Type* designation (i.e., N-aggregation state) helps to interpret how point defects, and the optical properties they impart to diamond, change (or are produced) due to heat and irradiation treatment (Green et al. 2022). From a geological perspective, additional classifications are often required to describe genetic aspects of a given diamond that are not apparent from its *Type* designation. Most commonly, the identity and composition of mineral inclusions in diamond are used to group samples based on their parageneses, e.g., as peridotitic, eclogitic, websteritic, lherzolitic or harzburgitic (Stachel et al. 2022; Curtolo et al. 2023). Several alternative classification schemes, based on properties such as

Always consult and cite the final published document. See https://msaweb.org/ or GeoScienceWorld

This is the peer-reviewed, final accepted version for American Mineralogist, published by the Mineralogical Society of America.
The published version is subject to change. Cite as Authors (Year) Title. American Mineralogist, in press.
DOI: https://doi.org/10.2138/am-2026-10296. https://msaweb.org/

crystal habit, surface morphology, transparency, color and deformation-related features, have also proven useful (e.g., Harris et al. 1975; Orlov 1984; Kurdumov et al. 1994; Hainschwang et al. 2020b, 2020a). Although genetic information (e.g., paragenesis, morphology, growth zonation) is absent in the *Type* classification, several important aspects of diamond residence in the mantle, post-diamond formation and pre-kimberlite eruption, can be obtained from the identity and concentration (at.ppm) of different N-defects measured by FTIR spectroscopy. For example, N forms a variety of point defects including ***C***-centers (single-substitutional N_s^0), ***A***-centers (dimeric N_2^0), and ***B***-centers (four N atoms surrounding a carbon (C) – vacancy (*V*); N_4V) (Table 1). Numerous other point- and extended defects are commonly observed in natural and synthetic diamond, many of which are described here. Substitutional and interstitial atoms (or ions) are indicated with a subscript "*s*" and "*i*", respectively and the defect charge-state is indicated with a superscript (e.g., N_s^0). Many different nitrogen(N) – vacancy(*V*) – hydrogen(H) – boron (B) defects are described where elements are written in normal font (e.g., B for boron) such that they are differentiated from the names of defects (e.g., ***B***-center) and IR features (e.g., *B*′ platelet peak). The N concentratio in ***C***-, ***A***- and ***B***-centers are indicated as N_C, N_A and N_B.

With progressive annealing, either naturally in Earth's mantle or as a result of heat treatment, ***C***-centers aggregate to form ***A***-centers, which in-turn, aggregate to form ***B***-centers. Because ***C***-, ***A***- and ***B***-centers each produce a characteristic signal (absorption spectrum) in the infrared region, the N-aggregation state (e.g., traditionally referred to as %IaB or %B, the proportion of N that occurs as ***B***-centers compared to ***A***-centers) can be calculated via decomposition of the IR spectrum. Determination of the $\boldsymbol{C} \rightarrow \boldsymbol{A}$ and $\boldsymbol{A} \rightarrow \boldsymbol{B}$ rate constants (activation energies and pre-exponential factors) has allowed the respective N-aggregation rates to be determined (Cooper 1990; Taylor et al. 1990, 1996; Kiflawi et al. 1997). Consequently, the time/temperature dependence of the $\boldsymbol{C} \rightarrow$

Always consult and cite the final published document. See https://msaweb.org/ or GeoScienceWorld

This is the peer-reviewed, final accepted version for American Mineralogist, published by the Mineralogical Society of America.
The published version is subject to change. Cite as Authors (Year) Title. American Mineralogist, in press.
DOI: https://doi.org/10.2138/am-2026-10296. https://msaweb.org/

121 ***A*** → ***B*** aggregation sequence, together with the N-aggregation state and total N concentration
122 (N_{tot}), can be used to calculate the temperature (T_{res}) of diamond residence in the mantle for an
123 assumed mantle residence time (t_{res}) or a known t_{res} calculated as the difference between the
124 diamond formation age (determined by radiometric dating, Heaman et al. 2019; Smit et al. 2023)
125 and the kimberlite eruption age (Stachel and Luth 2015; Nimis 2022) if one assumes T_{res} is the
126 same as the temperature of diamond formation (T_{form}). Alternatively, T_{res} may be significantly
127 cooler than T_{form}, providing insights into how a diamond may have been exhumed to cooler
128 residence environments after formation (e.g., Smit et al. 2018) or in some cases, T_{res} may be greater
129 than T_{form} where diamond formation occurs in cold subducting slabs. A t_{res} may also be calculated
130 using a known (or assumed) T_{res}, but as N-aggregation rates are much more sensitive to
131 temperature than time, calculated t_{res} may have relatively large errors. The N-defect content and
132 N-aggregation state of a given diamond may be highly heterogenous across individual diamonds,
133 reflecting primary growth zones that form from a single evolving parental fluid/melt and/or
134 secondary (tertiary etc.) growth zones indicating periods of later growth, potentially at different
135 P/T conditions and/or from different fluids/melts (Bulanova et al. 2002, 2017; Zedgenizov et al.
136 2006). When this information is combined with T_{res} (or t_{res}), detailed thermal reconstructions of
137 the mantle residence period of a given diamond can be obtained (Kohn et al. 2016).

138 Since the initial experiments of Robertson et al. (1934, 1936) and the subsequent first
139 definitive proposition of the modern *Type* classification ~60 years ago (Dyer et al. 1965), our
140 understanding of how N-defects aggregate (or disaggregate) with changing pressure and
141 temperature conditions has improved considerably. The continued discovery of new correlations
142 between different IR absorbance features (e.g., platelets, deformation-related features and new N-
143 defects) and the concentration of ***C***-, ***A***- and ***B***-centers (N_C, N_A and N_B) has expanded the amount

Always consult and cite the final published document. See https://msaweb.org/ or GeoScienceWorld

This is the peer-reviewed, final accepted version for American Mineralogist, published by the Mineralogical Society of America.
The published version is subject to change. Cite as Authors (Year) Title. American Mineralogist, in press.
DOI: https://doi.org/10.2138/am-2026-10296. https://msaweb.org/

of geological and gemological information that can be extracted from the FTIR spectra of natural, synthetic and treated diamonds. The current *Type* classification scheme includes the *Type I* and *Type II* groups which describe diamonds with N concentrations above and below the FTIR detection limit, respectively. The *Type I* group is further subdivided into *Type Ib* and *Type Ia* indicating the presence of ***C***-centers or ***A***- and ***B***-centers, respectively. Further subdivisions are based on the calculated N-aggregation state (e.g., the proportion of ***A***-centers that have aggregated to ***B***-centers), e.g., see section "Limitations of the Historical Type Classification Scheme". The *Type II* group is subdivided into *Type IIa* indicating the absence of detectable N and *Type IIb* also indicating the absence of N but the presence of boron defects.

The importance and utility of the *Type* classification has also been realized in the materials science community, where predicting and controlling different N/*V*/H-aggregation sequences (Stacey et al. 2012) is critical when designing experiments to produce particular defects in synthetic diamonds. The presence of certain defects has important technological applications for diamond semiconductors, e.g., doped *p*- and *n*-type diamonds (Ashfold et al. 2020; Zheng et al. 2021) and the production of NV^- defects for quantum computing purposes (Achard et al. 2020). Although the growing utility of the *Type* classification has led to numerous proposals for amendments and additions of specific *Type* groups (e.g., Klyuev et al. 1972; Woods et al. 1993; Collins 1997; Zaitsev 2001; Hainschwang 2014), a new updated and comprehensive scheme has yet to be formally proposed. The lack of rigorous and widely agreed upon definitions for each *Type* (sub)group often leads researchers to modify the *Type* classification scheme such that it can be used to organize their particular dataset (Hainschwang 2014; Day et al. 2024). This can lead to inconsistent and/or ambiguous terminology, particularly across different subdisciplines of diamond research.

Always consult and cite the final published document. See https://msaweb.org/ or GeoScienceWorld

This is the peer-reviewed, final accepted version for American Mineralogist, published by the Mineralogical Society of America.
The published version is subject to change. Cite as Authors (Year) Title. American Mineralogist, in press.
DOI: https://doi.org/10.2138/am-2026-10296. https://msaweb.org/

For these reasons, we propose an updated version of the *Type* classification scheme in which all the original *Type* (sub)groups are rigorously defined and several new groups and subgroups, based on particular absorption features, are included. Moreover, the geological and gemological data that can be extracted from different IR absorption features and/or particular *Type* designations are described. Different researchers classify diamonds for a variety of purposes and often do not want, nor need, to perform detailed classifications and instead may require a straightforward and efficient method of classification. Consequently, four Tiers are included in the classification scheme that represent increasing levels of detail. This allows users to perform basic classifications using Tiers 1–3, based solely on the presence and concentration of IR-active N-defects, or more advanced classifications using Tier 4, based on the presence of additional features observed in the infrared. A detailed review of previous work on such features (e.g., platelets, CO_2 inclusions, amber centers), in addition to descriptions of different point- and extended-defects commonly observed in diamond, is also provided.

Development of the Historical *Type* Classification Scheme

Robertson et al. (1934, 1936) were the first to identify general differences in the transparency of diamonds to ultraviolet (UV) and infrared (IR) light, classifying diamonds that absorbed UV light below 300 nm and IR light from 7000 – 20000 nm (1428.6 – 500 cm^{-1}) as *Type I*, and diamonds that were transparent to these wavelengths as *Type II*. Following these initial observations, an enormous amount of work was conducted in the 1940–60s, describing different N-related absorption features in UV–vis, EPR (electron paramagnetic resonance) and FTIR spectra (e.g., Sutherland and Willis 1945; Blackwell and Sutherland 1949; Sutherland et al. 1954; Clark et al. 1956a,b; Kaiser and Bond 1959; Anderson 1961; Lightowlers and Dean 1964). Custers (1952, 1954) was the first to extend Robertson's original classification, proposing that *Type II*

Always consult and cite the final published document. See https://msaweb.org/ or GeoScienceWorld

This is the peer-reviewed, final accepted version for American Mineralogist, published by the Mineralogical Society of America.
The published version is subject to change. Cite as Authors (Year) Title. American Mineralogist, in press.
DOI: https://doi.org/10.2138/am-2026-10296. https://msaweb.org/

diamonds be subdivided into *Type IIa* and *Type IIb* diamonds based on differences in color, electrical conductivity and phosphorescence that was later attributed to boron (B) in *Type IIb* diamond (Wentorf and Bovenkerk 1962; Chrenko 1973).

In the seminal work of Sutherland et al. (1954), absorption due to ***A***- and ***B***-centers (first described as *group A* and *B* bands by Sutherland et al. (1954) was differentiated in *Type I* diamonds. Later work by Kaiser and Bond (1959) confirmed that these groups of bands were indeed due to different forms of substitutional N. Originally, Sutherland et al. (1954) assigned several peaks between 1426 and 1372 cm^{-1} as *B*-type bands (hence the name *B′* peak) that were later attributed to {100} planar defects called *platelets* (Frank 1956; Caticha-Ellis and Cochran 1958; Evans and Phaal 1962). Later, it was shown that the position, width, and intensity of the platelet (*B′*) peak varied as a function of platelet size and shape (Sobolev et al. 1969; Davies 1977; Clark and Davey 1984; Speich et al. 2017), and that the intensity of the *B′* peak was correlated with both ***B***- and ***N3***-center (N_3V^0) absorption (Brozel et al. 1978; Davies 1981; Woods 1986). Also important was the discovery of the ***D***-center absorbance feature (Clark and Davey 1984), which was later correlated with the *B′* peak and attributed to platelet-stimulated lattice vibrational modes (Woods 1986).

With regards to *Type Ib* diamond, Charette (1961) was the first to observe a paramagnetic form of isolated N with UV and IR absorption signal distinct from that observed for ***A***- and ***B***-centers. These findings were confirmed by Dyer et al. (1965), who consequently proposed that *Type I* diamonds, containing aggregated (***A***- and ***B***-centers) and single substitutional N-defects, be classified as *Type Ia* and *Type Ib*, respectively. The absorbance spectrum characteristic of *Type Ib* diamond was first referred to as the *C spectrum* (hence the name ***C***-center) by Clark and Davey (1984), logically following the earlier observation of the *A* and *B spectra* (i.e., ***A***- and ***B***-centers)

Always consult and cite the final published document. See https://msaweb.org/ or GeoScienceWorld

This is the peer-reviewed, final accepted version for American Mineralogist, published by the Mineralogical Society of America.
The published version is subject to change. Cite as Authors (Year) Title. American Mineralogist, in press.
DOI: https://doi.org/10.2138/am-2026-10296. https://msaweb.org/

by Sutherland et al. (1954). Researchers began to further subdivide *Type Ia* diamonds as *Type IaA*, *Type IaB*, and a mixed *Type IaAB* based on the prevalence of absorption due to ***A***- and ***B***-centers. Compared to the ***C***-center, exact determination of the structure and composition of ***A***- and ***B***-centers as N_2 and N_4V defects took much longer (Davies 1977; Woods 1986). In fact, robust evidence for the identity of the ***A***- and ***B***-centers were not proposed until 1992 based on the theoretical work of Jones et al. 1992. The identity of the ***B***-center was confirmed later by Salustro et al. 2018. A variant of the ***C***-center, a positively charged isolated N_s^+ defect, called the ***X***-center, was shown to produce an absorption feature at 1332 cm^{-1} like the ***B***-center (Lawson and Kanda 1993; Lawson et al. 1998). Other common N-defects have been described more recently, for example the ***Y***-center (Hainschwang et al. 2012; Nadolinny et al. 2025; Day et al. 2026). The exact identity of the ***Y***-center remains unknown but has been tentatively attributed to a complex form of single-substitutional N_s and interpreted as a precursor (or intermediate) of ***C***-to-***A*** aggregation (Nadolinny et al. 2025; Day et al. 2026). Alternative identities for the ***Y***-center involving Ni and O-related defects have also been proposed (see section "Tier 4" and Table 1).

Determination of the IR calibration coefficients for ***C***- ***A***- ***B***- and ***X***-centers (Chrenko et al. 1971; Boyd et al. 1994, 1995; Kiflawi et al. 1994; Lawson et al. 1998; Liggins 2010) allowed for the concentration of different N-defects to be determined via standard decomposition of the one-phonon region (N-region, ~1400–1000 cm^{-1}) and thus calculation of the N-aggregation state (%IaA or %IaB) of a given diamond. This prompted the proposal of definitive sub-divisions in the Type classification based on the proportion of ***A***- and ***B***-centers in *Type Ia* diamonds (e.g., Stachel and Harris 1997; Banas et al. 2007; Stachel 2014; Day et al. 2023). Experimental confirmation that ***C*** $\rightarrow$ ***A*** and ***A*** $\rightarrow$ ***B*** aggregation proceeds according to second-order kinetics (Satoh et al. 1990; Mainwood 1994), and the determination of the corresponding rate constants and pre-exponential

Always consult and cite the final published document. See https://msaweb.org/ or GeoScienceWorld

This is the peer-reviewed, final accepted version for American Mineralogist, published by the Mineralogical Society of America.
The published version is subject to change. Cite as Authors (Year) Title. American Mineralogist, in press.
DOI: https://doi.org/10.2138/am-2026-10296. https://msaweb.org/

factors (Cooper 1990; Taylor et al. 1990, 1996; Kiflawi et al. 1997) allowed the time/temperature conditions of diamond residence to be calculated. This work marked the first important application of the *Type* classification scheme to the geological study of diamond formation.

Limitations of the Historical Type Classification Scheme

This rapid period of work on N impurities in diamond in the mid 20th century eventually led to a large and diverse nomenclature for both the names of different N-defects and the subsequent *Type* groups. It was commonplace for early experimentalists to name absorption features based on associated treatments (e.g., Clark et al. 1956a,b), for example, in the ***N3***-, ***H1***- and ***GR1***-centers, prefixes indicate natural-, heat- and general radiation-related origins, respectively. In modern studies, it is conventional to describe point defects (particularly optical centers) using the structure and/or composition of the defect or the wavelength or energy (eV) of the zero-phonon line (ZPL), or a particular characteristic local vibrational mode (LVM), corresponding to that defect. For example, the ***C***-center, named by Clark and Davey (1984), is often alternatively described as (1) *single-substitutional nitrogen*, (2) N_1^0 or N_s^0, (3) the 1130 cm^{-1} (or 8.85 μm) line, and (4) the 140.1 meV line. Multiple different descriptions of the same features have led to a disjointed cross-disciplinary nomenclature. For example, Nadolinny et al. (2025) assign a signal in their EPR spectra to the ***N3***-center, however this defect is markedly different than the more commonly observed optical center – N_3V^0, that is also referred to as the ***N3***-center. Moreover, naming of the ***C***-, ***A***-, and ***B***-centers, before the first descriptions of how such defects aggregate (Chrenko et al. 1977; Allen and Evans 1981; Evans and Qi 1982), resulted in the counterintuitive N-aggregation sequence $\boldsymbol{C} \rightarrow \boldsymbol{A} \rightarrow \boldsymbol{B}$.

The naming conventions for each *Type* group are also counterintuitive. For example, the name *Type IaA* is inherently problematic as, according to the current classification scheme, it

Always consult and cite the final published document. See https://msaweb.org/ or GeoScienceWorld

This is the peer-reviewed, final accepted version for American Mineralogist, published by the Mineralogical Society of America.
The published version is subject to change. Cite as Authors (Year) Title. American Mineralogist, in press.
DOI: https://doi.org/10.2138/am-2026-10296. https://msaweb.org/

represents three types of diamonds with drastically different mantle residence histories: (1) diamonds with mostly ***A***-centers and minor amounts of ***C***-centers, (2) diamonds with exclusively ***A***-centers, or (3) diamonds with mostly ***A***-centers and minor amounts of ***B***-centers. The *Type* subgroups *IaA*, *IaAB*, and *IaB* based on the concentration of N in ***A***- and ***B***-centers have been defined previously as (Stachel and Harris 1997; Banas et al. 2007; Stachel 2014; Day et al. 2023):

Type IaA: %IaB < 10%

Type IaAB: 10% < %IaB < 90%

Type IaB: %IaB > 90%

where:

[Eqn 1]: $\%IaB = 100 \times \frac{N_B}{N_B + N_A}$

Here, N_A and N_B are the concentrations (in at.ppm) of N in the form of ***A***- and ***B***-centers determined via decomposition of the IR spectrum normalized to a thickness of 1 cm. However, it is unclear when, or if, these subgroup definitions for *Type Ia* diamonds were formally proposed and it is unclear whether all authors adhere to these definitions. To compound these problems, it is also evident that several different methods for calculating %IaB (or %B) are currently employed. For example, one may wrongly assume that calculated concentration of N (determined via decomposition) in the form of ***A***- and ***B***-centers represent the concentration of the N_2 and N_4V defects themselves. Alternatively, %IaB may be erroneously calculated using the concentration of ***A***- and ***B***-center themselves (e.g., %IaB = $(N_B/4) / (N_B/4 + N_A/2)$) rather than the absolute amount of N associated with such defects leading to contradictory comparisons of diamonds studied by different researchers. The terms "%IaB", and "%IaA", are also problematic as they suggest that a

Always consult and cite the final published document. See https://msaweb.org/ or GeoScienceWorld

This is the peer-reviewed, final accepted version for American Mineralogist, published by the Mineralogical Society of America.
The published version is subject to change. Cite as Authors (Year) Title. American Mineralogist, in press.
DOI: https://doi.org/10.2138/am-2026-10296. https://msaweb.org/

given N-aggregation state represents the proportion of ***B***-centers compared to ***A***-centers (or the proportion of ***A***-centers compared to ***C***-centers) when in fact, it represents the relative proportion of N in ***B***-centers compared to ***A***-centers (or the proportion of N in ***A***-centers compared to ***C***-centers) as is shown in Eqn 1. Consequently, a new terminology for N-aggregation state is described in "Results and Discussion".

Despite their common use, the definitions for each *Type* group and the N-aggregation state (i.e. Eqn 1) have never been formally defined. Consequently, researchers often propose their own terminology based on the amount of information that is extractable from their IR spectra. For example, small diamonds (e.g., microdiamonds, <0.5 mm across) may result in low quality spectra, especially when not cleaned well, resulting in instances where accurate N-defect concentrations cannot be determined. In other cases, thick samples and/or diamonds with high total N concentrations may result in saturation in the two- and/or one-phonon regions preventing accurate thickness normalization and N-defect determination (see section "Tiers 1 and 2"). In these cases, authors often indicate qualitative differences between N-defect concentrations, e.g., IaA > IaB vs. IaA >> IaB (e.g., Hainschwang 2014; Day et al. 2024), or simply refer to *Type IaA* and *IaB* diamonds as those that contain exclusively ***A***- and ***B***-centers, respectively, and *Type IaAB* diamonds as those with any proportion of ***A***- and ***B***-centers (Pignatelli and Ferraris 2025). Perhaps the largest contributing factor to ambiguity in the *Type* group nomenclature is the fact that systematic subgroup definitions for *Type Ib* diamonds based on the normalized proportion of ***A***- and ***C***-centers do not exist (as opposed to the *Type* group definitions given above for *Type Ia* diamonds that are commonly used). Therefore, *Type Ib* diamonds have been described as those with >90% and/or >50% ***C***-centers (compared to ***A***-centers) or simply as any diamond that contains detectable amounts of ***C***-centers (Kvasnytsya and Kaminsky 2021). Moreover, since the modern

Always consult and cite the final published document. See https://msaweb.org/ or GeoScienceWorld

This is the peer-reviewed, final accepted version for American Mineralogist, published by the Mineralogical Society of America.
The published version is subject to change. Cite as Authors (Year) Title. American Mineralogist, in press.
DOI: https://doi.org/10.2138/am-2026-10296. https://msaweb.org/

303 *Type* classification was published (Dyer et al. 1965), several new defects (e.g., ***Y***-centers,
304 Hainschwang et al. 2012; Nadolinny et al. 2025; Day et al. 2026) have been discovered and new
305 diamond *Types* have been proposed. For example, *Type IbX*, *IbXY*, *IbY* for diamonds with almost
306 exclusively ***X***- and ***Y***-centers (Hainschwang 2014) and *Type Ib + IbXY*, *Ib + IaA*, and *Ib < IaA*,
307 etc. for *Type Ib* diamonds with variable N_X and N_Y and $\boldsymbol{C \rightarrow A}$ aggregation states (Day et al. 2024,
308 2026).

309 In recent years our understanding of different signals in the IR has greatly improved and
310 novel defects (and combinations of different defects) have been produced in synthetic diamond
311 and using HPHT and irradiation treatments. Consequently, many features in the FTIR spectra of
312 natural, synthetic and treated diamonds are not included in the historical classification scheme
313 despite the important geological and gemological information they may yield. Examples include
314 absorption due to both nitrogen and boron in an individual natural diamond and synthetic nitrogen-
315 and boron-doped semiconducting diamond (Eaton-Magaña and Ardon 2016); absorption in the
316 one-phonon region in *480 nm diamonds* (Lai et al. 2024; Hardman et al. 2025) and peaks associated
317 with different types of platelets (Speich et al. 2017, 2018), CO_2 inclusions (Barannik et al. 2021)
318 and amber centers – indicative of plastic deformation (Massi et al. 2005). Moreover, the historical
319 *Type* classification scheme assumes that during mantle or laboratory annealing, all ***C***-centers
320 (detectable by FTIR spectroscopy) aggregate to form ***A***-centers before ***B***-centers form. It follows
321 that no *Type* group currently exists for diamonds with ***C***-, ***A***- and ***B***-centers, other than alternative
322 terminology (e.g., *IaA > IaB >> Ib*, Hainschwang et al. 2020b, 2020a) which includes only
323 qualitative information about the relative concentration of N-defects. This is problematic as natural
324 ***C***-, ***A***- and ***B***-center bearing diamonds have been reported (Shigley et al. 1993; Hainschwang et al.
325 2006a) and it is well known that HPHT-treatment of *Type Ia* diamond produces ***C***-centers (Collins

Always consult and cite the final published document. See https://msaweb.org/ or GeoScienceWorld

This is the peer-reviewed, final accepted version for American Mineralogist, published by the Mineralogical Society of America.
The published version is subject to change. Cite as Authors (Year) Title. American Mineralogist, in press.
DOI: https://doi.org/10.2138/am-2026-10296. https://msaweb.org/

et al. 2000). It follows that such diamonds with detectable ***C***-, ***A***- and ***B***-centers cannot be rigorously classified according to their N-aggregation states using the historical *Type* classification scheme.

Additionally, several different mechanisms of N-defect aggregation, distinct from ***C*** → ***A*** → ***B***, have been shown to occur in both natural and synthetic diamond. For example, in N-doped CVD diamond, HPHT-treatment results in the production of primarily N_3VH^0 defects rather than ***B***-centers due to the high H content of such diamonds (Ashfold et al. 2020). Evidence of similar processes are observed for natural diamonds where an inverse correlation between N_B and the intensity of the 3107 cm^{-1} peak (due to N_3VH) is observed (Melton et al. 2013; Speich et al. 2017). This suggests that N-aggregation sequences in some diamonds involve the production of vacancy-bearing defects (e.g., ***N3***-centers) that may inhibit the transformation of ***A***-center to ***B***-centers (Day et al. 2024).

In irradiated *Type Ib* diamonds, large amounts of interstitial N_i are produced evidenced by the observation of the N_{2i} (***H1a***-center) in such diamonds (Ashfold et al. 2020). With progressive annealing, ***A***-centers are produced via N_{2i} → ***A***-center + C_i which in-turn, continues to drive the production of interstitials and ***A***-centers via $C_i + N_s \rightarrow N_i$; $N_i + N_s \rightarrow N_{2i}$; N_{2i} → ***A***-center + C_i (Ashfold et al. 2020). In fact, such interstitial C_i ($\pm N_i$) may also form small interstitial complexes (Goss et al. 2003), the coupling of such complexes with ***C***-centers has been tentatively attributed to ***Y***-center absorbance observed in *Type Ib* diamonds (Day et al. 2026). Moreover, in *Type Ib* diamonds with high N_C, "N_s–pair" defects (Newton and Baker 1991b; Mineeva and Speransky 2005; Etmimi et al. 2009) may form which comprise a group of defects (e.g., the ***NOC1***-, ***NOC2***- and ***NOC3***-centers, Nadolinny et al. 1999) where N_s^0 pairs are separated by different numbers of carbon atoms. For example, the ***N1***-center (N_s^0–C–N_s^+) (Cox et al. 1992) or the N_s^0–C–N_s^0 defect

Always consult and cite the final published document. See https://msaweb.org/ or GeoScienceWorld

This is the peer-reviewed, final accepted version for American Mineralogist, published by the Mineralogical Society of America.
The published version is subject to change. Cite as Authors (Year) Title. American Mineralogist, in press.
DOI: https://doi.org/10.2138/am-2026-10296. https://msaweb.org/

which has also been tentatively assigned to the ***Y***-center (Nadolinny et al. 2025) (see section "Tier 4"). As the historical classification scheme assumes that N-aggregation proceeds simply via ***C*** → ***A*** → ***B***, it is important that alternative aggregation sequences (as above) are described and that users of the scheme are aware that degree of annealing and N-aggregation state may not always be directly related from diamond to diamond (e.g., high H contents may inhibit ***A*** → ***B*** aggregation rates, Ashfold et al. 2020).

In the updated *Type* classification scheme, *Type* (sub)groups have been included to address the various issues described above and to allow classification (or at least systematic description) of a wider variety of IR-active features in natural, synthetic and/or treated diamond by geologists, gemologists or materials scientists.

Results and Discussion: The Updated *Type* Classification Scheme

As described above, the names of different N-defects and the *Type* groups in the historical classification scheme, currently in widespread use, limit the applications to different kinds of natural, treated and synthetic diamonds. Moreover, rigorous *Type* group definitions, based on N-aggregation states, have never been formally published leading to ambiguous *Type* group designations in some cases. However, because the *Type* classification terminology is deeply ingrained in the literature, and in the lexicon of diamond researchers, we suggest that proposing a completely new nomenclature would be counter-productive. For these reasons, an updated and expanded version of the existing *Type* classification scheme for diamond is proposed here, where the names of the traditional N-defects and *Type* groups are retained where possible. In an effort to make the updated *Type* classification scheme as accessible as possible, all *Type* group criteria are based solely on data extracted from the one-phonon region, ~1000–1400 cm^{-1} (10000–7143 nm) of the FTIR spectra of diamond. However, and in some cases, more detailed classification can be

Always consult and cite the final published document. See https://msaweb.org/ or GeoScienceWorld

This is the peer-reviewed, final accepted version for American Mineralogist, published by the Mineralogical Society of America.
The published version is subject to change. Cite as Authors (Year) Title. American Mineralogist, in press.
DOI: https://doi.org/10.2138/am-2026-10296. https://msaweb.org/

performed using *Type* subgroups based on features observed in higher wavenumber regions, specifically the two- and three-phonon regions, 1400–2700 cm^{-1} (7143–3704 nm) and 2700–4000 cm^{-1} (3704–2500 nm), respectively. The proposed classification scheme is not intended as a tool with which exhaustive descriptions of impurities, defects and/or structural features in diamond can be made. Complete spectroscopic characterization of diamond requires a variety of techniques (e.g., CL, UV–vis, PL, and EPR spectroscopy) to detect (and quantify) features that are IR-inactive or weakly absorbing and thus not observed in the IR. However, application of multiple techniques, particularly for large sample suites, is often impractical. As a consequence, to maximize the utility of the classification scheme proposed here, we rely solely on FTIR spectroscopy, which is relatively simple, cost efficient and widely available. New *Type* groups were only added for features that are commonly observed in the infrared (e.g., platelet-related absorption, see section "Tier 4"), or that the authors deem to be of relatively high-interest to the community using FTIR spectroscopy to study diamonds.

Regarding the terminology for point defects, we follow that described by Ashfold et al. (2020). Here, atoms or ions that substitute for carbon are indicated with the subscript "*s*" with the associated charge-state (i.e., -, 0, +) indicated, where known or useful, with a superscript e.g., ***C***-centers may be alternatively termed "N_s^0". For larger defects, the substitutional nature of atoms in often implicit e.g., ***A***-centers are typically termed "N_2" rather than "N_{2s}". Interstitial atoms or ions that occur in positions additional to the host structure are indicated with the subscript "*i*" e.g., ***H1a***-centers may be alternatively termed "N_{2i}". Here, we recommend that N/*V*/H-point defects are described by listing each atom in the order N, *V* and then H (e.g., N_3VH^0) where *V* (vacancy) is italicised such that it is differentiated from the element vanadium.

Always consult and cite the final published document. See https://msaweb.org/ or GeoScienceWorld

This is the peer-reviewed, final accepted version for American Mineralogist, published by the Mineralogical Society of America.
The published version is subject to change. Cite as Authors (Year) Title. American Mineralogist, in press.
DOI: https://doi.org/10.2138/am-2026-10296. https://msaweb.org/

In Fig. 1, a simplified version of the updated classification scheme is shown to allow easy visualization and comprehension. In Fig. 2, a detailed version of this scheme (in Fig. 1) is shown. The scheme in Fig. 2 can be used to classify the vast majority of natural (untreated) diamonds such that traditional thermochronometric methods (based on N-aggregation or platelets) can be used to determine mantle residence temperatures/times. In Fig. 3, the full extended and updated classification scheme is shown. This scheme can be used to classify a wide variety of natural, synthetic and treated diamonds and includes numerous options to indicate important geological and or gemological features observed in the diamond, and thus the FTIR spectrum, being investigated. It is important to note that when using the new schemes (Figs. 2 and 3), users do not necessarily have to classify their diamonds down to the complex Tier 4 level. In many cases, classification down to the Tier 2 or Tier 3 levels may be entirely sufficient for their purposes.

The updated *Type* classification scheme is divided into four tiers as described below where increasing degrees of information extracted from a given FTIR spectrum allow classification at higher level tiers. Classification at the Tier 1 level simply requires that one determine if the total concentration of IR-active N (and/or B) is above or below the FTIR detection limit. Classification at the Tier 2 level requires that different N-defects can be distinguished and at the Tier 3 and 4 levels, the relative abundance of different N-defects must be quantifiable via standard decomposition of signal in the one-phonon region. In most previous related work, decomposition of composite signal in the one-phonon region is typically referred to as “deconvolution”. However, as signal in this region does not convolute, but instead, combines according to the additivity principal, the term “decomposition” more accurately describes this process and is thus preferred here. A detailed description of all group-criteria (as shown in Fig. 3) is provided in Table B.1. (Supplementary Material, Appendix B).

Always consult and cite the final published document. See https://msaweb.org/ or GeoScienceWorld

This is the peer-reviewed, final accepted version for American Mineralogist, published by the Mineralogical Society of America.
The published version is subject to change. Cite as Authors (Year) Title. American Mineralogist, in press.
DOI: https://doi.org/10.2138/am-2026-10296. https://msaweb.org/

We propose that the N-aggregation state of *Type Ib* diamonds be described using the terms **$\%N_{TS}$ (or $\%N_A$)** and that they are calculated as follows;

[Eqn 2]: $\%N_{TS} = 100 \times \frac{N_{TS}}{N_C + N_X + N_Y + N_A + N_B}$

Here, N_{TS} indicates total single substitutional N and $N_{TS} = (N_C+N_X+N_Y)$ and includes the total amount of single-substitutional N (Lawson et al. 1998; Day et al. 2026) (***C***- and ***X***-centers) or N-defects associated with ***C***- and ***X***-centers (***Y***-centers) in *Type Ib* diamonds. The specific structure (composition) of the ***Y***-center remains a topic of debate. Therefore, until the exact identity and calibration coefficient of the ***Y***-center has been rigorously determined, some degree of uncertainty is inherent when determining the N-aggregation state of any ***Y***-center bearing *Type Ib* diamond.

It is important not to confuse N_{TS} with N_s^0 (***C***-centers) as N_{TS} also includes ***X***- and ***Y***-centers. Because ***C***-, ***X***- and ***Y***-centers are directly (or indirectly) involved in the formation of ***A***-centers (Nadolinny et al. 2025; Day et al. 2026), one cannot accurately indicate the N-aggregation state of a *Type Ib* diamond using $\%N_C$ (or $\%N_X$ or $\%N_Y$) if the diamond contains ***X***- and ***Y***-centers in addition to ***C***-centers. If only ***C***-, ***X***- or ***Y***-centers are observed, the N-aggregation state can be described using $\%N_C$, $\%N_X$ or $\%N_Y$. For example, for a diamond with N_C = 50 at.ppm and N_X and N_Y = 0 at.ppm, $\%N_{TS}$ or $\%N_C$ can be used to describe the N-aggregation state as $\%N_{TS} = \%N_C$ in this case. Alternatively, $\%N_A$ (see Eqn 6) can be used to describe the N-aggregation state of a *Type Ib* diamond where $\%N_A = (100 - \%N_{TS})$. Here, $\%N_C$, $\%N_X$ and $\%N_Y$ are calculated as follows;

[Eqn 3]: $\%N_C = 100 \times \frac{N_C}{N_C + N_X + N_Y + N_A + N_B}$

[Eqn 4]: $\%N_X = 100 \times \frac{N_X}{N_C + N_X + N_Y + N_A + N_B}$

Always consult and cite the final published document. See https://msaweb.org/ or GeoScienceWorld

This is the peer-reviewed, final accepted version for American Mineralogist, published by the Mineralogical Society of America.
The published version is subject to change. Cite as Authors (Year) Title. American Mineralogist, in press.
DOI: https://doi.org/10.2138/am-2026-10296. https://msaweb.org/

[Eqn 5]: $\%N_Y = 100 \times \frac{N_Y}{N_C + N_X + N_Y + N_A + N_B}$

For the reasons described in "Limitations of the historical Type classification scheme", we also propose that N-aggregation state of Type Ia diamonds be described using the terms **$\%N_B$ (or $\%N_A$)** instead of %IaB (or %IaA), and that $\%N_A$ and $\%N_B$ are calculated following Eqn 1 as follows;

[Eqn 6]: $\%N_A = 100 \times \frac{N_A}{N_C + N_X + N_Y + N_A + N_B}$

[Eqn 7]: $\%N_B = 100 \times \frac{N_B}{N_C + N_X + N_Y + N_A + N_B}$

In Eqns 2–4, N_B must be included such that $\%N_{TS}$ (or $\%N_C$, $\%N_X$ or $\%N_Y$) can also be used to describe ***Type Ib–Ia*** diamonds (those that contain ***C***-, ***A***- and ***B***-centers). For the same reason, N_C, N_X and N_Y must be included in Eqns 6 and 7. For most natural (untreated) diamonds, that do not contain significant N_C and N_B, N_B in Eqns 2–5 will have no effect on $\%N_{TS}$ (or $\%N_C$, $\%N_X$ or $\%N_Y$). Similarly, N_C, N_X and N_Y will often have no effect on $\%N_A$ or $\%N_B$ in Eqns 6–7. From here on, we refer to the N-aggregation state of *Type Ib*, *Type Ia* and *Type Ib–Ia* diamonds using these terms and classify diamonds using the *Type* designations as shown in Fig. 3. It is important to note that as ***A***-centers occur in both *Type Ib* and *Type Ia* diamonds and ***C***-, ***A***- and ***B***-centers occur in *Type Ib–Ia* diamonds, an N-aggregation state (e.g., a specific $\%N_{TS}$ or $\%N_A$ value) should not be stated independent of the corresponding diamond *Type* (i.e., $\%N_A$ describes the aggregation state of a *Type Ib*, *Ia* or *Ib–Ia* diamond).

In Fig. 1, the estimated proportion of natural *Type Ib*, *Ia*, *IIb* and *IIa* diamonds is provided (Harlow 1998; Breeding and Shigley 2009) but vary in the literature. Based on gemmological data, the proportion of *Type Ia* diamonds has been reported as ~99% (Eaton-Magana et al. 2020),

Always consult and cite the final published document. See https://msaweb.org/ or GeoScienceWorld

This is the peer-reviewed, final accepted version for American Mineralogist, published by the Mineralogical Society of America.
The published version is subject to change. Cite as Authors (Year) Title. American Mineralogist, in press.
DOI: https://doi.org/10.2138/am-2026-10296. https://msaweb.org/

459 slightly higher than the 95–98% reported by Harlow (1998). Based on the more recent geological
460 database of Stachel et al. (2022), the proportion of *Type I* diamonds appears to be significantly
461 lower (e.g., ~80%) than that previously reported. Based on a database of 13.8 million diamonds
462 submitted to the GIA, (Smith et al. 2018) reasoned that the proportion of *Type IIb* diamonds is
463 <0.02%. However, it is extremely likely that such estimates suffer from major selection biases
464 based on diamond color, size, clarity, the presence of visible mineral inclusions, and locality
465 (economic vs. non-economic deposits and subsequent production and recovery rates). Moreover,
466 it is well known that the proportion of different diamond *Types* vary significantly across different
467 deposits. In fact, it is likely that the proportion of *Type Ib* diamonds may be significantly
468 underestimated due to the smaller average size and distinct coloration (e.g., prevalent deformation
469 features) that makes such diamonds less economically desirable and harder to recover from ore
470 using techniques like X-ray luminescence.

471 **Tiers 1 and 2**

472 Tier 1 comprises *Type I* and *Type II* diamonds. *Type I* diamonds are traditionally defined
473 as containing N-defects at concentrations detectable via standard FTIR analysis. *Type II* diamonds
474 are often described as diamonds that do not contain N-defects, or more aptly, as diamonds that
475 contain N-defects at concentrations not detectable via standard FTIR analysis, but that may be
476 detectable with other techniques including PL and CL spectroscopy and Secondary Ion Mass
477 Spectrometry (SIMS). There is some discrepancy in the literature regarding the reported FTIR
478 detection limit of N in diamond which ranges from 1–3 to 20 at.ppm (Ashfold et al. 2020) but is
479 most commonly reported as 5–15 at.ppm (e.g., Stachel 2014; Carvalho et al. 2025). Contrasting
480 reports of the FTIR detection limit of N are likely the result of comparative studies on diamonds
481 with variable thicknesses (i.e., path lengths) and IR-active N-contents where different N-defects

Always consult and cite the final published document. See https://msaweb.org/ or GeoScienceWorld

This is the peer-reviewed, final accepted version for American Mineralogist, published by the Mineralogical Society of America.
The published version is subject to change. Cite as Authors (Year) Title. American Mineralogist, in press.
DOI: https://doi.org/10.2138/am-2026-10296. https://msaweb.org/

have different molar absorptivities (calibration coefficients). Here, it is useful to differentiate the *instrument detection limit* (IDL) and the *practical quantitation limit* (PQL) or the *limit of quantitation* (LOQ) (Gibbons et al. 1991). The IDL is the minimum total IR-active N concentration that will produce a detectable signal above background noise. The PQL is the minimum total IR-active N concentration that will produce a signal sufficiently high above background that it can be decomposed with a least-squares fit above a defined fit-quality threshold (see Supplementary Material, Appendix A). Both the IDL and PQL depend on the Beer-Lambert law and thus sample thickness (path length of the IR beam) and the absorptivity of the N-defects being analyzed, which ranges from 5.5 ± 1 at.ppm/cm^{-1} for ***X***-centers (Lawson et al. 1998) to 79.4 ± 8 at.ppm/cm^{-1} for ***B***-centers (Boyd et al. 1995).

Absorbance is a unitless, dimensionless measure of how much light is absorbed by a sample, while accounting for reflectance and scattering effects. The absorption coefficient is an intrinsic property of a homogeneous material that describes the decrease in light intensity per unit path length (cm^{-1}). In this work, the term "calibration coefficient" is used for the proportionality constant that converts the measured absorbance per unit thickness at a specified wavenumber into the concentration (e.g., N_B in at.ppm) of N in the corresponding N-defect (e.g., ***B***-centers). However, this relation is only valid within the linear regime of the Beer-Lambert law, i.e., under non-saturating conditions. In many cases, overly thick, or particularly N-rich diamonds, may result in saturation (complete absorption) in the two- or one-phonon (N) regions, respectively, thus preventing reliable spectral processing. In general, where absorbance in the two- and/or one-phonon regions is greater than 1.0–1.5, saturation will prevent reliable thickness normalization (via fitting of signal in the two-phonon region, e.g., with DiaMap, Howell et al. 2012a,b) and N-defect calculation via decomposition of signal in the one-phonon region. All spectra presented here

Always consult and cite the final published document. See https://msaweb.org/ or GeoScienceWorld

This is the peer-reviewed, final accepted version for American Mineralogist, published by the Mineralogical Society of America.
The published version is subject to change. Cite as Authors (Year) Title. American Mineralogist, in press.
DOI: https://doi.org/10.2138/am-2026-10296. https://msaweb.org/

are normalized to a thickness of 1 cm; hereafter, all reported peak intensities and defect concentrations are assumed to correspond to this normalized thickness.

For standard FTIR analyses, where the thickness normalized intensity of absorbance due to ***X***-, ***C***-, ***A***- and/or ***B***-centers is ≥ 0.10 cm^{-1}, fitting of such signal, and thus reasonably accurate determination of N-defect concentrations, can usually be performed. This minimum thickness normalized intensity value corresponding to the PQL was determined by decomposing 58 *Type Ia* and *Ib* spectra with low N_{tot} and comparing the resultant fit quality. This intensity threshold (0.10 cm^{-1}) was determined at 1282 cm^{-1} as this is the location of the absorbance maxima of ***A***-centers and overlaps with signal produced by ***C***- and ***B***-centers. To ensure validity of this value, and thus the PQL, the effect of different baseline correction procedures, sample thickness and spectrum resolution on the PQL was tested (see Supplementary Material A).

The PQL of ***X***-, ***C***-, ***A***-, and ***B***-centers may be expressed individually as;

[Eqn 8]: $PQL_X = 5.5 \pm 1.0 \times 0.10 = 0.55 \pm 0.10\ at.ppm$

[Eqn 9]: $PQL_C = 25.0 \pm 2.0 \times 0.10 = 2.50 \pm 0.20\ at.ppm$

[Eqn 10]: $PQL_A = 16.5 \pm 1.0 \times 0.10 = 1.65 \pm 0.10\ at.ppm$

[Eqn 11]: $PQL_B = 79.4 \pm 8.0 \times 0.10 = 7.94 \pm 0.80\ at.ppm$

Although it has not been experimentally proven yet, Day et al. (2026) suggested the ***Y***-center is associated with a single-substitutional N atom and has a calibration coefficient similar to the ***C***-center and thus one can assume $PQL_Y \approx PQL_C$. **The averaged (combined) PQL can thus be expressed as a function of $\%N_A$ for *Type Ib* diamonds as**;

[Eqn 12]: $PQL_{Ib} = \frac{(\%N_A \times 1.65 \pm 0.10) + (\%N_C \times 2.5 \pm 0.20)}{100}$

Always consult and cite the final published document. See https://msaweb.org/ or GeoScienceWorld

This is the peer-reviewed, final accepted version for American Mineralogist, published by the Mineralogical Society of America.
The published version is subject to change. Cite as Authors (Year) Title. American Mineralogist, in press.
DOI: https://doi.org/10.2138/am-2026-10296. https://msaweb.org/

If ***X***- and ***Y***-centers are observed in addition to ***C***- and ***A***-centers, the PQL_{Ib} is given as;

[Eqn 13]: $$PQL_{Ib} = \frac{(\%N_A \times 1.65 \pm 0.10) + (\%N_C \times 2.5 \pm 0.20) + (\%N_X \times 0.55 \pm 0.10) + (\%N_Y \times 2.5 \pm 0.20)}{100}$$

The combined PQL can be expressed as a function of $\%N_B$ for *Type Ia* diamonds as;

[Eqn 14]: $$PQL_{Ia} = \frac{(\%N_B \times 7.94 \pm 0.80) + (\%N_A \times 1.65 \pm 0.10)}{100}$$

The combined PQL can be expressed for *Type Ib–Ia* diamonds as;

[Eqn 15]:

$$PQL_{Ib-I} = \frac{(\%N_B \times 7.94 \pm 0.80) + (\%N_A \times 1.65 \pm 0.10) + (\%N_C \times 2.5 \pm 0.20) + (\%N_X \times 0.55 \pm 0.10) + (\%N_Y \times 2.5 \pm 0.20)}{100}$$

Here, $\%N_C$, $\%N_X$, $\%N_Y$ and $\%N_A$ for *Type Ib* diamonds, $\%N_B$ and $\%N_A$ for *Type Ia* diamonds, and $\%N_C$, $\%N_X$, $\%N_Y$, $\%N_A$, and $\%N_B$ for *Type Ib–IaA* diamonds are normalized to unity.

If the total N concentration (N_{tot}) of the diamond is greater than the combined PQL (Eqns 12–15), it may be classified at a Tier 3 level. For example, for a diamond with N_A and $N_B > PQL_{Ia}$ (and $N_C <$ IDL), $\%N_B$ (or $\%N_A$) can be determined and thus the diamond can be classified as *Type IaA*, I*aAB* or *IaB* (see Fig. 3). In cases where N_C, N_X, N_Y, N_A and/or N_B are greater than the IDL but less than the respective PQL, such N-defects will produce a detectable signal but one that cannot be reliably fit during decomposition. Such a diamond can be classified as *Type I* if N-defects can be identified but not rigorously differentiated by decomposition. If absorbance due to ***C***-, ***X***- and/or ***Y***-centers can be differentiated from that due to ***A***- or ***B***-centers, respectively, but not quantified, the diamond can be classified as *Type Ib* or *Type Ia* but cannot be classified further at the Tier 3a level (see Fig. 3). Similarly, if absorbance due to ***C***- (and/or ***X***- or ***Y***-centers), ***A***- and

Always consult and cite the final published document. See https://msaweb.org/ or GeoScienceWorld

This is the peer-reviewed, final accepted version for American Mineralogist, published by the Mineralogical Society of America.
The published version is subject to change. Cite as Authors (Year) Title. American Mineralogist, in press.
DOI: https://doi.org/10.2138/am-2026-10296. https://msaweb.org/

546 ***B***-centers can be identified but not quantified (IDL < N_{TS}, N_A, N_B < $PQL_{Ib–Ia}$), the diamond can be
547 classified as *Type Ib–Ia* but cannot be classified further at a Tier 3b level (see Fig. 3). *Type Ib–Ia*
548 diamonds also include samples where IDL < N_{TS}, N_B < $PQL_{Ib–Ia}$ and N_A < IDL, but if such samples
549 are to be classified at the Tier 3b level, N_{TS} and N_B must be greater than the $PQL_{Ib–Ia}$. If no signal,
550 or only signal that cannot be attributed to a particular N-defect, is observed, the diamond should
551 be classified as *Type II* (Table B.1., Supplementary Material, Appendix B).

552 For example, consider the spectrum in Fig. 4a where the thickness normalized intensity of
553 the fit line at 1282 cm^{-1} is 0.12 cm^{-1} corresponding to a N_B of 9.5 at.ppm. This fit is high-quality
554 (see Supplementary Material – Appendix A for methods for determining fit quality) and because
555 N_B (9.5 at.ppm) is greater than the PQL_{Ia} (7.94 at.ppm) for this spectrum, one can classify this
556 diamond as *Type IaB'* (%N_B = 100 and %N_A = 0). In Fig. 4b, the thickness normalized intensity of
557 the fit line at 1282 cm^{-1} is 0.05 cm^{-1}, corresponding to an N_B of 4.0 at.ppm. Here, N_B (4.0 at.ppm)
558 is less than the PQL_{Ia} (7.94 at.ppm) and the fit is relatively poor-quality, particularly around 1130
559 to 1000 cm^{-1} and from 1300 to 1230 cm^{-1}, the wavenumber range associated with the ***A***-center
560 absorbance maximum. It follows that one cannot reliably determine %N_B or exclude the presence
561 of ***A***-centers (>PQL_A) as N_B > IDL but not the PQL_{Ia}. Therefore, this diamond should be classified
562 at a Tier 2 level as *Type Ia* rather than at a Tier 3 level as *Type IaB', IaB* or *IaAB*. In Fig. 4b, it is
563 apparent that the background spectrum is contributing to the poor-quality nature of the fit as the
564 measured absorption coefficient is less than the reference spectrum (red line) across several
565 regions. Analogous issues related to the background spectrum occur in all fits albeit to different
566 degrees, here N_B is very low (4.0 at.ppm) and thus the effect of the background subtraction is
567 relatively prominent. In fact, the fit in Fig. 4b serves as an example of how the quality of
568 background spectra, among many other factors, contribute to the PQL (see section "Uncertainty

Always consult and cite the final published document. See https://msaweb.org/ or GeoScienceWorld

This is the peer-reviewed, final accepted version for American Mineralogist, published by the Mineralogical Society of America.
The published version is subject to change. Cite as Authors (Year) Title. American Mineralogist, in press.
DOI: https://doi.org/10.2138/am-2026-10296. https://msaweb.org/

associated with the bulk nature of FTIR spectra"). Although the spectrum in Fig. 4b should be classified as *Type Ia*, it is useful to indicate that the decomposition results (albeit based on a low-quality fit) suggest the majority of N is in the form of ***B***-centers. For this reason, it is suggested that Tier 2 *Types* are reported along with the results of decomposition, albeit qualitative in most cases. In Fig. 4c, a weak signal is observed in the one-phonon region but cannot be attributed to any N-defect and is likely due to a combination of noise, surface contamination, micrometric inclusions and/or irregularities in the background spectrum resulting in a problematic background subtraction. It follows that this spectrum (diamond) should be classified as *Type II*.

Caution must be exercised when assuming that a diamond, classified as *Type II*, does not contain N (in any form) as several N-defects are *IR-inactive* or are weakly absorbing and are thus rarely observed in FTIR spectra. For example, the ***N3***- and ***N2***-centers (N_3V), which produce characteristic absorption lines at 415 and 477 nm (24096 and 20964 cm^{-1}), have IR-active vibrational modes with absorptivities (absorption cross section) that are too low to be observed in the infrared, despite often occurring at concentrations in the at.ppm range (Thomaz and Davies 1978; Kiflawi and Bruley 2000; Dischler 2012; Shigley and Breeding 2013). Similarly, the N_3VH defect, which produces peaks at 3107 and 1405 cm^{-1} (due to C–H stretching and bending), also produces signal in the one-phonon region but that is not intense enough to be observed. The NV^0 and NV^- defects and the N–*V*–N^0 defect (***H3***-center) are not observed in the IR but play an important role in ***C*** → ***A*** aggregation sequences (Nadolinny et al. 2025; Day et al. 2026) and may occur in significant concentrations in some *Type Ib* diamonds. Moreover, other N-defects that are IR-active produce signal outside of the one-phonon region. For example, the N–*V*–N^- defect (***H2***-center), which absorbs at 988 nm (10125 cm^{-1}) (Shigley and Breeding 2013), or the (001) di-nitrogen split interstitial N_{2i} defect (***H1a***-center), which produces a sharp peak at 1450 cm^{-1}

Always consult and cite the final published document. See https://msaweb.org/ or GeoScienceWorld

This is the peer-reviewed, final accepted version for American Mineralogist, published by the Mineralogical Society of America.
The published version is subject to change. Cite as Authors (Year) Title. American Mineralogist, in press.
DOI: https://doi.org/10.2138/am-2026-10296. https://msaweb.org/

(Liggins et al. 2010). Nitrogen may also form different types of micro- or nanoscale inclusions. For example, octahedral inclusions of cubic δ–N_2 that are thought to form from the exsolution of N from ***B***-centers in super-deep diamonds at high P/T conditions (Navon et al. 2017; Kempe et al. 2025). Therefore, for the purposes of utility, we restrict the *Type* group criteria based on N-defects (Tiers 1–3) to signal observed in the defect-induced one-phonon region of the FTIR spectrum of diamond. In general, it is likely that most *Type II* diamonds contain N (in some form). More importantly, a *Type II* composition should not be used as an indicator of N-poor diamond-forming fluids/melts as N may be preferentially partitioned into other phases crystallizing from the same fluids/melts or may be stable in a molecular form that cannot be incorporated into diamond during growth (see section "Tier 3").

Typically, *Type II* diamonds are further subdivided as *Type IIa* and *Type IIb* diamonds based on the presence of boron (B) (Table B.1., Supplementary Material, Appendix B). The IR spectra of *Type IIb* diamonds show signal (at 2458, 2803 and 4090 cm^{-1}) due to substitutional boron defects but have total concentration of IR-active N below the IDL (Breeding and Shigley 2009; Gaillou et al. 2012). These *Type II* designations imply that all *Type IIb* diamonds are N-free (N_{tot} < IDL), which is of course not true for N- and B-doped synthetic diamond and even for natural *Type IIb* diamonds (Eaton-Magaña and Ardon 2016), some of which show characteristic absorption due to ***B***-centers (Van der Bogert et al. 2009; Borenstein and O'Neal 2021; Chan and Pradhan 2025). In several studies, this has led some authors to refer to natural *Type IIb* diamonds as "N-poor" rather than "N-free" (Smith et al. 2025). In part, such complications arise due to difficulties recognizing N in the spectra of *Type IIb* diamonds due to electrical compensation of boron acceptors by N donors, and signal overlap in the N-region (e.g., at ~1290 cm^{-1}) due to B-defects. It is unlikely that any *Type II* diamond actually contains no form of N, in fact N in

Always consult and cite the final published document. See https://msaweb.org/ or GeoScienceWorld

This is the peer-reviewed, final accepted version for American Mineralogist, published by the Mineralogical Society of America.
The published version is subject to change. Cite as Authors (Year) Title. American Mineralogist, in press.
DOI: https://doi.org/10.2138/am-2026-10296. https://msaweb.org/

commonly detected via SIMS in *Type II* diamonds. As instrumental detection limits continue to improve, it is likely that N in *Type II* diamonds will be routinely detected, even at the ppb level. Consequently, we propose that *Type IIa* diamonds include those that do not show signal in the one-phonon region due to N-defects (N_{tot} < IDL), or show signal that is sufficiently weak that it cannot be attributed to specific N-defects (N_{tot} > IDL and N_{tot} < PQL). Similarly, we suggest that *Type IIb* diamonds are described similarly (N_{tot} < IDL/PQL) but contain boron. However, when referring to the general presence of N (e.g., IR-inactive N-defects, cubic δ–N_2 inclusions, etc.), *Type II* diamonds are better described as "N-poor" rather than "N-free".

Tier 3

Type Ib* and *Type Ia* diamonds.** As described for the spectrum in Fig. 4a, diamonds with N-defect concentrations greater than their PQL can be classified at the Tier 3 level. Decomposition of the spectra of most untreated natural *Type I* diamonds will result in one of two outcomes; (1) N_A *and* N_B or (2) N_C (and/or N_X or N_Y) and N_A (see *Type* groups shown in blue, Figs. 2 and 3). Outcome (1) corresponds to the *Type Ia* group which can be further subdivided when N_B and N_A > PQL_{Ia} and N_{TS} < IDL. The *Type Ia* subgroups, *IaA*, *IaAB* and *IaB* are differentiated based on $\%N_A$ and $\%N_B$ (see Eqns 6 and 7). Outcome (2) corresponds to the *Type Ib* group which can be subdivided when N_C and/or N_X and/or N_Y and N_A > PQL_{Ib} and N_B < IDL. The *Type Ib* subgroups, *IbC*, *IbCA* and *IbA* are based on $\%N_{TS}$ and $\%N_A$ (see Eqns 2 and 6). As ***X- and ***Y***-centers are variants of single substitutional nitrogen (Lawson et al. 1998; Nadolinny et al. 2025; Day et al. 2026), they are grouped with ***C***-centers in the calculation of $\%N_{TS}$ (see Eqn 2).

Traditionally, the *Type IaA* group represents (1) *Type Ib* diamonds that contain predominately ***A***-centers and minor ***C***-centers, (2) *Type Ia* diamonds with $90 \leq \%N_A < 100$ (and $0 < \%N_B \leq 10$), and (3) *Type Ia* diamonds with exclusively ***A***-centers ($\%N_A = 100$). This is obviously

Always consult and cite the final published document. See https://msaweb.org/ or GeoScienceWorld

This is the peer-reviewed, final accepted version for American Mineralogist, published by the Mineralogical Society of America.
The published version is subject to change. Cite as Authors (Year) Title. American Mineralogist, in press.
DOI: https://doi.org/10.2138/am-2026-10296. https://msaweb.org/

problematic as (1) to (3) describe diamonds with drastically different mantle residence times/temperatures or annealing treatments. Consequently, in the updated classification scheme, groups (1) and (2) (as above) are differentiated as *Type IbA* and *Type IaA* and are defined as $90 \leq \%N_A < 100$ ($0 < \%N_{TS} \leq 10$); and $90 \leq \%N_A < 100$ ($0 < \%N_B \leq 10$), respectively (Fig. 3). For group (3), an additional *Type IaA′* group has been added which represents diamonds with exclusively ***A***-centers ($\%N_A = 100$ and $\%N_{TS}$ and $\%N_B = 0$) as such diamonds have unique thermal residence histories. Similarly, an additional *Type IaB′* group has been added, representing diamonds with exclusively ***B***-centers ($\%N_B = 100$ and $\%N_{TS}$ and $\%N_A = 0$), such that fully-aggregated diamonds can be easily differentiated from *Type IaAB* and *IaB* diamonds.

If standard decomposition reveals absorption due to only ***A***-centers (or only ***B***-centers), one may assume $\%N_A$ (or $\%N_B$) ≈ 100. However, it is possible that a given diamond with $\%N_A \approx 100$ contains minor $N_{TS} < PQL_C$ (or $N_B < PQL_B$) that would not be detected during decomposition. With decreasing N_{tot}, the corresponding degree of uncertainty in $\%N_{TS}$, $\%N_A$ and $\%N_B$ for pure *Type IbC*, *IaA′* and *IaB′* diamonds increases. For example, a *Type IaA′* diamond with $N_{tot} = 50$ at.ppm may have $N_B \leq 7.94$ at.ppm below the PQL_{Ia} or $N_{TS} \leq 5.55$ ($2.5(N_C)+0.55(N_X)+2.5(N_Y)$) at.ppm below the PQL_{Ib} and thus a large uncertainty in $\%N_A$ ranging from 11.1 to 15.9%. However, for a *Type IaA′* diamond with $N_{tot} = 500$ at.ppm, the uncertainty in $\%N_A$ (due to $N_B \leq PQL_{Ia}$ and $N_{TS} \leq PQL_{Ib}$) ranges from 1.1 to 1.6%.

The *Type IaB′* group allows identification of fully-aggregated diamonds which represent the *end-state* of normal N-aggregation and are a useful proxy in experiments focused on investigating the behaviour of defects (e.g., N/*V*/H-aggregation sequences) during laboratory annealing experiments (e.g., Day et al. 2024, 2025). Moreover, the *Type IaB′* group allows differentiation of super-deep (sublithospheric) diamonds, the majority of which are fully-

Always consult and cite the final published document. See https://msaweb.org/ or GeoScienceWorld

This is the peer-reviewed, final accepted version for American Mineralogist, published by the Mineralogical Society of America.
The published version is subject to change. Cite as Authors (Year) Title. American Mineralogist, in press.
DOI: https://doi.org/10.2138/am-2026-10296. https://msaweb.org/

aggregated and have been the topic of much recent work (e.g., see Shirey et al. 2024). The *Type IaA'* group is particularly useful as ~100 $\%N_A$ – *Type IaA''* diamonds are observed disproportionately more than *Type IbA* and *IaA* diamonds (Stachel 2014). Inspection of the database from Stachel et al. (2022), containing 3619 diamond samples for which N-aggregation states were determined, shows that ~9% of the samples have $\%N_A$ = 100.0% ($\%N_B$ = 0.0), significantly more than ~0.1% as would be expected based on a random distribution of $\%N_B$ from 0.0–100.0%. Approximately 13% of the samples from this database have $\%N_B$ = 0.0–5.0% and ~18% of the samples have $\%N_B$ = 0.0–10.0%.

In fact, some diamond populations from particular deposits (localities) have an unusually high proportion of *Type IaA''* diamonds, e.g., mixed-habit diamonds from Marange (Zimbabwe) (Smit et al. 2016); FALC kimberlite (Sask craton, Canada) (Leahy and Taylor 1997); A154–N/S and Jericho kimberlites (Slave craton, Canada) (Donnelly et al. 2007; Aulbach et al. 2012); the Wawa-Genesis diamond occurrences (Superior craton) (Stachel et al. 2006); and several kimberlite localities in the Kalahari craton (South Africa) (Mc Dade and Harris 1998; Phillips et al. 2004; Tappert et al. 2005; Deines et al. 2009; Thomassot et al. 2009; Weiss et al. 2018). Over-representation of *Type IaA''* diamonds reflects the difference in $\boldsymbol{C} \rightarrow \boldsymbol{A}$ and $\boldsymbol{A} \rightarrow \boldsymbol{B}$ activation energies, E_a = ~4.4–6.0 eV and 7.03 eV, respectively (Cooper 1990; Taylor et al. 1990, 1996; Kiflawi et al. 1997). Considering the significant difference in E_a, higher T_{res} (or significantly longer t_{res}) are required to convert ***A***-centers to ***B***-centers than ***C***-centers to ***A***-centers. As previously described by Weiss et al. (2018) and Timmerman et al. (2018), after $\boldsymbol{C} \rightarrow \boldsymbol{A}$ aggregation is complete, T_{res} may not be sufficiently high to drive $\boldsymbol{A} \rightarrow \boldsymbol{B}$ transformation at non-negligible rates and N-aggregation may effectively stall for a finite time period. Of course, at any temperature, $\boldsymbol{A} \rightarrow \boldsymbol{B}$ will inevitably proceed but at extremely slow rates where T_{res} is not sufficiently high. For

Always consult and cite the final published document. See https://msaweb.org/ or GeoScienceWorld

This is the peer-reviewed, final accepted version for American Mineralogist, published by the Mineralogical Society of America.
The published version is subject to change. Cite as Authors (Year) Title. American Mineralogist, in press.
DOI: https://doi.org/10.2138/am-2026-10296. https://msaweb.org/

example, a diamond with N_{tot} = 500 at.ppm would require times greater than the age of Earth (t_{res} = ~5.0 Gyr) at a T_{res} = 1124 °C to convert 50% of the ***A***-centers to ***B***-centers, and thus higher T_{res} would be required to produce a reasonable t_{res}.

Type Ib–Ia* diamonds.** It is now well established that HPHT treatment of *Type Ia* diamonds may result in disassociation of ***A- and/or ***B***-centers and the subsequent production of ***C***-centers. Since the mid-1990's, HPHT or HT treatments (in addition to irradiation) have been commonly used to modify the color and/or clarity of natural and synthetic diamonds (Shigley et al. 1993; Moses and McClure 2022). For example, yellow and yellow–green diamonds are often produced by HPHT treatment of natural *Type Ia* brown diamond (Collins et al. 2000; Reinitz et al. 2000). Brown diamonds owe their color to plastic deformation features. Some *Type Ia* and *Type Ib* diamonds show evidence of plastic deformation in the form of *amber centers* (Massi et al. 2005). It has been shown that annealing (e.g., HT and LPHT treatment) of such diamonds results in the breakdown of amber centers (Hainschwang et al. (2020a), releasing vacancies, subsequently producing N–*V*–N^0 (***H3***-center) among other vacancy-related defects (Eaton-Magaña et al. 2017). Here, HPHT treatment also acts to disassociate aggregated N to produce ***C***-centers that act as electron donors producing N–*V*–N^- (***H2***-centers) and the combination of ***H2***- and ***H3***-center absorption produces the yellow–green color observed in such diamonds (e.g., Collins et al. 2000).

Brozel et al. (1978) were the first to report (using EPR data) the production of ***C***-centers due to HPHT treatment of *Type Ia* diamonds at 1960 °C and 8.5 GPa. Although subsequent HPHT experiments at similar temperatures did not replicate the production of ***C***-centers (e.g., Evans and Qi 1982), subsequent experiments at higher temperatures (~2000–2650 °C and 6–9 GPa) clearly show the appearance of a peak at 1344 cm^{-1} due to ***C***-centers after HPHT treatment of *Type IaA* and *IaAB* diamond (Collins et al. 2000; Kiflawi and Bruley 2000). The temperatures and pressures

Always consult and cite the final published document. See https://msaweb.org/ or GeoScienceWorld

This is the peer-reviewed, final accepted version for American Mineralogist, published by the Mineralogical Society of America.
The published version is subject to change. Cite as Authors (Year) Title. American Mineralogist, in press.
DOI: https://doi.org/10.2138/am-2026-10296. https://msaweb.org/

of such HPHT treatments far exceed those associated with the formation of most natural diamonds (1160±100 °C and 5–6 GPa, Stachel and Harris 2009; Stachel and Luth 2015) and thus it is unlikely that temperature-induced disassociation of ***A***- and ***B***-centers occurs in natural diamonds. However, albeit rare, untreated diamonds that contain ***C***-, ***A***- and ***B***-centers have been reported (e.g., Woods and Collins 1983; Hainschwang et al. 2005) and were previously named "*ABC diamonds*" (Hainschwang et al. 2006a). In fact, ***C***-centers (***P1***-centers) have been detected via EPR in untreated plastically deformed *Type IaB* diamonds and have been attributed to the disassociation of ***B***-centers due to the propagation of dislocations associated with plastic deformation (Nadolinny et al. 2009; Rakhmanova et al. 2015). It is important to note that single growth zones in untreated natural diamonds that contain ***C***-, ***A***- and ***B***-centers are exceedingly rare. In many cases, reports of all three N-defects in untreated diamonds likely reflect analysis of several different growth zones which are often observed in diamonds that have experienced episodic growth where younger (less aggregated) rims containing ***C***-centers occur around older (more aggregated) cores containing predominately ***A***- and ***B***-centers (e.g., Timmerman et al. 2017; Lai et al. 2020b).

Diamonds with detectable N in the form of ***C***-, and/or ***X***- or ***Y***- and ***A***- and ***B***-centers (N_C and/or N_X and/or N_Y and N_A and N_B > IDL) are defined as *Type Ib–Ia* at the Tier 2 level (see *Type* groups shown in orange, Fig. 3). When N_C and/or N_X and/or N_Y and N_A and N_B > $PQL_{Ib–Ia}$, *Type Ib–Ia* diamonds can be subdivided based on $\%N_{TS}$, $\%N_A$ and $\%N_B$. Like the equivalent Tier 3a *Type* groups, the seven *Type* groups that comprise Tier 3b (Fig. 3) are mutually exclusive and represent all possible compositions in the $\%N_{TS}$–$\%N_A$–$\%N_B$ ternary space. These *Type* groups also include compositions that fall along the $\%N_{TS}$–$\%N_B$ binary join (contain exclusively ***C***-, ***X***-, and/or ***Y***-centers and ***B***-centers) although no such compositions have been reported yet via FTIR spectroscopy. For example, in Fig. 5, the decomposition results of a HPHT-treated yellow–green

Always consult and cite the final published document. See https://msaweb.org/ or GeoScienceWorld

This is the peer-reviewed, final accepted version for American Mineralogist, published by the Mineralogical Society of America.
The published version is subject to change. Cite as Authors (Year) Title. American Mineralogist, in press.
DOI: https://doi.org/10.2138/am-2026-10296. https://msaweb.org/

diamond (originally brown) are shown from Collins et al. (2000). Here, $\%N_{TS}$ ($\%N_C$) = 17.5, $\%N_A$ = 29.1, and $\%N_B$ = 53.4 allowing classification as *Type IaABC* (Fig. 3).

***Type I* diamonds with boron and *Type II* diamonds with H-related defects.** As described in "Tiers 1 and 2", it is unlikely that *Type II* diamonds have $N_{tot} \approx 0$ and thus are best described as "N-poor" where N_{tot} < IDL. As Diamonds with $N_{tot} \geq$ IDL and boron are technically *Type I*, we propose that such diamonds are described using the suffix "*–NB"* and classified at the Tier 2 level using the criteria for *Type Ib*, *Type Ib–Ia* and *Type Ia* diamonds (e.g., *Type Ia–NB*, Fig. 3). Where N_{tot} > PQL, and the identity and concentration of N-defects can be determined, the corresponding *Type* group can be assigned at the Tier 3 level. For example, boron-bearing diamonds with 90 < $\%N_B$ < 100 (Eaton-Magaña and Ardon 2016; Borenstein and O'Neal 2021) should be described as *Type IaB–NB* (see Fig. 3).

The observation of the 3107 cm^{-1} peak, due to the N_3VH defect (Goss et al. 2014), is a common example of N in *Type II* diamonds, albeit the total concentration of N_3VH required to produce a detectable 3107 cm^{-1} peak is relatively small compared to ***C***-, ***A***- and ***B***-centers (Coxon et al. 2020; Wood 2020; Kaminsky et al. 2024). Here, the presence of the 3107 cm^{-1} peak or other H-related peaks (e.g., 3236 cm^{-1}, assigned to N_4VH^0, Keat et al. 2024), can be indicated in *Type IIa* and *Type IIb* diamonds with the suffix "–H_n" where *n* is the position(s) of the H-related peaks in the IR (e.g., *Type IIa*–H_{3107}, Fig. 3). Although a large number of different peaks in the spectrum of *Type Ia* diamonds have been attributed to H-related impurities (Day et al. 2024, 2025), very few have been attributed to specific defects and more work is required before additional *Type* groups for H-defects can be included here. The same is true for other impurities like Ni, Co, Fe, Cr, Ti, S, Mn, Cu, Si, P, V, and O which have important effects on the properties of diamond but are still poorly understood regarding their expression in the infrared.

Always consult and cite the final published document. See https://msaweb.org/ or GeoScienceWorld

This is the peer-reviewed, final accepted version for American Mineralogist, published by the Mineralogical Society of America.
The published version is subject to change. Cite as Authors (Year) Title. American Mineralogist, in press.
DOI: https://doi.org/10.2138/am-2026-10296. https://msaweb.org/

A *Type I* vs. *Type II* designation is often used to make inferences about the N-content of the respective diamond-forming fluid. Due to the compatibility of N in diamond (N and C have similar charge and ionic radii), *Type II* diamonds are often thought to form from N-poor (or N-free) fluids. Similarly, *Type I* diamonds are often associated with N-bearing (or N-rich) fluids where the amount of N in a given *Type I* diamond reflects the N content of the diamond-forming fluid from which it grew. Based on recent works, it is now known this is often not the case. For example, in *Type II* super-deep diamonds, the absence of N has been attributed to siderophile behaviour of N in deep reducing environments and its preferential uptake by Fe-alloys (Smith and Kopylova 2014; Smith et al. 2016) and/or the formation of high-pressure nitrides (Dobrzhinetskaya et al. 2009), not necessarily N-poor diamond-forming fluids. Alternatively, Mikhail and Howell (2016), propose that specific redox or acid/base reactions are required to convert molecular forms of N, that are stable at diamond-forming conditions (e.g., NH_4^+, NH_3, N_2), to monatomic N^{3-} (which is unstable in the mantle) such that it can be incorporated into the diamond lattice. Therefore, the degree to which different molecular forms of N are in disequilibrium with the diamond-forming environment will dictate the rate at which, for example, N_2 is disassociated to form N-bearing diamond (i.e., $8CO_2 + N_2 + 2H_2 = 2NC_4$ (diamond) $+ 2H_2O + 7O_2$) (Mikhail and Howell 2016). It follows that, if molecular N species are in equilibrium with the diamond-forming environment, *Type II* diamond formation can occur from N-rich fluids/melts. As the reactions required to convert molecular N to monatomic N^{3-} may be more or less favoured depending on P, T, pH, N abundance, and in particular the redox state (Li and Keppler 2014; Mikhail and Sverjensky 2014), one cannot assume that N-rich and N-poor *Type I* and *Type II* diamonds form from N-rich and N-poor parental fluid/melts, respectively. Although more work is required to constrain the types and rates of reactions involving molecular N, and the electrochemical

Always consult and cite the final published document. See https://msaweb.org/ or GeoScienceWorld

This is the peer-reviewed, final accepted version for American Mineralogist, published by the Mineralogical Society of America.
The published version is subject to change. Cite as Authors (Year) Title. American Mineralogist, in press.
DOI: https://doi.org/10.2138/am-2026-10296. https://msaweb.org/

behaviour of N^{3-} at the diamond growth surface, it is clear that N-incorporation in diamond is not solely a kinetic process (Mikhail and Howell 2016). Similar processes are also likely operative for molecular H species (e.g., H_2O, NH_4^+, NH_3) in diamond-forming fluids.

480 nm diamonds. A group of diamonds named "*480 nm diamonds"* shows a broad band centered at ~480 nm in the visible absorption spectrum. These diamonds can only be reliably identified using UV–vis spectroscopy and thus a *Type* group is not proposed here for 480 nm diamonds. However, these diamonds show unique absorption features in the one-phonon region which can lead to difficulties when decomposition, and subsequent classification, based on N-defects, is attempted. This, in addition to the recent attention that commercially valuable 480 nm orange–yellow and chameleon diamonds have received (Breeding et al. 2020), warrants their description here. The 480 nm – orange–yellow diamonds have comparatively low N_{tot} and may show absorption due to ***A***-centers (peak at 1282 cm^{-1}) underlain by anomalous absorption in the one-phonon region making accurate decomposition difficult (Lai et al. 2024; Hardman et al. 2025). The 480 nm – chameleon diamonds typically have higher N_{tot} compared to the 480 nm – orange-yellow diamonds and are typically *Type IaA'*, and more rarely contain ***C***- or ***B***-centers (Hainschwang et al. 2005). Reasonably accurate decomposition of 480 nm – chameleon diamonds may be possible in some cases when anomalous absorption in the one-phonon region is minimal.

For 480 nm – orange–yellow diamonds, anomalous absorption is often characterized by a peak at ~1093–1095 cm^{-1}, with a weak shoulder at ~1053 cm^{-1}, and a peak at ~1228–1235 cm^{-1}, with a shoulder at ~1216 cm^{-1} (e.g., see Lai et al. 2024; Hardman et al. 2025). This anomalous absorbance is observed in both *Type Ib* and *Ia* diamonds and identification of such peaks is often difficult due to accompanying absorbance due to ***A***-centers and ***C***-centers (evidenced by peaks at 1130 and 1344 cm^{-1}) or more rarely ***B***-centers (evidenced by a peak at 1175 cm^{-1}) (Breeding et al.

Always consult and cite the final published document. See https://msaweb.org/ or GeoScienceWorld

This is the peer-reviewed, final accepted version for American Mineralogist, published by the Mineralogical Society of America.
The published version is subject to change. Cite as Authors (Year) Title. American Mineralogist, in press.
DOI: https://doi.org/10.2138/am-2026-10296. https://msaweb.org/

2020; Lai et al. 2024; Hardman et al. 2025). Additional broad peaks are observed at 1430, 1500, 1540 and 1578 cm^{-1} (Lai et al. 2024). Absorption in the one-phonon region associated with 480 nm diamonds should be recognized as a potential source of error during decomposition and classification.

A series of relatively weak and sharp peaks between ~1350–1380 cm^{-1} are also observed in 480 nm diamonds but are weak or absent when one-phonon absorbance is dominated by ***A***-centers (Lai et al. 2024). Similar peaks were observed in *Type Ib* diamonds by Day et al. (2026) who attributed them to small interstitial complexes associated with ***Y***-centers. In other studies, HPHT treatment of ***Y***-center bearing diamonds results in a reduction in ***Y***-center absorbance and the production of the 480 nm band, in addition to a 690 nm red luminescence band and ***C***-centers. Consequently, the ***Y***-center has been interpreted as a potential precursor to the defect(s) giving rise to the 480 nm feature observed in some yellow-orange diamonds (i.e., "480 nm diamonds") (Hainschwang et al. 2012, 2013). Related studies have tentatively attributed the 480 nm band to oxygen or nickel-related defects (Kupriyanov et al. 2020; Lai et al. 2024).

Tier 4

Type Ib* and *Type Ib–Ia* diamonds with *X*- and *Y*-centers.** The ***X- and ***Y***-centers are only observed in *Type Ib* diamonds and represent different forms of single-substitutional nitrogen (i.e., ***C***-centers). The ***X***-center has been assigned to the N^+ defect (Lawson et al. 1998) and ***Y***-centers have been attributed to variety of defects involving oxygen, nickel (Hainschwang 2014; Kupriyanov et al. 2020; Lai et al. 2024) and/or single-substitutional N_s in different charge states (Titkov et al. 2015). In some studies, HPHT treatment results in the disassociation of ***Y***-centers and subsequent production of ***C***-centers, a 480 nm band and a 690 nm red luminescence band, but no production of ***A***-centers (Hainschwang 2014). Other HPHT studies show the disassociation of

Always consult and cite the final published document. See https://msaweb.org/ or GeoScienceWorld

This is the peer-reviewed, final accepted version for American Mineralogist, published by the Mineralogical Society of America.
The published version is subject to change. Cite as Authors (Year) Title. American Mineralogist, in press.
DOI: https://doi.org/10.2138/am-2026-10296. https://msaweb.org/

Y-centers, but also the production of a peak at 1060 cm^{-1} and ***A***-centers instead (Kupriyanov et al. 2020). For natural untreated diamonds, Day et al. (2026) describe ***Y***-centers as an intermediate form of N_s^0 coupled with singular or small interstitial complexes of C_i ($\pm N_i$) where ***Y***-centers play a key role in the interstitial-assisted aggregation sequences that produce ***A***-centers, in agreement with the findings of Kupriyanov et al. (2020). Nadolinny et al. (2025) came to a similar conclusion, assigning ***Y***-centers to the N_s^0–C–N_s^0 defect and attributing it to a precursor to ***A***-centers, based on HPHT treatment of cubic, plastically deformed *Type Ib* diamonds. Although neither of these assignments has been rigorously proven, both suggest ***Y***-centers are directly (or indirectly) related to ***C*** → ***A*** aggregation sequences. For these reasons, N_X and N_Y are grouped with N_C (as N_{TS}) in the calculation of $\%N_{TS}$ (see Eqn 2) and thus the proportion of ***C***-, ***X***- and ***Y***-centers is not accessible at the Tier 3 level. Here $\%N_X$ and $\%N_Y$ can be calculated using Eqns 4 and 5.

Following the work of Hainschwang (2014), who described natural diamonds with almost exclusively ***X***- and ***Y***-centers, additional Tier 4 subgroups have been included to describe *Type Ib* (and *Type Ib–Ia*) diamonds with ≥50 $\%N_X$ or ≥50 $\%N_Y$. In Tier 3a, only the *Type IbC* and Type *IbCA* (Tier 3) groups may contain ≥50 $\%N_{TS}$, and thus corresponding Tier 4a subgroups are only included for these compositions (Fig. 3). For example, *Type IbC* (Tier 3a) is defined as $90 < \%N_C \leq 100$ ($0 \leq \%N_A < 10$), and can be further described at a Tier 4a level as *Type IbY* if $\%N_Y \geq 50$, $0 \leq \%N_A < 10$ and $0 \leq \%N_{TS}–\%N_Y \leq 50$. Similarly, in Tier 3b, only the *Type IbCB* and *Type IbCAB* groups may contain ≥50 $\%N_{TS}$ and thus these are the only groups for which additional Tier 4b subgroups involving $\%N_X$ and $\%N_Y$ are provided (Fig. 3). However, in many *Type Ib* diamonds, ***X***- and ***Y***-centers occur in subordinate proportions (Day et al. 2026) and where $\%N_X$ and/or $\%N_Y$ are <50 it may still be useful to indicate their presence. This can be done using the suffix "–*X*", "–*Y*" or "–*XY*", for example, a *Type IbCA* diamond with $\%N_Y < 50$ and $\%N_X = 0$ can be described as

Always consult and cite the final published document. See https://msaweb.org/ or GeoScienceWorld

This is the peer-reviewed, final accepted version for American Mineralogist, published by the Mineralogical Society of America.
The published version is subject to change. Cite as Authors (Year) Title. American Mineralogist, in press.
DOI: https://doi.org/10.2138/am-2026-10296. https://msaweb.org/

"*Type IbCA–Y*" or as "*Type IbCA–XY*" if both ***X***- and ***Y***-centers are observed and $\%N_X + \%N_Y < 50$. Alternatively, a diamond with ≥50 $\%N_Y$ (or $\%N_X$) and <50 $\%N_X$ (or $\%N_Y$) can be described similarly, e.g., a *Type IbY* diamond with minor N_X can be classified as "*Type IbY–X*". For example, the decomposition results of a *Type IbY–X* diamond are shown in Fig. 6a and the decomposition results of a *Type IbCA–XY* diamond are shown in Fig. 6b.

As described in "Tier 3", the intensity of several peaks at ~1350–1374 cm^{-1} (Fisher and Lawson 1998; Lai et al. 2020b, 2020a; Day et al. 2026) are positively correlated with N_Y and are attributed to platelet-like, small (self-)interstitial complexes containing interstitial nitrogen (N_i) and carbon (C_i) that may serve as the building blocks for platelets in *Type Ia* diamonds (Humble 1982; Goss et al. 2003, 2004; Day et al. 2026). Inclusion of such features in the updated *Type* classification may be useful to differentiate genetic complexities amongst these N-defects in *Type Ib* and *Type Ib–Ia* diamonds but more work is required before this can be done rigorously.

Type Ia* and *Type Ib–Ia* diamonds with platelets.** Additional Tier 4 subgroups for *Type Ia* and *Type Ib–Ia* diamonds are proposed based on the presence of platelets. Platelets are extremely common in *Type Ia* diamonds and are a type of extended defect consisting of [001] layers of interstitial C_i (Humble 1982) that may contain subordinate amounts of N_i, H and *V* (Humble 1982; Goss et al. 2003; Gu et al. 2020). Platelets produce a characteristic *B*′ peak in the IR between ~1360–1375 cm^{-1}. Speich et al. (2017) provide a detailed description of how the characteristics of this peak change due to platelet density, shape, and size. Most platelet-bearing diamonds contain *regular* platelets where the integrated absorption of the *B*′ peak is positively correlated with absorption due to ***B-centers (i.e., N_B). This correlation is attributed to platelet formation as a bi-product of ***A*** → ***B*** aggregation and the simultaneous generation and accumulation of C_i (via $N_2 + N_2 = N_4V + C_i$) (Woods 1986). However, some diamonds contain *irregular* platelets where the

Always consult and cite the final published document. See https://msaweb.org/ or GeoScienceWorld

This is the peer-reviewed, final accepted version for American Mineralogist, published by the Mineralogical Society of America.
The published version is subject to change. Cite as Authors (Year) Title. American Mineralogist, in press.
DOI: https://doi.org/10.2138/am-2026-10296. https://msaweb.org/

integrated absorption of the *B′* peak is significantly lower than what would be expected based on N_B due to platelet degradation associated with high temperature annealing (Woods 1986; Speich et al. 2017). In fact, HPHT-treatment also acts to broaden (increase the FWHM – full-width-at-half-maximum) of the *B′* peak and can be used to identify treated natural stones (Fisher 2009). A third group, *subregular* platelets, may also have a weaker than expected *B′* peak and smaller platelet sizes than expected for the respective N_B (Speich et al. 2018). We stress that the terms regular, irregular and subregular should only be used to describe platelets and not the platelet-bearing diamonds themselves. Similar terms (i.e., irregular) are frequently used to describe the morphology of diamonds, e.g., CLIPPIR (Cullinan-like, Large, Inclusion-Poor, Pure, Irregular, and Resorbed) diamonds (Smith et al. 2016).

For natural *Type Ia* diamonds, detailed analysis of the *regular, irregular* and *subregular* platelet groups has shown that each group reflects important differences in T_{res} and t_{res} (Speich et al. 2017, 2018). Consequently, *Type* subgroups denoting such differences have been previously proposed (e.g., Zaitsev 2001; Stachel et al. 2022) but are often indicated inconsistently e.g., "*Type IaB′′* and "*Type IaB′ regular*" or with the suffixes "*–B′* " and/or "*–p"*. Following Speich et al. (2018), we propose that the presence or absence of platelets in *Type Ia* diamonds is indicated at the Tier 4 level using the suffixes "*–p*" (platelets) and "*–np*" (no platelets), respectively (Figs. 2 and 3). As the formation of platelets is a by-product of ***A*** → ***B*** aggregation, we restrict this Tier 4 scheme to compositions where $N_B > PQL_B$. In cases where the type of platelet can be identified, the following sub-divisions (and associated suffixes) are proposed:

[1] *regular platelets* are indicated with the suffix "$–p_{reg}$" (e.g., *Type IaB*$–p_{reg}$) and reflect a potentially wide range of T_{res}, typically 1120–1220 °C (Speich et al. 2018).

Always consult and cite the final published document. See https://msaweb.org/ or GeoScienceWorld

This is the peer-reviewed, final accepted version for American Mineralogist, published by the Mineralogical Society of America.
The published version is subject to change. Cite as Authors (Year) Title. American Mineralogist, in press.
DOI: https://doi.org/10.2138/am-2026-10296. https://msaweb.org/

890 [2] *subregular platelets* are indicated with the suffix "–p_{subreg}" (e.g., *Type IaB–*p_{subreg}) and reflect
891 relatively low T_{res} and/or short t_{res} where there is potential for continued platelet growth.

892 [3] *irregular platelets* are indicated with the suffix "–p_{ireg}" (e.g., *Type IaB–*p_{ireg}) and reflect varying
893 degrees of platelet degradation due to relatively high T_{res}.

894 It follows those diamonds with *irregular* platelets (e.g., *Type IaB–*p_{ireg}) form a continuum
895 with those that do not contain platelets (e.g., *Type IaB–np*) reflecting varying degrees of platelet
896 degradation (see Figs. 2 and 3). Speich et al. (2018) calibrated a mantle thermometer based on the
897 degree of platelet degradation allowing calculation of the T_{res} for *Type Ia* diamonds (see equation
898 [13] in Speich et al. 2018). This is particularly useful as only a minimum T_{res} for pure *Type IaB′*
899 diamonds (%N_B = 100) can be calculated using the $\boldsymbol{A} \rightarrow \boldsymbol{B}$ aggregation rate. Although the
900 thermochronometric (geological) applications of platelets may not be useful for treated, natural or
901 synthetic diamond, platelets have been observed in such diamonds (Allen and Evans 1981; Kiflawi
902 et al. 1998; Fisher 2009) and may still provide insights into mechanisms of N-aggregation.
903 Therefore, this scheme may also be used to further describe *Type Ib–Ia* diamonds at the Tier 3b
904 level.

905 To determine the regularity of platelets, the integrated absorption of the *B′* peak (I(*B′*)) can
906 be compared to the thickness normalized absorption due to ***B***-centers (μB where $N_B = 79.4 \times \mu B$)
907 using the relation of Woods (Woods 1986). In Fig. 7a, the one-phonon region of two *Type IaAB*
908 diamonds and one *Type IaB′* diamond is shown. As shown in Fig. 7b, the platelet (*B′*) peak (1364
909 cm^{-1}) of one *Type IaAB* diamond (shown in red) follows the regularity relation of Woods (1986)
910 and therefore this diamond can be classified as *Type IaAB–*p_{reg}. The *B′* peak (1360 cm^{-1}) for the
911 other *Type IaAB* diamond (shown in blue) does not follow the regularity relation and therefore this
912 diamond can be classified as *Type IaAB–*p_{ireg}. Here, the integrated absorbance of the irregular *B′*

Always consult and cite the final published document. See https://msaweb.org/ or GeoScienceWorld

This is the peer-reviewed, final accepted version for American Mineralogist, published by the Mineralogical Society of America.
The published version is subject to change. Cite as Authors (Year) Title. American Mineralogist, in press.
DOI: https://doi.org/10.2138/am-2026-10296. https://msaweb.org/

peak is less than expected based on μB due to platelet degradation. In diamonds where platelets have been completely degraded (typically *Type IaB′*), the *B′* peak is absent as shown by the black spectrum in Fig. 7a.

Using a large dataset of platelet-bearing diamonds, Speich et al. (2018) describe the relation between the *B′* peak position (cm^{-1}) and the integrated absorbance of the *B′* peak (I(*B′*) in cm^{-2}), in addition to the symmetry and FWHM of the *B′* peak, and describe how such relations can be used to determine platelet type. For example, *subregular* platelets cannot be differentiated from *regular* platelets by comparison of I(*B′*) and μB (i.e., using the regularity relations of Woods (1986); Fig. 7b), and instead are identified by comparing I(*B′*) and the platelet peak position (Speich et al. 2018). Here, subregular platelets produce a *B′* at higher wavenumbers (cm^{-1}) than would be expected for a given I(*B′*). As the *B′* peak position is controlled by platelet size, it follows that *subregular* platelets are smaller than *regular* platelets for a given I(*B′*). To rigorously determine the properties of platelets, Speich and Kohn (2020) included a routine in the QUIDDIT program allowing one to produce "quadplots" (e.g., see Speich et al. 2018) in which μB, I(*B′*) and the position (cm^{-1}), symmetry and FWHM of the *B′* are compared. As the relations of different *B′* peak parameters determined by Speich et al. (2018) are based on data collected for single growth zones in polished diamond plates, inspection of quadplots may also reveal sampling of two or more growth zones which can lead to erroneous interpretations (see section "Uncertainty associated with the bulk nature of FTIR spectra").

CO_2-bearing diamonds. Since the early 1990s, a tremendous amount of work has been done characterizing CO_2 in natural and treated diamond using FTIR spectroscopy (e.g., Chinn et al. 1995, 1998; Hainschwang et al. 2006b, 2008; Barannik et al. 2021; Wu et al. 2022). From a geological perspective, such work was driven by the potential of CO_2 in diamond to be used as a

Always consult and cite the final published document. See https://msaweb.org/ or GeoScienceWorld

This is the peer-reviewed, final accepted version for American Mineralogist, published by the Mineralogical Society of America.
The published version is subject to change. Cite as Authors (Year) Title. American Mineralogist, in press.
DOI: https://doi.org/10.2138/am-2026-10296. https://msaweb.org/

barometer as pressure-induced shifts of different CO_2-related modes had been previously calibrated (e.g., Hanson and Jones 1981; Lu and Hofmeister 1995). Schrauder and Navon (1993) were the first to describe shifts in the ν_2 and ν_3 vibrational modes of CO_2 in one diamond and concluded that such CO_2 occurs as solid inclusions as CO_2–ice (CO_2–I) at a residual pressure of ~5 GPa. However, later work has described significant variations in the positions, widths (FWHM) and relative intensities of ν_2 and ν_3 vibrational modes (IR absorption peaks) across single diamond samples (e.g., Fig. 8a,b) (Chinn 1995) that are not compatible with solid (pure) CO_2–I inclusions at different residual pressures (Hainschwang et al. 2006b, 2008). Consequently, a more complex model for CO_2-bearing inclusions (or precipitates) was proposed that invokes the presence of impurities (e.g., H_2O, N_2, CO and other O-related impurities) in CO_2-bearing phases to explain the anomalous variation in the ν_2 and ν_3 absorption peaks (Barannik et al. 2021; Shiryaev et al. 2023). For these reasons, using shifts in the absorption peaks due to CO_2–I in diamond as a barometer may yield erroneous results. However, if Davydov splitting of the ν_2 band is observed one can assume the CO_2–I phase is relatively pure and barometric calibrations will likely yield accurate results (Barannik et al. 2021).

Although classification of different types of CO_2-bearing diamonds has been previously proposed (e.g., "CO_2" vs. "Pseudo CO_2" diamonds, Hainschwang 2003), here, we are simply interested in providing a means by which the presence of CO_2–I can be indicated in the *Type* group for that diamond. For variable pressures of ~5–20 GPa, the IR-active modes for the CO_2–I polymorphs (cubic phase I and orthorhombic phase III) include bending modes ν_{2a} (~649–661 cm^{-1}), ν_{2b} (636–650 cm^{-1}), and the stretching modes ν_{3a} (2368–2438 cm^{-1}), ν_{3b} (2342–2440 cm^{-1}) in addition to higher frequency overtones (Lu and Hofmeister 1995). However, these frequency ranges were determined for pure CO_2–I and as the frequency (peak position) may vary significantly

Always consult and cite the final published document. See https://msaweb.org/ or GeoScienceWorld

This is the peer-reviewed, final accepted version for American Mineralogist, published by the Mineralogical Society of America.
The published version is subject to change. Cite as Authors (Year) Title. American Mineralogist, in press.
DOI: https://doi.org/10.2138/am-2026-10296. https://msaweb.org/

due to pressure and composition, it is not surprising that ν_3 modes reported for CO_2–I in diamond are slightly different, ranging from 2339–2415 cm^{-1} (Chinn 1995; Barannik et al. 2021). Here we suggest that CO_2–I in diamonds be identified through observation of both the ν_2 and ν_3 modes (Fig. 8a,b). The presence of CO_2 can be indicated at the Tier 4 level by using the suffix "–CO_2" following the given Type designation (e.g., *Type IaAB*–CO_2, Fig. 8b). However, some CO_2-rich diamonds (or growth zones) are characterized by anomalous absorption in the one-phonon region that cannot be attributed to known N-defects (Hainschwang et al. 2008) and thus classification down to the Tier 3 level may not always be possible. For example, the one-phonon region of the spectrum in Fig. 8a shows broad anomalous absorption, however a broad peak at 1285 cm^{-1}, likely due to ***A***-centers, allows classification as *Type I*–CO_2. It is advisable to record spectra of CO_2-bearing diamonds in an N-purged atmosphere as the ν_2 and ν_3 vibrational modes of gaseous (atmospheric) CO_2 at 1 atm produce peaks at ~667 and ~2350 cm^{-1}, respectively (Lu and Hofmeister 1995).

Amber centers as an indicator of plastic deformation. Amber centers are commonly observed as a series of broad peaks that typically occur from 3400–4300 cm^{-1} for natural untreated diamonds (Massi et al. 2005; Hainschwang et al. 2020a; Mashkovtsev et al. 2021). However, many other peaks associated with amber centers are observed up to 9000 cm^{-1} where the position of amber centers varies depending on the nature of the diamond (i.e., synthetic, irradiated, (HP)HT-treated, etc.) as observed in Hainschwang et al. (2020a). Amber centers are most commonly observed in natural *Type Ib* (Massi et al. 2005) diamonds but also in natural *Type Ia* diamonds and are more intense in *Type IaA* compared to *Type IaB'* diamonds (Eaton-Magaña et al. 2018; Gu and Wang 2018). Amber centers are not observed in *Type IIa* or *Type IIb* diamonds, they have been produced by neutron irradiation and heat-treatment of natural (Hainschwang et al. 2020a) and

Always consult and cite the final published document. See https://msaweb.org/ or GeoScienceWorld

This is the peer-reviewed, final accepted version for American Mineralogist, published by the Mineralogical Society of America.
The published version is subject to change. Cite as Authors (Year) Title. American Mineralogist, in press.
DOI: https://doi.org/10.2138/am-2026-10296. https://msaweb.org/

CVD (Khomich et al. 2023) diamonds and are observed in heat-treated natural diamond but are typically annealed-out at temperatures > 1900 °C (Eaton-Magaña et al. 2017).

Due to the ubiquity of amber centers in natural brown *Type Ib* diamonds where they are always accompanied by deformation lamellae, often referred to as "brown graining" (e.g., see Fig. 9a) (Hainschwang et al. 2013), the formation of amber centers is attributed to plastic deformation. Based on the absence of amber centers in *Type II* diamonds and their prevalence in diamond with ***A***-centers, Massi et al. (2005) suggested plastic deformation may produce the defective ***A***-center, N_s^0–C–C–N_s^0, that is responsible for amber center absorbance. This suggestion is in accordance with the findings of Newton and Baker (1991a) who described the W7 defect, N_s^0–C–C–N_s^+, that is only observed in plastically deformed brown *Type Ib* diamond with predominately ***A***-centers. To explain the large variability in the position and relative intensity of different amber centers, a more complex defect involving vacancy clusters that contain ***A***- or ***B***-centers was proposed and supported by genetic relationships between the amber centers at ~4063 cm^{-1} and the ***H1b***- and ***H1c***-centers (Hainschwang et al. 2020a). The ***H1b***- and ***H1c***-centers have been interpreted as ***A***- and ***B***-centers coupled with extended vacancy-defects (Table 1) that anneal out together with the 4063 cm^{-1} amber center (Collins et al. 1986; Hainschwang et al. 2020a). The formation of these defects is associated with the production of vacancies or interstitials during irradiation and annealing (Collins et al. 1986). The ***H1b and H1c***-centers produce peaks in the infrared spectrum at 4935 and 5165 cm^{-1}, respectively (Breeding and Ahline 2024). It follows that indicating the presence of these defects may be of use when describing such treated stones, we recommend this is done using the suffixes "*–H1b*" and "*–H1c*", e.g., *Type IbA–H1b/c*. Similar suffixes can be used to describe the presence of ***H1a***-centers which produce a characteristic peak at 1450 cm^{-1}.

Always consult and cite the final published document. See https://msaweb.org/ or GeoScienceWorld

This is the peer-reviewed, final accepted version for American Mineralogist, published by the Mineralogical Society of America.
The published version is subject to change. Cite as Authors (Year) Title. American Mineralogist, in press.
DOI: https://doi.org/10.2138/am-2026-10296. https://msaweb.org/

Plastically deformed, untreated, natural *Type Ib* and *Type Ia* diamonds are characterized by amber centers most commonly observed at 3462, 4063–4065, 4073, 4165–4167 and 4111–4113 cm^{-1} (Eaton-Magaña et al. 2017; Hainschwang et al. 2020a). Hainschwang et al. (2020a) proposed a detailed classification scheme for deformation-related *Type Ib* brown diamonds incorporating different amber centers. However, in this *Type* classification scheme, we are simply interested in indicating the presence of amber centers, and thus plastic-deformation. This can be done at the Tier 4 level (Fig. 3) using the suffix "–Amb_n" where *n* is the position of the observed amber center. For example, in Figs. 9a and 9b, two spectra recorded from a *Type IaA′* diamond with amber centers at 4065 cm^{-1} and a *Type IaAB* diamond with amber centers at 4167 cm^{-1} are shown and can be classified as *Type IaA′*–Amb_{4065} (Fig. 9b) and *Type IaAB*–Amb_{4167} (Fig. 9a), respectively.

Uncertainty associated with the bulk nature of FTIR spectra

Designating a particular *Type* to a given diamond based on a single FTIR spectrum assumes the identity and concentration of N-defects in that diamond is largely homogenous. Of course, this is rarely the case, especially for natural diamonds. Here, we must consider heterogeneity at scales both larger and smaller than that detectable by standard FTIR spectroscopy (i.e., larger and smaller than the volume of diamond sampled by the IR beam).

Fourier-transform IR profiles and maps of natural diamond plates often show complex and/or oscillatory growth zones marked by core-to-rim differences in $\delta^{13}C$ (Smart et al. 2011), different inclusion ages in cores and rims (Rudnick et al. 1993; Wiggers de Vries et al. 2013; Timmerman et al. 2017), and differences in N-content and aggregation state (Kohn et al. 2016). Moreover, irregular (patchy) zoning is also observed in some diamonds where variations in impurities such as H, in addition to N, have been described (e.g., Smit et al. 2018; Day et al. 2025). From a geological perspective, this is particularly important as bulk sampling of two or more

Always consult and cite the final published document. See https://msaweb.org/ or GeoScienceWorld

This is the peer-reviewed, final accepted version for American Mineralogist, published by the Mineralogical Society of America.
The published version is subject to change. Cite as Authors (Year) Title. American Mineralogist, in press.
DOI: https://doi.org/10.2138/am-2026-10296. https://msaweb.org/

growth zones will produce a volume-averaged N-aggregation state and erroneous mantle residence temperatures/times (Kohn et al. 2016). Zoning is also commonly observed in in synthetic HPHT diamonds in the form of dominant cubic and octahedral growth sectors which preferentially incorporate different impurities and as a result, are often observed as different coloured zones (Eaton-Magaña et al. 2017). Similarly, natural mixed-habit diamonds contain cuboid and octahedral growth sectors with distinct colouration, transparency, or impurity levels (Harris et al. 2023). In CVD diamond, smaller scale striations (or banding), related to layered growth, are commonly observed (Eaton-Magana and Shigley 2016) and influence the distribution of N-defects, particularly in N-doped CVD diamond (Zaitsev et al. 2020; Zhang et al. 2024). Where possible, imaging and spectroscopic analyses of polished diamond plates may allow identification of different zones (sectors) and *Type* classification of each zone (e.g., a *Type IaA'* core surrounded by a *Type IbA* rim). However, laborious sample preparation (polished plates) and preliminary imaging is not always possible nor practical for large sample suites. In such cases, the *Type* group assigned to a given diamond may not be representative of the entire diamond and, depending on the scale of heterogeneity, may reflect an averaged concentration of N-defects and N-aggregation states. Even if spectra are collected from singular growth zones or sectors, the resultant data are inevitably "bulk" in nature as it is likely that the distribution of N/*V*/H-defects, in terms of both concentrations and identity, is heterogenous at scales far below the spatial resolution of standard FTIR spectroscopy (at best 10 μm, typically 100 μm). For samples that are not doubly flat-polished (i.e., faceted or natural unpolished samples) the optical absorption path cannot be reliably determined and one should be aware of spectral irregularities that may occur due to variable degrees of scattering and/or reflection of IR light.

Always consult and cite the final published document. See https://msaweb.org/ or GeoScienceWorld

This is the peer-reviewed, final accepted version for American Mineralogist, published by the Mineralogical Society of America.
The published version is subject to change. Cite as Authors (Year) Title. American Mineralogist, in press.
DOI: https://doi.org/10.2138/am-2026-10296. https://msaweb.org/

Due to the complex and ubiquitous nature of zoning in both natural and synthetic diamonds (as described above), the *Type* classification scheme should be considered as a method by which one can assign a *Type* name to a spectrum (i.e., the 3D volume of diamond sampled by the IR beam) rather than the entire individual diamond from which that spectrum was recorded. A single *Type* name can only be reliably assigned to an entire diamond where flat polishing, imaging (e.g., CL) and spectroscopic mapping confirm that such a diamond is homogenous in terms of the concentration and aggregation state of N-defects. For example, consider the *Type IIb* diamond shown in Fig. 10a which contains a small concentrically zoned *Type IaB* region (bright region in Fig. 10b). If a bulk FTIR spectrum of this entire diamond were recorded (the IR beam samples the entirety of the diamond), boron and ***A***-/***B***-centers from both regions would contribute to the composite signals observed in the IR and standard decomposition would allow classification as *Type IaB–NB* (see Fig. 3). However, it is likely that by using a smaller (and more realistic) aperture size, spectra could sample exclusively the boron-bearing or N-bearing regions resulting in classification as *Type IIb* or *Type IaB*, respectively. Here, the *Type IIb* or *Type IaB* designations aptly describe the corresponding spectrum but not the entirety of the diamond. The *Type IaB–NB* designation indicates the presence of both boron and ***A***-/***B***-centers, but contains no information about the distribution of such defects (i.e., that N is not homogenously distributed throughout the diamond). In general, one should never assume a single spectrum is representative of the entire corresponding diamond and where possible, imaging or spectroscopic mapping should be performed to identify zonation.

In terms of systematic error, appropriate baseline and background corrections and thickness normalization routines, in addition to high signal-to-noise ratios, are critical to ensure accurate N-defect concentrations are obtained. These processes have been standardized through the use of

Always consult and cite the final published document. See https://msaweb.org/ or GeoScienceWorld

This is the peer-reviewed, final accepted version for American Mineralogist, published by the Mineralogical Society of America.
The published version is subject to change. Cite as Authors (Year) Title. American Mineralogist, in press.
DOI: https://doi.org/10.2138/am-2026-10296. https://msaweb.org/

spreadsheets (e.g., DiaMap and *Caxbd_Inherit_2024-Ib*, Howell et al. 2012a, 2012b; Day et al. 2026) and the QUIDDIT program (Speich and Kohn 2020) increasing consistency amongst different samples and sample suites processed by different researchers. Errors are typically assumed to be 10–15%, but determining the errors in the concentration and aggregation state of N due to the uncertainties associated with the calibration coefficients for ***C***-, ***A***- and ***B***-centers are not incorporated in the data reduction spreadsheets and should be considered in future work. Moreover, aspects of spectral resolution are often overlooked when automated decomposition is performed. For example, sample and reference spectra should be recorded at the same resolution (e.g., 2 cm^{-1}) as calibration coefficients for particular absorption peaks (e.g., 1344 cm^{-1}) for some N-defects (e.g., ***C***-centers) are dependant on the spectral resolution (Liggins 2010).

Implications

The basis of the historical *Type* classification scheme for diamond, based on N-defects, was proposed ~100 years ago by Robertson et al. (1934, 1936) and systematized ~60 years ago by Dyer et al. (1965). Since then, our understanding of the common N-defects (***C***-, ***A***- and ***B***-centers), and several new defects (e.g., ***Y***-centers), in addition to other IR-active features (e.g., platelets, CO_2 inclusions, amber centers, etc.), has outgrown the constraints of the historical classification scheme. Consequently, authors from a variety of disciplines often modify the definitions and the names of each *Type* group to suit their purposes or produce classification schemes for specific groups of diamonds (e.g., deformation and non-deformation related brown diamonds, (Hainschwang et al. 2020a,b). Moreover, the lack of formally defined *Type* groups, differences in the methods used to calculate N-aggregation states, and use of both quantitative (using decomposition) and qualitative (visual estimates) determination of relative concentrations of different N-defects, has led to a body of literature where *Type* designations can be ambiguous or

Always consult and cite the final published document. See https://msaweb.org/ or GeoScienceWorld

This is the peer-reviewed, final accepted version for American Mineralogist, published by the Mineralogical Society of America.
The published version is subject to change. Cite as Authors (Year) Title. American Mineralogist, in press.
DOI: https://doi.org/10.2138/am-2026-10296. https://msaweb.org/

ill-defined. To remedy this issue, a simplified classification scheme, applicable to most natural untreated diamonds (Figs. 1 and 2), is provided and is appropriate for most geological purposes (i.e., the application of thermochronometric methods) and for basic and efficient classification of diamonds. An extended *Type* classification scheme (Fig. 3) is also provided for more detailed classification where high-quality spectra allow rigorous decomposition to be completed. This detailed scheme is applicable to a wider variety of natural, synthetic and treated diamonds such that particular defects (impurities) of interest in gemological and materials science (physics) studies can also be described using the *Type* classification scheme.

To accommodate classification based on spectra of variable quality, e.g., due to thick samples with high N concentrations leading to saturation and erroneous N-defect determination (see section "Tiers 1 and 2"), the *Type* classification scheme is structured using four *Tiers*. Each Tier represents a requirement for increasing spectral quality and the consequent amount (accuracy) of information than can be extracted from such spectra. Here, rigorous divisions between *Type* groups are described, namely *Type I* and *Type II* diamonds where the *practical quantitation limit* (PQL) and *instrumental detection limit* (IDL) of different N-defects in the IR are used. New *Type* group criteria are proposed for *Type Ib* diamonds and several new *Type* groups are described for *Type Ib* diamonds with ***X***- and ***Y***-centers (e.g., *Type IbCA–XY* and *Type IbY–X*). The thermometric systematics of diamonds with exclusively ***A***-centers (~100 $\%N_A$ or ~0 $\%N_B$) and exclusively ***B***-centers (~100 $\%N_B$ or ~0 $\%N_A$) are used to justify the addition of the *Type IaA′* and *Type IaB′* group to the updated *Type* classification scheme. *Type IaB′* diamonds express the end-state of normal N-aggregation processes and represent the majority of super-deep diamonds that form (and reside) at relatively high temperatures in the sublithospheric mantle. Natural *Type IaA′* diamonds reside in the mantle at sufficiently low T_{res} (for a given t_{res}) such that $\boldsymbol{A} \rightarrow \boldsymbol{B}$ aggregation proceeds

Always consult and cite the final published document. See https://msaweb.org/ or GeoScienceWorld

This is the peer-reviewed, final accepted version for American Mineralogist, published by the Mineralogical Society of America.
The published version is subject to change. Cite as Authors (Year) Title. American Mineralogist, in press.
DOI: https://doi.org/10.2138/am-2026-10296. https://msaweb.org/

at negligible rates, effectively halting N-aggregation after $\boldsymbol{C \rightarrow A}$ aggregation is complete. This process explains the disproportionately high number of *Type IaA′* diamonds observed in nature and may point towards relatively lower N_{tot} and T_{res} and/or shorter t_{res} for *Type IaA′* diamonds in general and/or particular geological/geothermal residence conditions associated with localities where *Type IaA′* diamonds are over-represented.

Additional Tier 2 groups have been added to the classification scheme to describe diamonds with total concentrations of IR-active N and B above the IDL such that they can be differentiated from *Type IIb* diamonds. At the Tier 4 level, groups describing the presence and type of platelets, CO_2–I inclusions, and plastic deformation in the form of amber centers, have been included. In recent years, the use of large diamond databases to advance our understanding of diamond formation, growth, and material properties has become commonplace; therefore, it is crucial that clear and informative *Type* group designations be included in these databases.

Always consult and cite the final published document. See https://msaweb.org/ or GeoScienceWorld

This is the peer-reviewed, final accepted version for American Mineralogist, published by the Mineralogical Society of America.
The published version is subject to change. Cite as Authors (Year) Title. American Mineralogist, in press.
DOI: https://doi.org/10.2138/am-2026-10296. https://msaweb.org/

Funding. This work was funded by the European Union (ERC, INHERIT, Starting Grant No.101041620). Views and opinions expressed are, however, those of the author(s) only and do not necessarily reflect those of the European Union or the European Research Council Executive Agency. Neither the European Union nor the granting authority can be held responsible for them.

Declaration of competing interest. The authors have no financial interests and have no other conflicts of interest to disclose. The authors confirm that this work is original and has not been published elsewhere, nor is it currently under consideration for publication elsewhere.

Data Availability – Appendices A and B. The online version contains Supplementary Material (Appendices A and B) available at https://XXXX. Supplementary Material can also be accessed from the University of Padova repository at https://XXXX (*link to be provided after acceptance*). All data is also available upon request to Maxwell C. Day.

Acknowledgements. We thank Stefano Castelli for assistance taking photographs of diamond specimens used in this work and Simone Molinari for providing samples from the mineral collection at the Museum of Nature and Humankind, University of Padova.

Always consult and cite the final published document. See https://msaweb.org/ or GeoScienceWorld

This is the peer-reviewed, final accepted version for American Mineralogist, published by the Mineralogical Society of America.
The published version is subject to change. Cite as Authors (Year) Title. American Mineralogist, in press.
DOI: https://doi.org/10.2138/am-2026-10296. https://msaweb.org/

References

Achard, J., Jacques, V., and Tallaire, A. (2020) Chemical vapour deposition diamond single crystals with nitrogen-vacancy centres: a review of material synthesis and technology for quantum sensing applications. Journal of Physics D: Applied Physics, 53, 313001.

Allen, B.P., and Evans, T. (1981) Aggregation of nitrogen in diamond, including platelet formation. Proceedings of the Royal Society of London. A. Mathematical and Physical Sciences, 375, 93–104.

Anderson, B.W. (1961) Some notes on an important discovery: Nitrogen in diamond. The Gemmologist, 30, 21–22.

Ashfold, M.N.R., Goss, J.P., Green, B.L., May, P.W., Newton, M.E., and Peaker, C. V. (2020) Nitrogen in Diamond. Chemical Reviews, 120, 5745–5794.

Aulbach, S., Stachel, T., Seitz, H.-M., and Brey, G.P. (2012) Chalcophile and siderophile elements in sulphide inclusions in eclogitic diamonds and metal cycling in a Paleoproterozoic subduction zone. Geochimica et Cosmochimica Acta, 93, 278–299.

Banas, A., Stachel, T., Muehlenbachs, K., and McCandless, T.E. (2007) Diamonds from the Buffalo Head Hills, Alberta: Formation in a non-conventional setting. Lithos, 93, 199–213.

Barannik, E.P., Shiryaev, A.A., and Hainschwang, T. (2021) Shift of CO2-I absorption bands in diamond: A pressure or compositional effect? A FTIR mapping study. Diamond and Related Materials, 113, 108280.

Blackwell, D.E., and Sutherland, G.B.B.M. (1949) The vibrational spectrum of diamond. Journal de Chimie Physique, 46, 9–15.

Borenstein, G., and O'Neal, S. (2021) Rare Mixed Type IaB-IIb Diamond with a Long-Lasting Phosphorescence. Gems & Gemology, 57, 177–178.

Boyd, S.R., Kiflawi, I., and Woods, G.S. (1994) The relationship between infrared absorption and the A defect concentration in diamond. Philosophical Magazine B, 69, 1149–1153.

——— (1995) Infrared absorption by the B nitrogen aggregate in diamond. Philosophical Magazine B, 72, 351–361.

Breeding, C.M., and Shigley, J.E. (2009) The "Type" Classification System of Diamonds and Its Importance in Gemology. Gems & Gemology, 45, 96–111.

Breeding, C.M., Eaton-Magaña, S., and Shigley, J.E. (2020) Naturally Colored Yellow and Orange Gem Diamonds: The Nitrogen Factor. Gems & Gemology, 56, 194–219.

Breeding, C.M., and Ahline, N.J. (2024) Infrared Spectroscopy and Its Use in Gemology. Gems & Gemology, 60, 474–492.

Always consult and cite the final published document. See https://msaweb.org/ or GeoScienceWorld

This is the peer-reviewed, final accepted version for American Mineralogist, published by the Mineralogical Society of America.
The published version is subject to change. Cite as Authors (Year) Title. American Mineralogist, in press.
DOI: https://doi.org/10.2138/am-2026-10296. https://msaweb.org/

Brozel, M.R., Evans, T., and Stephenson, R.F. (1978) Partial Dissociation of Nitrogen Aggregates in Diamond by High Temperature-High Pressure Treatments. Proceedings of the Royal Society of London. Series A, Mathematical and Physical Sciences, 361, 109–127.

Bulanova, G.P., Pearson, D.G., Hauri, E.H., and Griffin, B.J. (2002) Carbon and nitrogen isotope systematics within a sector-growth diamond from the Mir kimberlite, Yakutia. Chemical Geology, 188, 105–123.

Bulanova, G.P., Smith, C.B., Kohn, S.C., and Speich, L. (2017) Natural diamond growth conditions recorded by their internal structures. International Kimberlite Conference: Extended Abstracts, 11.

Carvalho, L.D.V., Doyle, B., Stachel, T., Stern, R., Steele-MacInnis, M., Nestola, F., and Pearson, D.G. (2025) The Sequoia kimberlite complex, central Slave Craton – A new superdeep diamond location. Mineralogy and Petrology.

Caticha-Ellis, S., and Cochran, W. (1958) The X-ray diffraction spikes of diamond. Acta Crystallographica, 11, 245–249.

Chan, N., and Pradhan, S. (2025) Type IIa/IaB Diamond Showing Transient Type IIb Responses. Gems & Gemology, 61, 295–296.

Charette, J.J. (1961) Essai de classification des bandes d'absorption infrarouge du diamant. Physica, 27, 1061–1073.

Chinn, I. (1995) A Study of Unusual Diamonds From the George Creek K1 Kimberlite Dyke, Colorado. Ph.D., University of Cape Town.

Chinn, I.L., Gurney, J.J., Milledge, H.J., Taylor, W.R., and Woods, P.A. (1995) Cathodoluminescence of CO2-bearing and CO2-free diamonds from the George Creek K1 kimberlite dyke, Colorado-Wyoming state line district. International Kimberlite Conference abstract.

Chinn, I.L., McCallum, M.E., Harris, C., Milledge, H.J., and Gurney, J.J. (1998) CO2-bearing diamonds in eclogite xenoliths from the Sloan 2 kimberlite, Colorado. International Kimberlite Conference abstract.

Chrenko, R.M. (1973) Boron, the Dominant Acceptor in Semiconducting Diamond. Physical Review B, 7, 4560–4567.

Chrenko, R.M., Strong, H.M., and Tuft, R.E. (1971) Dispersed paramagnetic nitrogen content of large laboratory diamonds. Philosophical Magazine, 23, 313–318.

Chrenko, R.M., Tuft, R.E., and Strong, H.M. (1977) Transformation of the state of nitrogen in diamond. Nature, 270, 141–144.

Clark, C.D., and Davey, S.T. (1984) One-phonon infrared absorption in diamond. Journal of Physics C: Solid State Physics, 17.

Always consult and cite the final published document. See https://msaweb.org/ or GeoScienceWorld

This is the peer-reviewed, final accepted version for American Mineralogist, published by the Mineralogical Society of America.
The published version is subject to change. Cite as Authors (Year) Title. American Mineralogist, in press.
DOI: https://doi.org/10.2138/am-2026-10296. https://msaweb.org/

Clark, C.D., Ditchburn, R.W., and Dyer, H.B. (1956a) The absorption spectra of irradiated diamonds after heat treatment. Proceedings of the Royal Society of London. Series A. Mathematical and Physical Sciences, 237, 75–89.

Clark, C. D., Ditchburn, R.W., and Dyer, H.B. (1956b) The absorption spectra of natural and irradiated diamonds. Proceedings of the Royal Society of London. Series A. Mathematical and Physical Sciences, 234, 363–381.

Collins, A.T. (1997) The electronic and optical properties of diamond. The Physics of Diamond, Ios Press, 273–354.

Collins, A.T., Davies, G., and Woods, G.S. (1986) Spectroscopic studies of the H1b and H1c absorption lines in irradiated, annealed type-Ia diamonds. Journal of Physics C: Solid State Physics, 19, 3933–3944.

Collins, A.T., Kanda, H., and Kitawaki, H. (2000) Colour changes produced in natural brown diamonds by high-pressure, high-temperature treatment. Diamond and Related Materials, 9, 113–122.

Cooper, G.I. (1990) Infra-red microspectroscopy of diamond in relation to mantle processes. Ph.D., University College London.

Cox, A., Newton, M.E., and Baker, J.M. (1992) ENDOR studies on the N1 di-nitrogen centre in diamond. Journal of Physics: Condensed Matter, 4, 8119–8130.

Coxon, D.J.L., Staniforth, M., Breeze, B.G., Greenough, S.E., Goss, J.P., Monti, M., Lloyd-Hughes, J., Stavros, V.G., and Newton, M.E. (2020) An Ultrafast Shakedown Reveals the Energy Landscape, Relaxation Dynamics, and Concentration of the N_3VH^0 Defect in Diamond. The Journal of Physical Chemistry Letters, 11, 6677–6683.

Curtolo, A., Novella, D., Logvinova, A., Sobolev, N. V., Davies, R.M., Day, M.C., Pamato, M.G., and Nestola, F. (2023) Petrology and geochemistry of Canadian diamonds: An up-to-date review. Earth-Science Reviews, 246, 104588.

Custers, J.F.H. (1952) Unusual phosphorescence of a diamond. Physica, 18, 489–493.

——— (1954) Letter to the Editor: Type IIb diamonds. Physica, 20, 183–184.

Davies, G (1977) Charge states of the vacancy in diamond. Nature, 269, 498–500.

Davies, G. (1977) The optical properties of diamond. In P.A. Thrower and P.L. Walker Jr., Eds., Chemistry and physics of carbon Vol. 13, pp. 1–143. Marcel Dekker, New York.

——— (1981) Decomposing the IR absorption spectra of diamonds. Nature, 290, 40–41.

Day, M.C., Pamato, M.G., Novella, D., and Nestola, F. (2023) Imperfections in natural diamond: the key to understanding diamond genesis and the mantle. La Rivista del Nuovo Cimento, 46, 381–471.

Always consult and cite the final published document. See https://msaweb.org/ or GeoScienceWorld

This is the peer-reviewed, final accepted version for American Mineralogist, published by the Mineralogical Society of America.
The published version is subject to change. Cite as Authors (Year) Title. American Mineralogist, in press.
DOI: https://doi.org/10.2138/am-2026-10296. https://msaweb.org/

Day, M.C., Jollands, M.C., Novella, D., Nestola, F., Dovesi, R., and Pamato, M.G. (2024) Hydrogen-related defects in diamond: A comparison between observed and calculated FTIR spectra. Diamond and Related Materials, 143, 110866.

Day, Maxwell C., Balan, E., Caracas, R., Jollands, M.C., Innocenzi, F., Novella, D., Nestola, F., and Pamato, M.G. (2025) The first-formed hydrogen and nitrogen defects in natural diamond. Diamond and Related Materials, 158, 112654.

Day, M.C., Jollands, M.C., Innocenzi, F., Novella, D., Nestola, F., and Pamato, M.G. (2026) Infrared spectroscopy of natural Type Ib + IaA diamond: insights into the formation of Y-centers and the early aggregation of nitrogen. American Mineralogist, 111, 360-375.

Deines, P., Stachel, T., and Harris, J.W. (2009) Systematic regional variations in diamond carbon isotopic composition and inclusion chemistry beneath the Orapa kimberlite cluster, in Botswana. Lithos, 112, 776–784.

Dischler, B. (2012) Handbook of Spectral Lines in Diamond. Handbook of Spectral Lines in Diamond.

Dobrzhinetskaya, L.F., Wirth, R., Yang, J., Hutcheon, I.D., Weber, P.K., and Green, H.W. (2009) High-pressure highly reduced nitrides and oxides from chromitite of a Tibetan ophiolite. Proceedings of the National Academy of Sciences, 106, 19233–19238.

Donnelly, C.L., Stachel, T., Creighton, S.., Muehlenbachs, K., and Whiteford, S. (2007) Diamonds and their mineral inclusions from the A154 South pipe, Diavik Diamond Mine, Northwest territories, Canada. Lithos, 98, 160–176.

Dyer, H.B., Raal, F.A., Du Preez, L., and Loubser, J.H.N. (1965) Optical absorption features associated with paramagnetic nitrogen in diamond. Philosophical Magazine, 11, 763–774.

Eaton-Magaña, S., and Ardon, T. (2016) Temperature effects on luminescence centers in natural type IIb diamonds. Diamond and Related Materials, 69, 86–95.

Eaton-Magaña, S., and Shigley, J.E. (2016) Observations on CVD-Grown Synthetic Diamonds: A Review. Gems & Gemology, 52, 222–245.

Eaton-Magaña, S., Ardon, T., and Zaitsev, A.M. (2017) LPHT annealing of brown-to-yellow type Ia diamonds. Diamond and Related Materials, 77, 159–170.

Eaton-Magaña, S., Ardon, T., Smit, K.V., Breeding, C.M., and Shigley, J.E. (2018) Natural-Color Pink, Purple, Red, and Brown Diamonds: Band of Many Colors. Gems & Gemology, 54, 352–377.

Eaton-Magaña, S., Ardon, T., Breeding, C.M., and Shigley, J.E. (2020) Natural-Color D-to-Z Diamonds: A Crystal-Clear Perspective. Gems & Gemology, 56, 318–335.

Etmimi, K.M., Ahmed, M.E., Briddon, P.R., Goss, J.P., and Gsiea, A.M. (2009) Nitrogen-pair paramagnetic defects in diamond: A density functional study. Physical Review B, 79, 205207.

Always consult and cite the final published document. See https://msaweb.org/ or GeoScienceWorld

This is the peer-reviewed, final accepted version for American Mineralogist, published by the Mineralogical Society of America.
The published version is subject to change. Cite as Authors (Year) Title. American Mineralogist, in press.
DOI: https://doi.org/10.2138/am-2026-10296. https://msaweb.org/

1295 Evans, T., and Phaal, C. (1962) Imperfections in type I and type II diamonds. Proceedings of the
1296 Royal Society of London. Series A. Mathematical and Physical Sciences, 270, 538–552.

1297 Evans, T., and Qi, Z. (1982) The Kinetics of the Aggregation of Nitrogen Atoms in Diamond.
1298 Proceedings of the Royal Society of London. Series A, Mathematical and Physical
1299 Sciences, 381, 159–178.

1300 Fisher, D. (2009) Brown diamonds and high pressure high temperature treatment. Lithos, 112,
1301 619–624.

1302 Fisher, D., and Lawson, S.C. (1998) The effect of nickel and cobalt on the aggregation of
1303 nitrogen in diamond. Diamond and Related Materials, 7, 299–304.

1304 Frank, F.C. (1956) On the X-ray diffraction spikes of diamond. Proceedings of the Royal Society
1305 of London. Series A. Mathematical and Physical Sciences, 237, 168–174.

1306 Gaillou, E., Post, J.E., Rost, D., and Butler, J.E. (2012) Boron in natural type IIb blue diamonds:
1307 Chemical and spectroscopic measurements. American Mineralogist, 97, 1–18.

1308 Gibbons, R.D., Grams, N.E., Jarke, F.H., and Stoub, K.P. (1991) Practical quantitation limits.
1309 Chemometrics and Intelligent Laboratory Systems, 12, 225–235.

1310 Goss, J.P., Coomer, B.J., Jones, R., Fall, C.J., Briddon, P.R., and Öberg, S. (2003) Extended
1311 defects in diamond: The interstitial platelet. Physical Review B - Condensed Matter and
1312 Materials Physics, 67.

1313 Goss, J.P., Briddon, P.R., Papagiannidis, S., and Jones, R. (2004) Interstitial nitrogen and its
1314 complexes in diamond. Physical Review B, 70, 235208.

1315 Goss, J.P., Briddon, P.R., Hill, V., Jones, R., and Rayson, M.J. (2014) Identification of the
1316 structure of the 3107 cm-1 H-related defect in diamond. Journal of Physics: Condensed
1317 Matter, 26, 145801.

1318 Green, B.L., Collins, A.T., and Breeding, C.M. (2022) Diamond Spectroscopy, Defect Centers,
1319 Color, and Treatments. In Reviews in Mineralogy and Geochemistry Vol. 88.

1320 Gu, T., and Wang, W. (2018) Optical defects in milky type IaB diamonds. Diamond and Related
1321 Materials, 89, 322–329.

1322 Gu, T., Ritterbex, S., Tsuchiya, T., and Wang, W. (2020) Novel configurations of VN4 and
1323 VN4H defects in diamond platelets: Structure, energetics and vibrational properties.
1324 Diamond and Related Materials, 108, 107957.

1325 Hainschwang, T. (2003) Classification and Color Origin of Brown Diamonds . DUG dissertation,
1326 France.

1327 Hainschwang, T. (2014) Diamants de type Ib: Relations entre les propriétés physiques et
1328 gemmologiques des diamants contenant de l’azote isolé . PhD Thesis, Université de Nantes,
1329 Nantes.

Always consult and cite the final published document. See https://msaweb.org/ or GeoScienceWorld

This is the peer-reviewed, final accepted version for American Mineralogist, published by the Mineralogical Society of America.
The published version is subject to change. Cite as Authors (Year) Title. American Mineralogist, in press.
DOI: https://doi.org/10.2138/am-2026-10296. https://msaweb.org/

Hainschwang, T., Simic, D., Fritsch, E., Deljanin, B., Woodring, S., and DelRe, N. (2005) A Gemological Study of A Collection of Chameleon Diamonds. Gems & Gemology, 41, 20–34.

Hainschwang, T., Notari, F., Fritsch, E., and Massi, L. (2006a) Natural, untreated diamonds showing the A, B and C infrared absorptions ("ABC diamonds"), and the H2 absorption. Diamond and Related Materials, 15, 1555–1564.

Hainschwang, T, Notari, F., Fritsch, E., Massi, L., Breeding, C.M., and Rondeau, B. (2006b) Natural CO2-rich Colored Diamonds. Gems & Gemology, 42.

Hainschwang, T., Notari, F., Fritsch, E., Massi, L., Rondeau, B., Breeding, C.M., and Vollstaedt, H. (2008) HPHT treatment of CO2 containing and CO2-related brown diamonds. Diamond and Related Materials, 17, 340–351.

Hainschwang, T., Fritsch, E., Notari, F., and Rondeau, B. (2012) A new defect center in type Ib diamond inducing one phonon infrared absorption: The Y center. Diamond and Related Materials, 21, 120–126.

Hainschwang, T., Fritsch, E., Notari, F., Rondeau, B., and Katrusha, A. (2013) The origin of color in natural C center bearing diamonds. Diamond and Related Materials, 39, 27–40.

Hainschwang, T., Notari, F., and Pamies, G. (2020a) A Defect Study and Classification of Brown Diamonds with Deformation-Related Color. Minerals, 10, 903.

——— (2020b) A Defect Study and Classification of Brown Diamonds with Non-Deformation-Related Color. Minerals, 10, 914.

Hanson, R.C., and Jones, L.H. (1981) Infrared and Raman studies of pressure effects on the vibrational modes of solid CO2. The Journal of Chemical Physics, 75, 1102–1112.

Hardman, M.F., Lai, M.Y., Breeding, C.M., Eaton-Magaña, S.C., and Schwartz, V.A. (2025) A statistical evaluation of the spectroscopic features in natural diamonds with the 480 nm absorption band. Diamond and Related Materials, 155, 112277.

Harlow, G.E. (1998) The Nature of Diamonds, 1st ed., 1–278 p. Cambridge University Press, Cambridge, UK.

Harris, J.W., Hawthorne, J.B., Oosterveld, M.M., and Wehmeyer, E. (1975) A classification scheme for diamond and a comparative study of South African diamond characteristics. Physics and Chemistry of the Earth, 9, 765–783.

Harris, J.W., Smit, K. V., Fedortchouk, Y., and Moore, M. (2023) Morphology of Monocrystalline Diamond and its Inclusions. In Diamond: Genesis, Mineralogy and Geochemistry.

Heaman, L.M., Phillips, D., and Pearson, G. (2019) Dating Kimberlites: Methods and Emplacement Patterns Through Time. Elements, 15, 399–404.

Always consult and cite the final published document. See https://msaweb.org/ or GeoScienceWorld

This is the peer-reviewed, final accepted version for American Mineralogist, published by the Mineralogical Society of America.
The published version is subject to change. Cite as Authors (Year) Title. American Mineralogist, in press.
DOI: https://doi.org/10.2138/am-2026-10296. https://msaweb.org/

Howell, D., O'Neill, C.J., Grant, K.J., Griffin, W.L., O'Reilly, S.Y., Pearson, N.J., Stern, R.A., and Stachel, T. (2012a) Platelet development in cuboid diamonds: insights from micro-FTIR mapping. Contributions to Mineralogy and Petrology, 164, 1011–1025.

Howell, D., O'Neill, C.J., Grant, K.J., Griffin, W.L., Pearson, N.J., and O'Reilly, S.Y. (2012b) μ-FTIR mapping: Distribution of impurities in different types of diamond growth. Diamond and Related Materials, 29.

Humble, P. (1982) The structure and mechanism of formation of platelets in natural type Ia diamond. Proceedings of the Royal Society of London. A. Mathematical and Physical Sciences, 381, 65–81.

Jones, R., Briddon, P.R., and Öberg, S. (1992) First-principles theory of nitrogen aggregates in diamond. Philosophical Magazine Letters, 66, 67–74.

Kaiser, W., and Bond, W.L. (1959) Nitrogen, A Major Impurity in Common Type I Diamond. Physical Review, 115, 857–863.

Kaminsky, F. V., Polyakov, V.B., Ber, B.Ya., Kazantsev, D.Yu., Khachatryan, G.K., and Shilobreeva, S.N. (2024) Hydrogen in natural diamond: Quantification of N3VH defects using SIMS and FTIR data. Chemical Geology, 661, 122185.

Keat, T.J., Coxon, D.J.L., Cruddace, R.J., Stavros, V.G., Newton, M.E., and Lloyd-Hughes, J. (2024) The 3237 cm−1 diamond defect: Ultrafast vibrational dynamics, concentration calibration, and relationship to the N3VH0 defect. Diamond and Related Materials, 141, 110661.

Kempe, Y., Remennik, S., Tschauner, O., Navon, O., Holland, T.J.B., and Weiss, Y. (2025) Redox state of the deep upper mantle recorded by nickel-rich diamond inclusions. Nature Geoscience.

Khomich, A.A., Khmelnitskii, R., Kozlova, M., Khomich, A. V., and Ralchenko, V. (2023) IR Spectroscopy of Vacancy Clusters (Amber Centers) in CVD Diamonds Nanostructured by Fast Neutron Irradiation. Journal of Carbon Research, 9, 55.

Kiflawi, I., and Bruley, J. (2000) The nitrogen aggregation sequence and the formation of voidites in diamond. Diamond and Related Materials, 9, 87–93.

Kiflawi, I., Mayer, A.E., Spear, P.M., Van Wyk, J.A., and Woods, G.S. (1994) Infrared absorption by the single nitrogen and A defect centres in diamond. Philosophical Magazine B, 69, 1141–1147.

Kiflawi, I., Kanda, H., Fisher, D., and Lawson, S.C. (1997) The aggregation of nitrogen and the formation of A centres in diamonds. Diamond and Related Materials, 6, 1643–1649.

Kiflawi, I., Bruley, J., Luyten, W., and Van Tendeloo, G. (1998) 'Natural' and 'man-made' platelets in type-Ia diamonds. Philosophical Magazine B, 78, 299–314.

Always consult and cite the final published document. See https://msaweb.org/ or GeoScienceWorld

This is the peer-reviewed, final accepted version for American Mineralogist, published by the Mineralogical Society of America.
The published version is subject to change. Cite as Authors (Year) Title. American Mineralogist, in press.
DOI: https://doi.org/10.2138/am-2026-10296. https://msaweb.org/

Klyuev, Y.A., Nepsha, V.I., Dudenkov, Y.A., Zvonkov, S.D., and Zubkov, V.M. (1972) Absorption spectra of diamonds of different types. Dokl. Akad. Nauk SSSR, 203, 1054–1057.

Kohn, S.C., Speich, L., Smith, C.B., and Bulanova, G.P. (2016) FTIR thermochronometry of natural diamonds: A closer look. Lithos, 265.

Kupriyanov, I.N., Palyanov, Y.N., Kalinin, A.A., and Shatsky, V.S. (2020) Effect of HPHT Treatment on Spectroscopic Features of Natural Type Ib-IaA Diamonds Containing Y Centers. Crystals, 10, 378.

Kurdumov, A. V., Malogolovets, V.G., and Novikov, N.V. et al. (1994) Polymorphous modification of carbon and boron nitride. Metallurgija, Moscow (in Russian).

Kvasnytsya, V.M., and Kaminsky, F. V. (2021) Unusual green Type Ib–Iab Dniester–type diamond from Ukrainian placers. Mineralogy and Petrology, 115, 149–160.

Lai, M.Y., Breeding, C.M., Stachel, T., and Stern, R.A. (2020a) Spectroscopic features of natural and HPHT-treated yellow diamonds. Diamond and Related Materials, 101, 107642.

Lai, M.Y., Stachel, T., Breeding, C.M., and Stern, R.A. (2020b) Yellow diamonds with colourless cores – evidence for episodic diamond growth beneath Chidliak and the Ekati Mine, Canada. Mineralogy and Petrology, 114, 91–103.

Lai, M.Y., Hardman, M.F., Eaton-Magaña, S., Breeding, C.M., Schwartz, V.A., and Collins, A.T. (2024) Spectroscopic characterization of diamonds colored by the 480 nm absorption band. Diamond and Related Materials, 142, 110825.

Lawson, S.C., and Kanda, H. (1993) An annealing study of nickel point defects in high-pressure synthetic diamond. Journal of Applied Physics, 73, 3967–3973.

Lawson, S.C., Fisher, D., Hunt, D.C., and Newton, M.E. (1998) On the existence of positively charged single-substitutional nitrogen in diamond. Journal of Physics: Condensed Matter, 10, 6171–6180.

Leahy, K., and Taylor, W.R. (1997) The influence of the Glennie domain deep structure on the diamonds in Saskatchewan kimberlites. Russ.Geol.Geophys., 38, 481–491.

Li, Y., and Keppler, H. (2014) Nitrogen speciation in mantle and crustal fluids. Geochimica et Cosmochimica Acta, 129, 13–32.

Liggins, S. (2010) Identification of point defects in treated single crystal diamond. PhD Thesis, University of Warwick, Warwick.

Liggins, S., Newton, M.E., Goss, J.P., Briddon, P.R., and Fisher, D. (2010) Identification of the dinitrogen (001) split interstitial H1a in diamond. Physical Review B, 81, 085214.

Lightowlers, E.C., and Dean, P.J. (1964) Measurement of nitrogen concentrations in diamond by photon activation analysis and optical absorption. Diamond Research, 21–25.

Always consult and cite the final published document. See https://msaweb.org/ or GeoScienceWorld

This is the peer-reviewed, final accepted version for American Mineralogist, published by the Mineralogical Society of America.
The published version is subject to change. Cite as Authors (Year) Title. American Mineralogist, in press.
DOI: https://doi.org/10.2138/am-2026-10296. https://msaweb.org/

Lu, R., and Hofmeister, A.M. (1995) Infrared fundamentals and phase transitions in CO2 up to 50 GPa. Physical Review B, 52, 3985–3992.

Mainwood, A. (1994) Nitrogen and nitrogen-vacancy complexes and their formation in diamond. Physical Review B, 49.

Mashkovtsev, R.I., Rakhmanova, M.I., and Zedgenizov, D.A. (2021) Specific spectroscopic features of yellow cuboid diamonds from placers in the north-eastern Siberian Platform. Journal of Geosciences, 117–126.

Massi, L., Fritsch, E., Collins, A.T., Hainschwang, T., and Notari, F. (2005) The "amber centres" and their relation to the brown colour in diamond. Diamond and Related Materials, 14, 1623–1629.

Mc Dade, P., and Harris, J.W. (1998) Syngenetic inclusion bearing diamonds from Letseng-la-Terai, Lesotho. International Kimberlite Conference: Extended Abstracts, 7, 561–563.

Melton, G.L., Stachel, T., Stern, R.A., Carlson, J., and Harris, J.W. (2013) Infrared spectral and carbon isotopic characteristics of micro- and macro-diamonds from the Panda kimberlite (Central Slave Craton, Canada). Lithos, 177.

Mikhail, S., and Sverjensky, D.A. (2014) Nitrogen speciation in upper mantle fluids and the origin of Earth's nitrogen-rich atmosphere. Nature Geoscience, 7, 816–819.

Mikhail, S., and Howell, D. (2016) A petrological assessment of diamond as a recorder of the mantle nitrogen cycle. American Mineralogist, 101, 780–787.

Mineeva, R.M., and Speransky, A. V. (2005) EPR studies on the di-nitrogen centers with nonequivalent atoms in a reddish-brown plastically deformed diamond. Applied Magnetic Resonance, 28, 355–364.

Moses, T.M., and McClure, S.F. (2022) HPHT-processed Natural Type Ia Diamond. Gems & Gemology, 58, 48–58.

Nadolinny, V.A., Yelisseyev, A.P., Baker, J.M., Twitchen, D.J., Newton, M.E., Hofstaetter, A., and Feigelson, B. (1999) EPR spectra of separated pairs of substitutional nitrogen atoms in diamond with a high concentration of nitrogen. Physical Review B, 60, 5392–5403.

Nadolinny, V.A., Yurjeva, O.P., and Pokhilenko, N.P. (2009) EPR and luminescence data on the nitrogen aggregation in diamonds from Snap Lake dyke system. Lithos, 112S, 865–869.

Nadolinny, V.A., Palyanov, Yu.N., Rakhmanova, M.I., Borzdov, Yu.M., Komarovskikh, A.Yu., Shatsky, V.S., Ragozin, A.L., and Yurjeva, O.P. (2025) Investigation of the Y centers in cubic plastically deformed type Ib diamonds (Yakutia placers). Diamond and Related Materials, 151, 111821.

Navon, O., Wirth, R., Schmidt, C., Jablon, B.M., Schreiber, A., and Emmanuel, S. (2017) Solid molecular nitrogen (δ-N2) inclusions in Juina diamonds: Exsolution at the base of the transition zone. Earth and Planetary Science Letters, 464, 237–247.

Always consult and cite the final published document. See https://msaweb.org/ or GeoScienceWorld

This is the peer-reviewed, final accepted version for American Mineralogist, published by the Mineralogical Society of America.
The published version is subject to change. Cite as Authors (Year) Title. American Mineralogist, in press.
DOI: https://doi.org/10.2138/am-2026-10296. https://msaweb.org/

Newton, M.E., and Baker, J.M. (1991a) ENDOR studies on the W7 di-nitrogen centre in brown diamond. Journal of Physics: Condensed Matter, 3, 3591–3603.

——— (1991b) Models for the di-nitrogen centres found in brown diamond. Journal of Physics: Condensed Matter, 3, 3605–3616.

Nimis, P. (2022) Pressure and Temperature Data for Diamonds. In Reviews in Mineralogy and Geochemistry Vol. 88.

Orlov, Yu.L. (1984) Mineralogy of Diamond, second ed. [in Russian]. Nauka , Moscow.

Phillips, D., Harris, J.W., and Viljoen, K.S. (2004) Mineral chemistry and thermobarometry of inclusions from De Beers Pool diamonds, Kimberley, South Africa. Lithos, 77, 155–179.

Pignatelli, I., and Ferraris, C. (2025) A Rare Yellow Diamond: Reconstruction of the Possible Geological History. Crystals, 15, 461.

Rakhmanova, M.I., Nadolinny, V.A., Yuryeva, O.P., Pokhilenko, N.P., and Logvinova, A.M. (2015) Peculiarities of nitrogen impurity aggregation in diamonds from the Sytykanskaya pipe, Yakutia. European Journal of Mineralogy, 27, 51–56.

Reinitz, I.M., Buerki, P.R., Shigley, J.E., McClure, S.F., and Moses, T.M. (2000) Identification of HPHT-Treated Yellow to Green Diamonds. Gems & Gemology, 36, 128–137.

Robertson, R., Fox, J.J., and Martin, A.E. (1934) Two types of diamond. Philosophical Transactions of the Royal Society of London. Series A, Containing Papers of a Mathematical or Physical Character, 232, 463–535.

Robertson, R., Fox, J.J., and Martin, A.E. (1936) Further work on two types of diamond. Proceedings of the Royal Society of London. Series A - Mathematical and Physical Sciences, 157, 579–593.

Rudnick, R.L., Eldridge, S.C., and Bulanova, G.P. (1993) Diamond growth history from in situ measurement of Pb and S isotopic compositions of sulfide inclusions. Geology, 21, 13–16.

Salustro, S., Ferrari, A.M., Gentile, F.S., Desmarais, J.K., Rérat, M., and Dovesi, R. (2018) Characterization of the B-Center Defect in Diamond through the Vibrational Spectrum: A Quantum-Mechanical Approach. The Journal of Physical Chemistry A, 122, 594–600.

Satoh, S., Sumiya, H., Tsuji, K., and Yazu, S. (1990) Difference in nitrogen concentration and aggregation among (111) and (110) growth sectors of large synthetic diamonds. In S. et al. Saito, Ed., Science and Technology of New Diamond pp. 351–355. Terra Scientific Publishing.

Schrauder, M., and Navon, O. (1993) Solid carbon dioxide in a natural diamond. Nature, 365, 42–44.

Shigley, J.E., and Breeding, C.M. (2013) Optical Defects in Diamond: A Quick Reference Chart. Gems & Gemology, 49, 107–111.

Always consult and cite the final published document. See https://msaweb.org/ or GeoScienceWorld

This is the peer-reviewed, final accepted version for American Mineralogist, published by the Mineralogical Society of America.
The published version is subject to change. Cite as Authors (Year) Title. American Mineralogist, in press.
DOI: https://doi.org/10.2138/am-2026-10296. https://msaweb.org/

Shigley, J.E., Fritsch, E., Koivula, J.I., Sobolev, N. V., Malinovsky, I.Y., and Pal'yanov, Y.N. (1993) The Gemological Properties of Russian Gem-Quality Synthetic Yellow Diamonds. Gems & Gemology, 29, 228–248.

Shirey, S.B., Pearson, D.G., Stachel, T., and Walter, M.J. (2024) Sublithospheric Diamonds: Plate Tectonics from Earth's Deepest Mantle Samples. Annual Review of Earth and Planetary Sciences, 52, 249-293.

Shiryaev, A.A., Chesnokov, Y., Vasiliev, A.L., and Hainschwang, T. (2023) Exsolution of oxygen impurity from diamond lattice and formation of pressurized CO2-I precipitates. Carbon Trends, 11, 100270.

Smart, K.A., Chacko, T., Stachel, T., Muehlenbachs, K., Stern, R.A., and Heaman, L.M. (2011) Diamond growth from oxidized carbon sources beneath the Northern Slave Craton, Canada: A δ13C–N study of eclogite-hosted diamonds from the Jericho kimberlite. Geochimica et Cosmochimica Acta, 75, 6027–6047.

Smit, K. V., Shirey, S.B., Stern, R.A., Steele, A., and Wang, W. (2016) Diamond growth from C–H–N–O recycled fluids in the lithosphere: Evidence from CH4 micro-inclusions and δ13C–δ15N–N content in Marange mixed-habit diamonds. Lithos, 265.

Smit, K. V., D'Haenens-Johansson, U.F.S., Howell, D., Loudin, L.C., and Wang, W. (2018) Deformation-related spectroscopic features in natural Type Ib-IaA diamonds from Zimmi (West African craton). Mineralogy and Petrology, 112, 243–257.

Smit, K. V., Timmerman, S., Aulbach, S., Shirey, S.B., Richardson, S.H., Phillips, D., and Pearson, D.G. (2023) Geochronology of Diamonds. In Diamond: Genesis, Mineralogy and Geochemistry.

Smith, E.M., and Kopylova, M.G. (2014) Implications of metallic iron for diamonds and nitrogen in the sublithospheric mantle. Canadian Journal of Earth Sciences, 51.

Smith, E.M., Shirey, S.B., Nestola, F., Bullock, E.S., Wang, J., Richardson, S.H., and Wang, W. (2016) Large gem diamonds from metallic liquid in Earth's deep mantle. Science, 354.

Smith, E.M., Shirey, S.B., Richardson, S.H., Nestola, F., Bullock, E.S., Wang, J., and Wang, W. (2018) Blue boron-bearing diamonds from Earth's lower mantle. Nature, 560.

Smith, E.M., Chinn, I., and Timmerman, S. (2025) Large irregular Type IIa and Type IIb diamonds: valuable sublithospheric gems that elude conventional indicators. Mineralogy and Petrology.

Sobolev, E. V., Lenskaya, S. V., and Lisoivan, V.I. (1969) Lamellar formations in the structure of natural diamonds. Journal of Structural Chemistry, 9, 917–920.

Speich, L., and Kohn, S.C. (2020) QUIDDIT - QUantification of infrared active Defects in Diamond and Inferred Temperatures. Computers and Geosciences, 144.

Always consult and cite the final published document. See https://msaweb.org/ or GeoScienceWorld

This is the peer-reviewed, final accepted version for American Mineralogist, published by the Mineralogical Society of America.
The published version is subject to change. Cite as Authors (Year) Title. American Mineralogist, in press.
DOI: https://doi.org/10.2138/am-2026-10296. https://msaweb.org/

Speich, L., Kohn, S.C., Wirth, R., Bulanova, G.P., and Smith, C.B. (2017) The relationship between platelet size and the B′ infrared peak of natural diamonds revisited. Lithos, 278–281.

Speich, L., Kohn, S.C., Bulanova, G.P., and Smith, C.B. (2018) The behaviour of platelets in natural diamonds and the development of a new mantle thermometer. Contributions to Mineralogy and Petrology, 173.

Stacey, A., Karle, T.J., McGuinness, L.P., Gibson, B.C., Ganesan, K., Tomljenovic-Hanic, S., Greentree, A.D., Hoffman, A., Beausoleil, R.G., and Prawer, S. (2012) Depletion of nitrogen-vacancy color centers in diamond via hydrogen passivation. Applied Physics Letters, 100.

Stachel, T. (2014) Chapter 1: Diamonds. In Mineralogical Association of Canada Short Course 44 pp. 1–28. Tucson AZ.

Stachel, T., and Harris, J.W. (1997) Syngenetic inclusions in diamond from the Birim field (Ghana) - a deep peridotitic profile with a history of depletion and re-enrichment. Contributions to Mineralogy and Petrology, 127, 336–352.

Stachel, T., and Harris, J.W. (2009) Formation of diamond in the Earth's mantle. Journal of Physics Condensed Matter, 21.

Stachel, T., and Luth, R.W. (2015) Diamond formation - Where, when and how? Lithos.

Stachel, T., Banas, A., Muehlenbachs, K., Kurszlaukis, S., and Walker, E.C. (2006) Archean diamonds from Wawa (Canada): samples from deep cratonic roots predating cratonization of the Superior Province. Contributions to Mineralogy and Petrology, 151, 737–750.

Stachel, T., Aulbach, S., and Harris, J.W. (2022) Mineral Inclusions in Lithospheric Diamonds. Reviews in Mineralogy and Geochemistry, 88, 307–391.

Sutherland, G.B.B.M., and Willis, H.A. (1945) Some new peculiarities in the infra-red spectrum of diamond. Transactions of the Faraday Society, 41, 289–292.

Sutherland, G.B.B.M., Blackwell, D.E., and Simeral, W.G. (1954) The Problem of the Two Types of Diamond. Nature, 174, 901–904.

Tappert, R., Stachel, T., Harris, J.W., Muehlenbachs, K., Ludwig, T., and Brey, G.P. (2005) Diamonds from Jagersfontein (South Africa): messengers from the sublithospheric mantle. Contributions to Mineralogy and Petrology, 150, 505–522.

Taylor, W.R., Jaques, A.L., and Ridd, M. (1990) Nitrogen-defect aggregation characteristics of some Australasian diamonds: time-temperature constraints on the source regions of pipe and alluvial diamonds. American Mineralogist, 75.

Taylor, W.R., Canil, D., and Judith Milledge, H. (1996) Kinetics of Ib to IaA nitrogen aggregation in diamond. Geochimica et Cosmochimica Acta, 60, 4725–4733.

Always consult and cite the final published document. See https://msaweb.org/ or GeoScienceWorld

This is the peer-reviewed, final accepted version for American Mineralogist, published by the Mineralogical Society of America.
The published version is subject to change. Cite as Authors (Year) Title. American Mineralogist, in press.
DOI: https://doi.org/10.2138/am-2026-10296. https://msaweb.org/

Thomassot, E., Cartigny, P., Harris, J.W., Lorand, J.P., Rollion-Bard, C., and Chaussidon, M. (2009) Metasomatic diamond growth: A multi-isotope study (13C, 15N, 33S, 34S) of sulphide inclusions and their host diamonds from Jwaneng (Botswana). Earth and Planetary Science Letters, 282, 79–90.

Thomaz, M.F., and Davies, G. (1978) The decay time of N3 luminescence in natural diamond. Proceedings of the Royal Society of London. A. Mathematical and Physical Sciences, 362, 405–419.

Timmerman, S., Koornneef, J.M., Chinn, I.L., and Davies, G.R. (2017) Dated eclogitic diamond growth zones reveal variable recycling of crustal carbon through time. Earth and Planetary Science Letters, 463, 178–188.

Timmerman, S., Chinn, I.L., Fisher, D., and Davies, G.R. (2018) Formation of unusual yellow Orapa diamonds. Mineralogy and Petrology, 112, 209–218.

Titkov, S. V., Mineeva, R.M., Zudina, N.N., Sergeev, A.M., Ryabchikov, I.D., Shiryaev, A.A., Speransky, A. V., and Zhikhareva, V.P. (2015) The luminescent nature of orange coloration in natural diamonds: optical and EPR study. Physics and Chemistry of Minerals, 42, 131–141.

Van der Bogert, C.H., Smith, C.P., Hainschwang, T., and McClure, S.F. (2009) Gray-to-Blue-to-Violet Hydrogen-Rich Diamonds from the Argyle Mine, Australia. Gems and Gemology, 45, 20–37.

Weiss, Y., Navon, O., Goldstein, S.L., and Harris, J.W. (2018) Inclusions in diamonds constrain thermo-chemical conditions during Mesozoic metasomatism of the Kaapvaal cratonic mantle. Earth and Planetary Science Letters, 491, 134–147.

Wentorf, R.H., and Bovenkerk, H.P. (1962) Preparation of Semiconducting Diamonds. The Journal of Chemical Physics, 36, 1987–1990.

Wiggers de Vries, D.F., Pearson, D.G., Bulanova, G.P., Smelov, A.P., Pavlushin, A.D., and Davies, G.R. (2013) Re–Os dating of sulphide inclusions zonally distributed in single Yakutian diamonds: Evidence for multiple episodes of Proterozoic formation and protracted timescales of diamond growth. Geochimica et Cosmochimica Acta, 120, 363–394.

Wood, J.O. (2020) An elusive impurity: studying hydrogen in natural diamonds. University of Bristol, Bristol.

Woods, G.S. (1986) Platelets and the infrared absorption of type Ia diamonds. Proceedings of the Royal Society of London, Series A, 407.

Woods, G.S., and Collins, A.T. (1983) Infrared absorption spectra of hydrogen complexes in type I diamonds. Journal of Physics and Chemistry of Solids, 44.

Woods, G.S., Kiflawi, I., Luyten, W., and Tendeloo, G. Van (1993) Infrared spectra of type IaB diamonds. Philosophical Magazine Letters, 67, 405–411.

Always consult and cite the final published document. See https://msaweb.org/ or GeoScienceWorld

This is the peer-reviewed, final accepted version for American Mineralogist, published by the Mineralogical Society of America.
The published version is subject to change. Cite as Authors (Year) Title. American Mineralogist, in press.
DOI: https://doi.org/10.2138/am-2026-10296. https://msaweb.org/

Wu, G.-C., Yu, X.-Y., Liu, F., Li, H.-B., Long, Z.-Y., and Wang, H. (2022) Color Genesis of Brown Diamond from the Mengyin Kimberlite, China. Crystals, 12, 449.

Zaitsev, A.M. (2001) Optical Properties of Diamond. Springer Berlin Heidelberg, Berlin, Heidelberg.

Zaitsev, A.M., Kazuchits, N.M., Kazuchits, V.N., Moe, K.S., Rusetsky, M.S., Korolik, O.V., Kitajima, K., Butler, J.E., and Wang, W. (2020) Nitrogen-doped CVD diamond: Nitrogen concentration, color and internal stress. Diamond and Related Materials, 105, 107794.

Zedgenizov, D.A., Harte, B., Shatsky, V.S., Politov, A.A., Rylov, G.M., and Sobolev, N. V. (2006) Directional chemical variations in diamonds showing octahedral following cuboid growth. Contributions to Mineralogy and Petrology, 151, 45–57.

Zhang, Y., Shi, G., and Xie, Z. (2024) Spectral Characteristics of Nitrogen-Doped CVD Synthetic Diamonds and the Origin of Surface Blue Fluorescence. Crystals, 14, 804.

Zheng, Y., Li, C., Liu, J., Wei, J., and Ye, H. (2021) Diamond with nitrogen: states, control, and applications. Functional Diamond, 1, 63–82.

Always consult and cite the final published document. See https://msaweb.org/ or GeoScienceWorld

This is the peer-reviewed, final accepted version for American Mineralogist, published by the Mineralogical Society of America.
The published version is subject to change. Cite as Authors (Year) Title. American Mineralogist, in press.
DOI: https://doi.org/10.2138/am-2026-10296. https://msaweb.org/

Figure Captions:

Figure 1. The *Type* classification scheme for natural untreated diamond simplified to allow for easy visualization and comprehension. The criteria for all groups at the Tier 1–3 levels are indicated in the extended version of this scheme in Fig. 2. At the Tier 2 level, the estimated proportions of natural diamonds globally are given though proportions will vary depending on the individual deposit and depending on the size fraction of diamonds examined (see above discussion).

Figure 2. The *Type* classification scheme for natural diamond (extended version of Fig. 1). This scheme is applicable to most natural untreated diamonds to which thermochronometric methods can be applied for geological purposes. The criteria for Tiers 1–4, and for each *Type* group at the Tier 3 and 4 levels, are listed for each respective group. The Tier 4 groups for ***X***- and ***Y***-bearing diamonds specify the identity of single substitutional N_{TS} (i.e., ***C***-, ***X***- or ***Y***-centers) where $\%N_{TS} \geq 50$, and are thus only applicable to the *Type IbC* and *Type IbCA* groups. Tier 4 groups for regular, subregular and irregular platelets are included as the platelet peak can also be used for thermochronometric (geological) applications. To show how different types of platelets (or the absence of platelets) are indicated in the *Type* name, *Type IaAB* is used as an example. The IDL, PQL_{Ib} and PQL_{Ia} are defined in section "Tiers 1 and 2".

Figure 3. The extended *Type* classification scheme for diamond. This scheme is applicable to natural, treated and synthetic diamonds. The scheme for natural *Type I* diamonds (as shown in Fig. 2) is shown in blue. The scheme for diamonds with detectable ***C***-, ***A***- and ***B***-centers (*Type Ib–Ia* diamonds) is shown in orange. The criteria for Tiers 1–4 and for each *Type* group at the Tier 3a, 3b, 4a and 4b levels are listed. The Tier 4a and 4b groups for ***X***- and ***Y***-bearing diamonds specify the identity of single substitutional N_{TS} (i.e., ***C***-, ***X***- or ***Y***-centers) where $\%N_{TS} \geq 50$, and are thus only applicable to the Tier 3a – *Type IbC* and *Type IbCA* groups and the Tier 3b – *Type IbCB* and *Type IbCAB* groups. A classification scheme for diamonds with boron and N-defects is provided (see section "Tier 3"). Additional Tier 4 – *Type* groups based on the presence of platelets (*B′* peak), CO_2 inclusions and amber centers are also provided (see section "Tier 4"). To show how different types of platelets (or the absence of platelets) are indicated in the *Type* name, *Type IaAB* is used as an example. Similarly, *Type IaA′–Amb$_n$* is used as an example to indicate the presence of an amber center peak at n cm^{-1}, *Type IaA–CO$_2$* and *Type IIa–CO$_2$* are used as examples to indicate the presence of CO_2, and *Type IIa–H$_{3107}$* is used as an example to indicate the presence of the N_3VH defect, if other H-related peaks are observed (e.g., 3237 cm^{-1} due to the N_4VH defect), this *Type* name can be modified accordingly (e.g., *Type IIa–H$_{3237}$*). The IDL, PQL_{Ib}, PQL_{Ia} and $PQL_{Ia–Ib}$ are defined in section "Tiers 1 and 2".

Figure 4. Results of decomposition via least-squares fitting of **(a)** a *Type IaB′* diamond where $N_B > PQL_{Ia}$ and a high-quality fit ($S_C = 0.2676$) is obtained allowing classification at the Tier 3 level. **(b)** a *Type Ia* diamond where $N_B < PQL_{Ia}$ and a poor-quality fit ($S_C = 2.2215$) is obtained, here the presence (or concentration) of ***A***-centers cannot be ruled out and thus this diamond can only be classified at the Tier 2 level. **(c)** a *Type II* diamond where signal cannot be attributed to ***A***- and/or ***B***-centers (shown in blue and green, respectively) and instead is likely due to background-related issues, noise, contamination and/or micro-inclusions. Thickness normalization to 1 cm, baseline

Always consult and cite the final published document. See https://msaweb.org/ or GeoScienceWorld

This is the peer-reviewed, final accepted version for American Mineralogist, published by the Mineralogical Society of America.
The published version is subject to change. Cite as Authors (Year) Title. American Mineralogist, in press.
DOI: https://doi.org/10.2138/am-2026-10296. https://msaweb.org/

correction and decomposition were performed with the *DiaMap* Excel spreadsheet (Howell et al. 2012a, 2012b).

Figure 5. Decomposition results of the one-phonon region of the FTIR spectra of a yellow–green diamond HPHT-treated at 2025 °C and 6 GPa for ~30 minutes. Originally, the diamond was brown and *Type IaAB* and after HPHT-treatment, disassociation of ***A***- and ***B***-centers resulted in the formation of ***C***-centers. Here, $40 < \%N_B\ (53.4) < 90$; $0 < \%N_C\ (17.5) \leq 40$; and $0 < \%N_A\ (29.1) \leq 40$ allowing classification as *Type IaABC*. Thickness normalized (to 1 cm) and baseline corrected data was taken from Collins et al. (2000) and decomposition was preformed using the *Caxbd_Inherit_2024-Ib* Excel spreadsheet (Day et al. 2026).

Figure 6. Decomposition results of the one-phonon region of the FTIR spectra of untreated, natural **(a)** *Type IbY–X* and **(b)** *Type IbCA–XY* diamonds. In **(a)** $\%N_Y\ (52.7) \geq 50$; $0 \leq \%N_A\ (8.1) < 10$; $0 \leq \%N_{TS}–\%N_Y\ (39.2) \leq 50$; and $\%N_X\ (3.1) < 50$ allowing classification as *Type IbY–X*. In **(b)** $10 < \%N_{TS}\ (31.1) \leq 90$; $10 \leq \%N_A\ (68.7) < 90$; and $\%N_X\ (2.7)$ and $\%N_Y\ (14.8) < 50$ allowing classification as *Type IbCA–XY*. Raw spectra were thickness normalized to 1 cm and baseline corrected using the *DiaMap* Excel spreadsheet (Howell et al. 2012a, 2012b) and decomposition was preformed using the *Caxbd_Inherit_2024-Ib* Excel spreadsheet (Day et al. 2026).

Figure 7. (a) spectra in the one-phonon region (1000–1400 cm^{-1}) of two platelet-bearing *Type IaAB* diamonds (blue and red) and of one *Type IaB′* diamond (black) that does not contain platelets. **(b)** The regularity relation between the integrated absorbance of the *B′* peak (I(*B′*) in cm^{-2}) and the thickness normalized absorption due to ***B***-centers (μB) is from Woods, (Woods 1986). The *B′* peak in the red spectrum **(a)** follows this relation (shown with red point in **(b)**) and thus the diamond contains *regular* platelets and can be classified as *Type IaAB–*p_{reg}. The *B′* peak in the blue spectrum **(b)** does not follow this relation (shown with blue point in **(b)**) and thus the diamond contains *irregular* platelets and can be classified as *Type IaAB–*p_{ireg}. Irregular platelets result from platelet degradation, eventually resulting in the complete absence of the *B′* peak as observed in the spectrum of the *Type IaB′* diamond shown in black. Raw spectra were thickness normalized to 1 cm, baseline corrected and decomposed using the *DiaMap* Excel spreadsheet (Howell et al. 2012a, 2012b).

Figure 8. FTIR spectra recorded from a single CO_2–I bearing diamond in the range 600 to 4000 cm^{-1} showing the peaks at 650 and 660 cm^{-1} (ν_{2b} and ν_{2a}) and 2369–2373 cm^{-1} (ν_{3b}) and 2415 cm^{-1} (ν_{3a}) due to CO_2–I inclusions (cubic phase I). Spectrum **(a)** shows anomalous absorption in the one-phonon region and can be classified as *Type I*–CO_2. Spectrum **(b)** shows additional peaks at 2850–2960 cm^{-1} due to C–H stretching modes associated with molecular hydrocarbons and a peak at 3107 cm^{-1} due to the C–H stretching mode of the N_3VH^0 defect. Spectrum **(b)** shows absorption in the one-phonon region due to ***A***- and ***B***-centers and decomposition results in $\%N_B = 31$ allowing classification as *Type IaAB*–CO_2. An image of dark CO_2–I (quasi)hexagonal inclusions from a CO_2-bearing diamond from the Museum of Nature and Humankind, University of Padova. Thickness normalized (to 1 cm) spectra were taken from Barannik et al. (2021).

Figure 9. FTIR spectra recorded from two diamonds in the range 750 to 5000 cm^{-1} that contain amber centers. Spectrum **(a)** (shown in black) is recorded from a brown–orange *Type IaAB* ($\%N_B$

Always consult and cite the final published document. See https://msaweb.org/ or GeoScienceWorld

This is the peer-reviewed, final accepted version for American Mineralogist, published by the Mineralogical Society of America.
The published version is subject to change. Cite as Authors (Year) Title. American Mineralogist, in press.
DOI: https://doi.org/10.2138/am-2026-10296. https://msaweb.org/

= 60) diamond, and shows amber centers at 4167 cm^{-1}, and is classified as *Type IaAB*–Amb_{4167}. Spectrum **(b)** (shown in red) is recorded from a yellow–brown *Type IaA′* diamond that shows amber centers at 4065 cm^{-1} and is classified as *Type IaA′*–Amb_{4065}. In both spectra, a peak at 3107 cm^{-1} due to the C–H stretching mode of the N_3VH^0 defect is observed. In spectrum **(b)** additional peaks at 2850–2960 cm^{-1} due to C–H stretching modes associated with molecular hydrocarbons (contamination) are observed. Images of both diamonds are shown along with linear (plastic) deformation lamellae observed in sample **(a)**. Spectra are thickness normalized to 1 cm but not otherwise processed. Samples are from the Museum of Nature and Humankind, University of Padova.

Figure 10. (a,b) Composite secondary-electron and cathodoluminescence images (CL–VPSE overlay) of a faceted *Type IIb* diamond with a small *Type IaB* region. In (b), dislocation networks in the *Type IIb* region are observed and fine, concentric growth zonation is observed in the bright (***N3***-center bearing) *Type IaB* region. Images: U. D'Haenens-Johansson (GIA).

Always consult and cite the final published document. See https://msaweb.org/ or GeoScienceWorld

This is the peer-reviewed, final accepted version for American Mineralogist, published by the Mineralogical Society of America.
The published version is subject to change. Cite as Authors (Year) Title. American Mineralogist, in press.
DOI: https://doi.org/10.2138/am-2026-10296. https://msaweb.org/

1737 **Supplementary Materials:**

1738 **Appendix A.** Determination of the thickness normalized absorption intensity and practical

1739 quantitation limit (PQL) for *Type Ib*, *Type Ia* and *Type Ib–Ia* diamonds (Sections A.1 – A.3 and

1740 Figures A.1 – A.5).

1741 **Appendix B.** Updated and extended Type Classification for diamond and associated group and

1742 subgroup criteria (tabulated data from Figure 3) (Table B.1**)**

Always consult and cite the final published document. See https://msaweb.org/ or GeoScienceWorld

This is the peer-reviewed, final accepted version for American Mineralogist, published by the Mineralogical Society of America.
The published version is subject to change. Cite as Authors (Year) Title. American Mineralogist, in press.
DOI: https://doi.org/10.2138/am-2026-10296. https://msaweb.org/

Table 1. Name, composition and identifying signals for point- and extended-defects in diamond used in the *Type* classification scheme.

Defect	Name(s)	Frequency (cm^{-1})	Wavelength (μm)	Energy (meV)	Type	Description/Comment
N_s^0	***C***-center	**1130** 1344 (narrow)	8.849 7.442	140.1 166.6	*IbC* to *IbA*	Single-substitutional N in the neutral charge state
N_2^0	***A***-center	**1282** 1215 1186	7.802 8.232 8.412	158.9 150.6 147.0	*IbC* to *IaB* *IaA'*	Substitutional N dimer in the neutral charge state
N_4V^0	***B***-center	**1175** 1332 (narrow)	8.509 7.509	145.7 165.1	*IaA* to *IaB* *IaB'*	A carbon vacancy surrounded by four substitutional N atoms in the neutral charge state
N_s^+	***X***-center	**1332** (narrow)	7.509	165.1	*Ib–X/Y*	Single-substitutional N in the positive charge state
N_s^0–C–N_s^0 or N_s^0 + C_i/N_i complex	***Y***-center	**1145** 1358 (narrow)	8.734 7.364	141.9 168.4	*Ib–X/Y*	N_s^0–C–N_s^0 or N_s^0 coupled with interstitial complexes of C_i (±N_i) associated with *platelet-like* peaks from ~1350–1390 cm^{-1}.
Platelet-related $(C_{2n})_i$	***D***-center	**1328** 1259 1210	7.532 7.942 8.265	164.6 156.1 150.0	*IaA* to *IaB'*	Platelet-stimulated lattice vibrational modes
Platelet-related	*B'* peak	~1360–1375	7.353–7.273	168.6–170.5	*IaA* to *IaB'*	Accumulations of C_i (±N_i) produced by ***A***-to-***B*** aggregation.
Platelet-related	C_i/N_i - complex	~1350–1390	7.407–7.194	167.4–172.3	*IbC* to *IbA*	Platelet-like interstitial complexes of C_i (±N_i) common in *Type Ib–XY*
N_3VH^0	-	**3107**	3.219	385.2	*IbC* to *IaB'*	Other H-peaks include 3050, 3144, 3154, 3182, 3310, 3343, and 3394 cm^{-1}. NVH^0 common in synthetic CVD diamond.
N_4VH^0 (platelet-centered)	-	3236–3237	3.090–3.089	401.2–401.3	*IaA'* to *IaB'*	

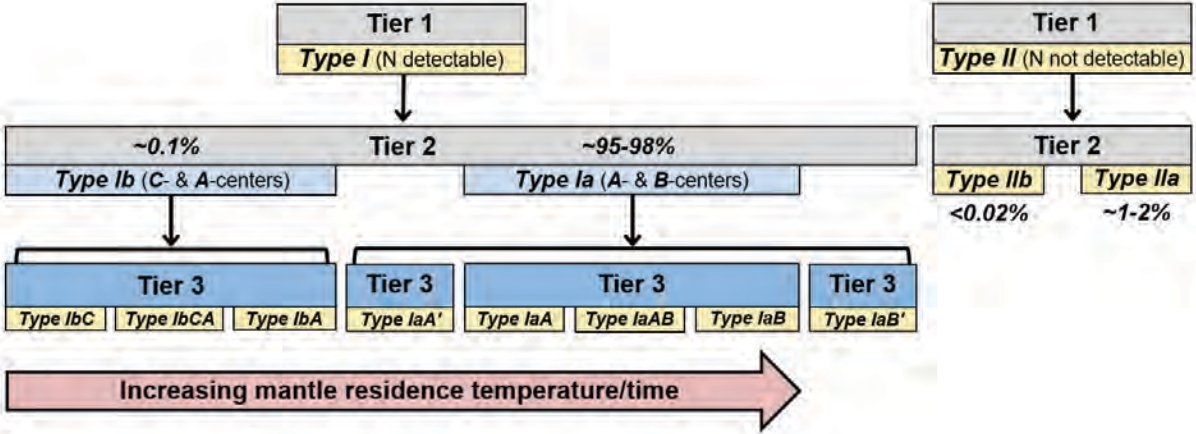
Always consult and cite the final published document. See https://msaweb.org/ or GeoScienceWorld

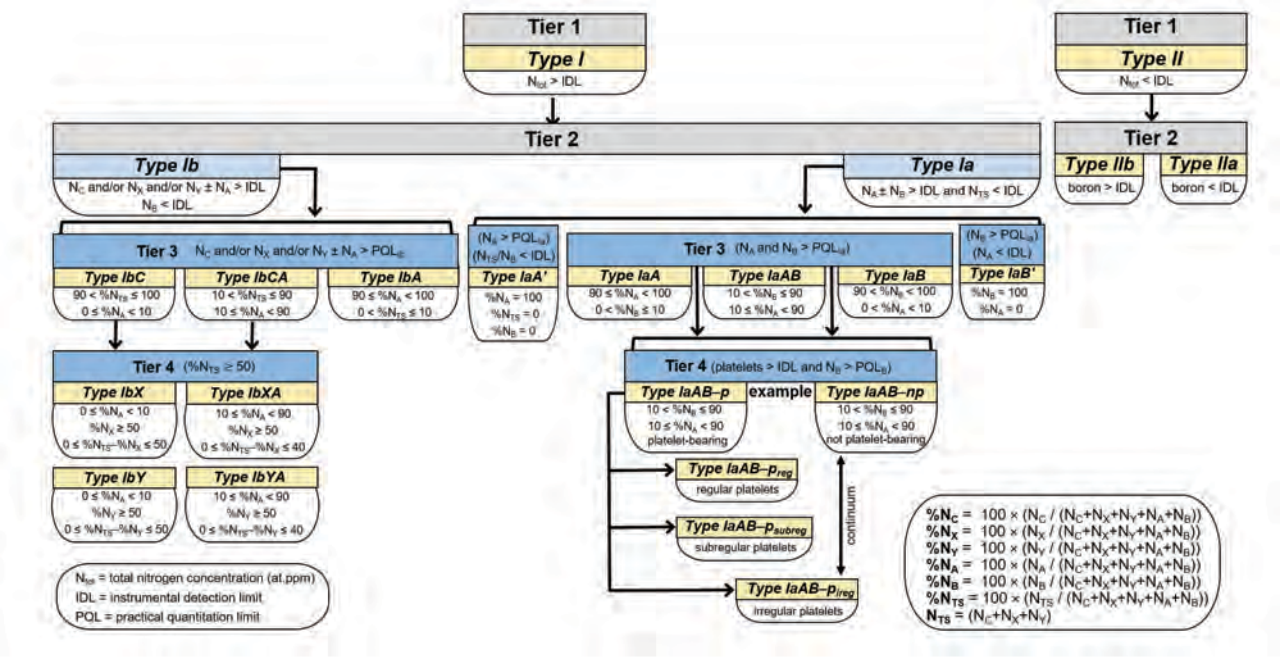
This is the peer-reviewed, final accepted version for American Mineralogist, published by the Mineralogical Society of America.
The published version is subject to change. Cite as Authors (Year) Title. American Mineralogist, in press.
DOI: https://doi.org/10.2138/am-2026-10296. https://msaweb.org/

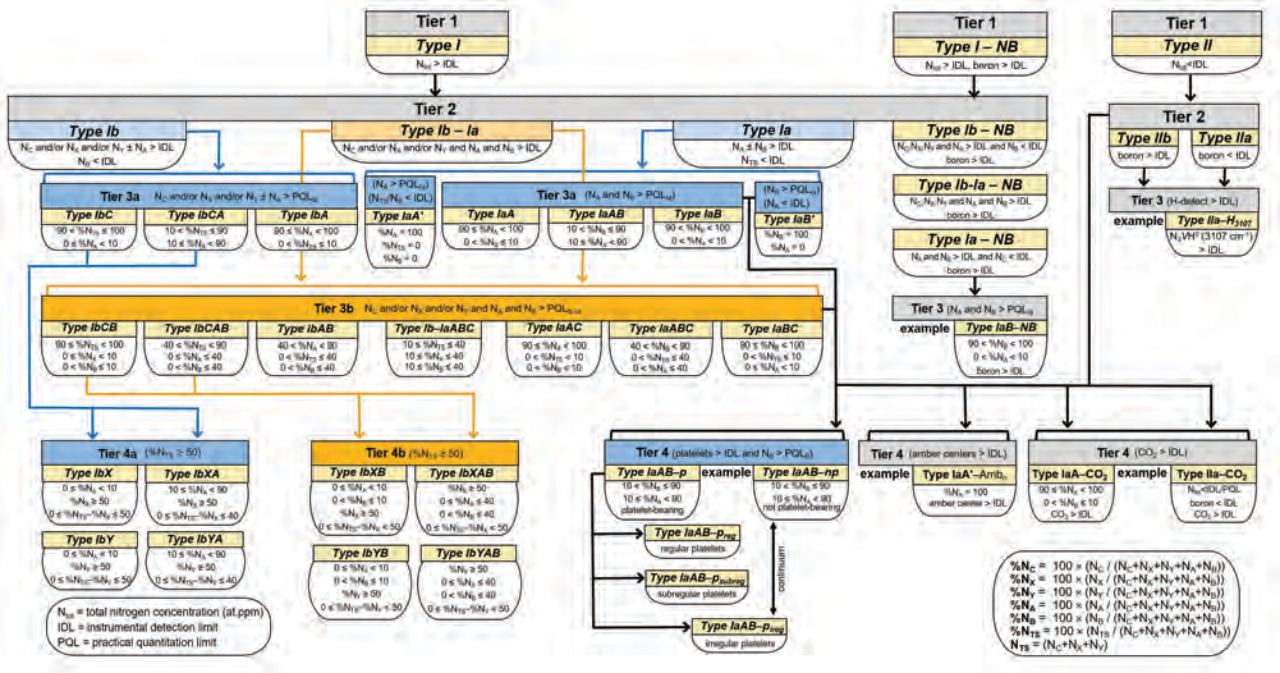
N*V*H^0	-	3123–3124	3.202–3.201	387.2–387.3	*IbC* to *IaA′*	
CO_2–I inclusion	-	649–661 (ν_{2a}) 636–650 (ν_{2b}) 2368–2438 (ν_{3a}) **2339–2440** (ν_{3b})	15.408–15.129 15.723–15.385 4.223–4.102 4.275–4.098	80.5–82.0 78.9–80.6 293.6–302.3 290.0–302.5	*IbC* to *IaB′*	Low P (cubic Phase I). High P (orthorhombic Phase III). May show anomalous one-phonon region.
Vacancy cluster (+N)	Amber center (AC)	3462, **4063-4065**, 4073, **4165–4167** and 4111–4113	2.889, 2.461–2.460, 2.455, 2.401–2.400, 2.432–2.431	429.2, 503.7–504.0, 505.0, 516.4–516.6, 509.7–509.9	*IbC* to *IaB′*	Indicative of plastic deformation. Common in brown diamonds.
Di-nitrogen split interstitial (N_{2i})	***H1a***-center	~1450	6.897	179.8	*IbC* to *IaB′*	Indicative of plastic deformation and or irradiation
N_2 + extended vacancy defect	***H1b***-center	~4935	2.026	611.9	*IbC* to *IaB′*	Indicative of plastic deformation and or irradiation Defect assignment is tentative
N_4V + extended vacancy defect	***H1c***-center	~5165	1.936	640.4	*IbC* to *IaB′*	Indicative of plastic deformation and or irradiation Defect assignment is tentative

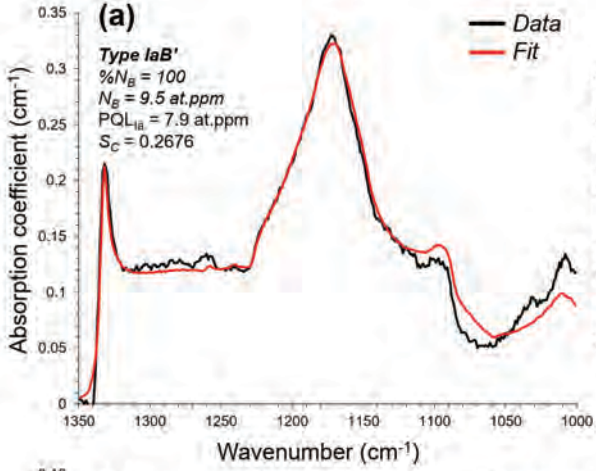
For each absorption system, only the main peak positions are listed and the diagnostic (most intense) peaks for each are shown in bold.
References: Dischler (2012), Shigley and Breeding (2013) and (Day et al. 2026)

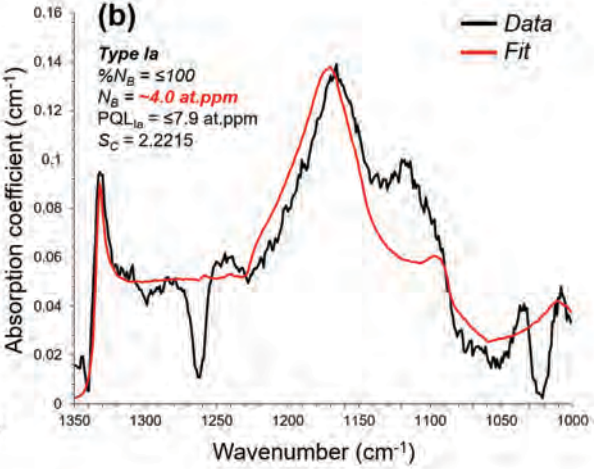
Always consult and cite the final published document. See https://msaweb.org/ or GeoScienceWorld

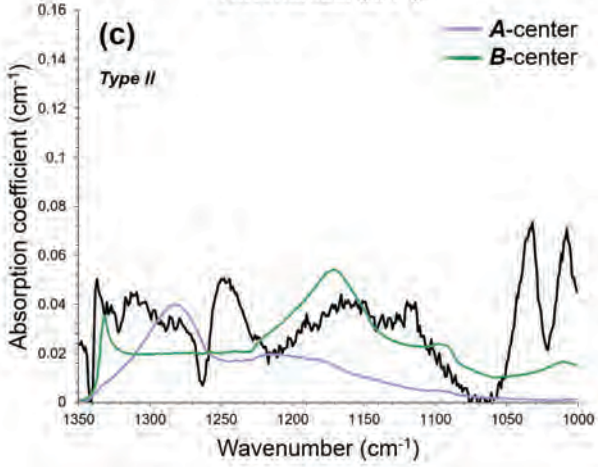

Tier 1
Type I (N detectable)
Tier 1
Type II (N not detectable)
~0.1%
Tier 2
~95-98%
Type Ib (C- & A-centers)
Type Ia (A- & B-centers)
Tier 2
Type IIb
Type IIa
<0.02%
~1-2%
Tier 3
Type IbC
Type IbCA
Type IbA
Tier 3
Type IaA'
Tier 3
Type IaA
Type IaAB
Type IaB
Tier 3
Type IaB'
Increasing mantle residence temperature/time

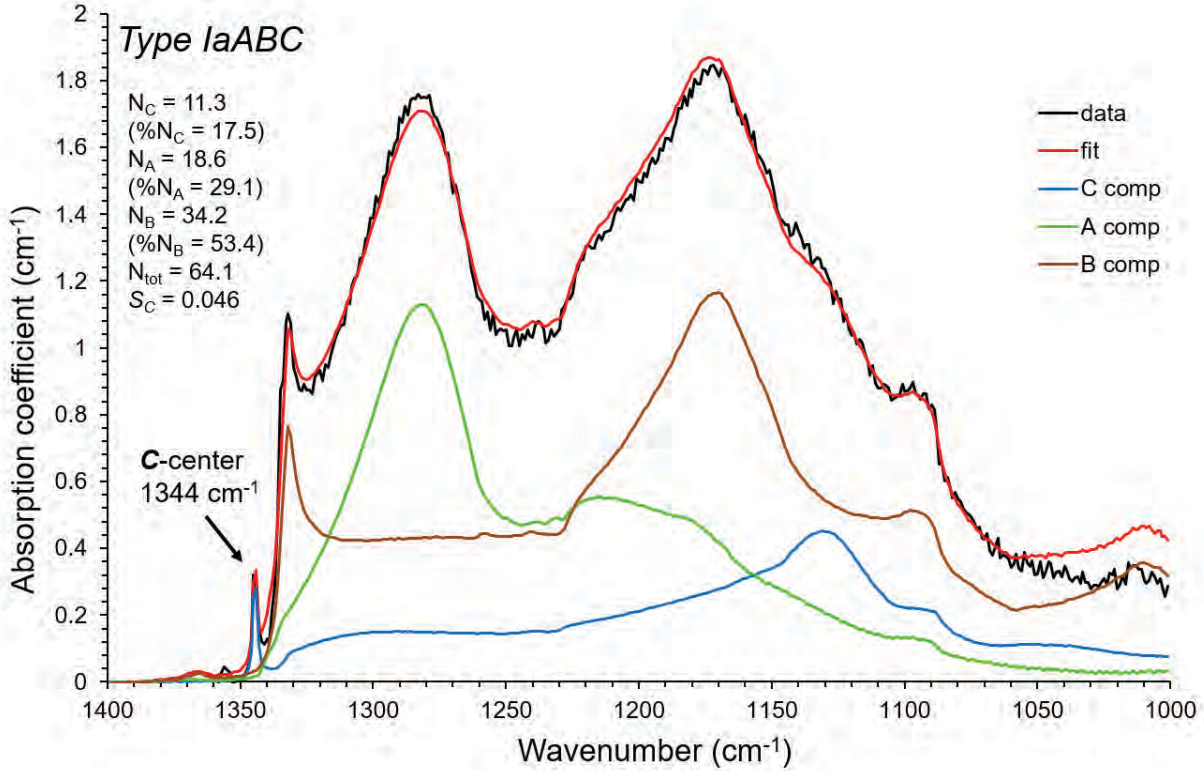

Tier 1
Type I
N_{tot} > IDL
Tier 1
Type II
N_{tot} < IDL
Tier 2
Type Ib
N_C and/or N_X and/or N_Y ± N_A > IDL
N_B < IDL
Type Ia
N_A ± N_B > IDL and N_{TS} < IDL
Tier 2
Type IIb
boron > IDL
Type IIa
boron < IDL
Tier 3 N_C and/or N_X and/or N_Y ± N_A > POL_E
Type IbC
90 < %N_{TS} ≤ 100
0 ≤ %N_A < 10
Type IbCA
10 < %N_{TS} ≤ 90
10 ≤ %N_A < 90
Type IbA
90 ≤ %N_A < 100
0 < %N_{TS} ≤ 10
(N_A > POL_{Ia})
(N_{TS}/N_B < IDL)
Type IaA'
%N_A = 100
%N_{TS} = 0
%N_B = 0
Tier 3 (N_A and N_B > POL_{Ia})
Type IaA
90 ≤ %N_A < 100
0 < %N_B ≤ 10
Type IaAB
10 < %N_B ≤ 90
10 ≤ %N_A < 90
Type IaB
90 < %N_B < 100
0 < %N_A < 10
(N_B > POL_{Ia})
(N_A < IDL)
Type IaB'
%N_B = 100
%N_A = 0
Tier 4 (%N_{TS} ≥ 50)
Type IbX
0 ≤ %N_A < 10
%N_X ≥ 50
0 ≤ %N_{TS}–%N_X ≤ 50
Type IbXA
10 ≤ %N_A < 90
%N_X ≥ 50
0 ≤ %N_{TS}–%N_X ≤ 40
Type IbY
0 ≤ %N_A < 10
%N_Y ≥ 50
0 ≤ %N_{TS}–%N_Y ≤ 50
Type IbYA
10 ≤ %N_A < 90
%N_Y ≥ 50
0 ≤ %N_{TS}–%N_Y ≤ 40
Tier 4 (platelets > IDL and N_B > POL_B)
Type IaAB–p
10 < %N_B ≤ 90
10 ≤ %N_A < 90
platelet-bearing
example
Type IaAB–np
10 < %N_B ≤ 90
10 ≤ %N_A < 90
not platelet-bearing
Type IaAB–p_{reg}
regular platelets
Type IaAB–p_{subreg}
subregular platelets
Type IaAB–p_{irreg}
irregular platelets
continuum
N_{tot} = total nitrogen concentration (at.ppm)
IDL = instrumental detection limit
POL = practical quantitation limit
%N_C = 100 × (N_C / (N_C+N_X+N_Y+N_A+N_B))
%N_X = 100 × (N_X / (N_C+N_X+N_Y+N_A+N_B))
%N_Y = 100 × (N_Y / (N_C+N_X+N_Y+N_A+N_B))
%N_A = 100 × (N_A / (N_C+N_X+N_Y+N_A+N_B))
%N_B = 100 × (N_B / (N_C+N_X+N_Y+N_A+N_B))
%N_{TS} = 100 × (N_{TS} / (N_C+N_X+N_Y+N_A+N_B))
N_{TS} = (N_C+N_X+N_Y)

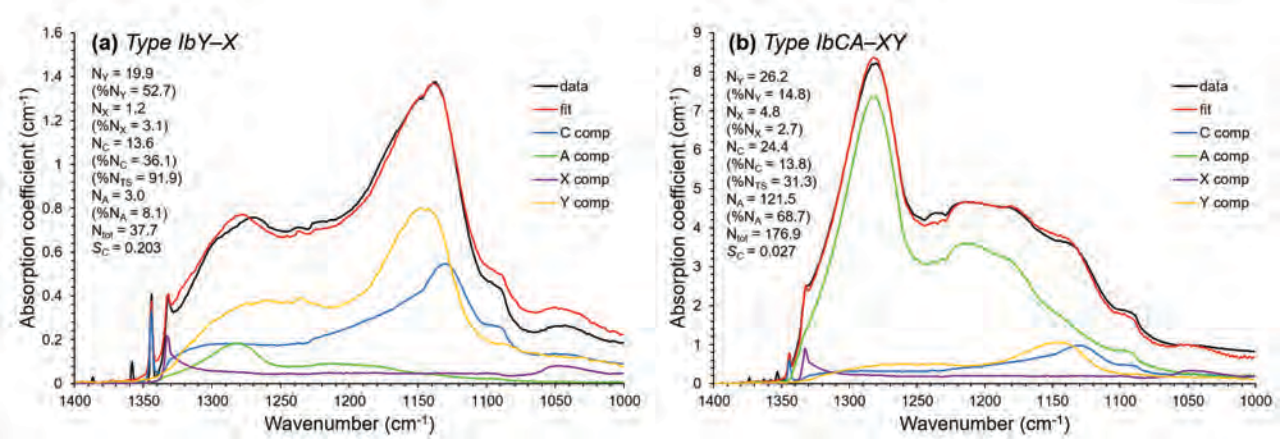

Tier 1
Type I
N_{tot} > IDL
Tier 2
Type Ib
N_C and/or N_N and/or $N_Y \pm N_A$ > IDL
N_B < IDL
Type Ib – Ia
N_C and/or N_N and/or N_Y and N_A and N_B > IDL
Type Ia
$N_A \pm N_B$ > IDL
N_{TS} < IDL
Tier 3a N_C and/or N_N and/or $N_Y \neq N_A$ > PQL_{tot}
Type IbC
90 < %N_{TS} ≤ 100
0 ≤ %N_A < 10
Type IbCA
10 < %N_{TS} ≤ 90
10 ≤ %N_A < 90
Type IbA
90 ≤ %N_A < 100
0 < %N_{TS} ≤ 10
(N_A > PQL_{tot})
(N_{TS}/N_B < IDL)
Type IaA'
%N_A = 100
%N_{TS} = 0
%N_B = 0
Tier 3a (N_A and N_B > PQL_{tot})
Type IaA
90 ≤ %N_A < 100
0 < %N_B ≤ 10
Type IaAB
10 < %N_B ≤ 90
10 ≤ %N_A < 90
Type IaB
90 < %N_B < 100
0 < %N_A < 10
(N_B > PQL_{tot})
(N_A < IDL)
Type IaB'
%N_B = 100
%N_A = 0
Tier 3b N_C and/or N_N and/or N_Y and N_A and N_B > $PQL_{tot,ca}$
Type IbCB
90 ≤ %N_{TS} < 100
0 ≤ %N_A < 10
0 < %N_B ≤ 10
Type IbCAB
40 < %N_{TS} ≤ 90
0 ≤ %N_A ≤ 40
0 < %N_B ≤ 40
Type IbAB
40 < %N_A < 80
0 < %N_{TS} ≤ 40
0 < %N_B ≤ 40
Type Ib–IaABC
10 ≤ %N_{TS} ≤ 40
10 ≤ %N_A ≤ 40
10 ≤ %N_B ≤ 40
Type IaAC
90 ≤ %N_A < 100
0 < %N_{TS} < 10
0 < %N_B < 10
Type IaABC
40 < %N_B < 90
0 < %N_{TS} ≤ 40
0 < %N_A ≤ 40
Type IaBC
90 ≤ %N_B < 100
0 < %N_{TS} ≤ 10
0 ≤ %N_A < 10
Tier 4a (%N_{TS} ≥ 50)
Type IbX
0 ≤ %N_A < 10
%N_B ≥ 50
0 ≤ %N_{TS}–%N_B ≤ 50
Type IbXA
10 ≤ %N_A < 90
%N_B ≥ 50
0 ≤ %N_{TS}–%N_B ≤ 40
Type IbY
0 ≤ %N_A < 10
%N_B ≥ 50
0 ≤ %N_{TS}–%N_B ≤ 50
Type IbYA
10 ≤ %N_A < 90
%N_B ≥ 50
0 ≤ %N_{TS}–%N_B ≤ 40
Tier 4b (%N_{TS} ≥ 50)
Type IbXB
0 ≤ %N_A < 10
0 < %N_B ≤ 10
%N_{TS} ≥ 90
0 ≤ %N_{TS}–%N_B < 50
Type IbXAB
%N_B ≥ 50
0 ≤ %N_A ≤ 40
0 < %N_B ≤ 40
0 ≤ %N_{TS}–%N_B < 50
Type IbYB
0 ≤ %N_A < 10
0 < %N_B ≤ 10
%N_Y ≥ 90
0 ≤ %N_{TS}–%N_Y < 50
Type IbYAB
%N_B ≥ 50
0 ≤ %N_A ≤ 40
0 < %N_B ≤ 40
0 ≤ %N_{TS}–%N_Y < 50
N_{tot} = total nitrogen concentration (at.ppm)
IDL = instrumental detection limit
PQL = practical quantitation limit
Tier 4 (platelets > IDL and N_B > PQL_B)
Type IaAB–p
10 ≤ %N_A ≤ 90
10 ≤ %N_B < 90
platelet-bearing
example
Type IaAB–np
10 < %N_A ≤ 90
10 ≤ %N_B < 90
not platelet-bearing
Type IaAB–p_{reg}
regular platelets
Type IaAB–p_{subreg}
subregular platelets
Type IaAB–p_{irreg}
irregular platelets
continuum
Tier 4 (amber centers > IDL)
example
Type IaA'–Amb_n
%N_A = 100
amber centre > IDL
Tier 4 (CO_2 > IDL)
Type IaA–CO_2
90 ≤ %N_A < 100
0 < %N_B ≤ 10
CO_2 > IDL
example
Type IIa–CO_2
N_{tot}<IDL/PQL
boron < IDL
CO_2 > IDL
%N_C = 100 × (N_C / (N_C+N_N+N_Y+N_A+N_B))
%N_N = 100 × (N_N / (N_C+N_N+N_Y+N_A+N_B))
%N_Y = 100 × (N_Y / (N_C+N_N+N_Y+N_A+N_B))
%N_A = 100 × (N_A / (N_C+N_N+N_Y+N_A+N_B))
%N_B = 100 × (N_B / (N_C+N_N+N_Y+N_A+N_B))
%N_{TS} = 100 × (N_{TS} / (N_C+N_N+N_Y+N_A+N_B))
N_{TS} = (N_C+N_N+N_Y)
Tier 1
Type Ib – NB
N_C,N_N,N_Y and N_A > IDL and N_B < IDL
boron > IDL
Type Ib-Ia – NB
N_C,N_N,N_Y and N_A and N_B > IDL
boron > IDL
Type Ia – NB
N_A and N_B > IDL and N_C < IDL
boron > IDL
Tier 3 (N_A and N_B > PQL_{tot})
example
Type IaB–NB
90 < %N_B < 100
0 < %N_A < 10
boron > IDL
Tier 1
Type II
N_{tot}<IDL
Tier 2
Type IIb
boron > IDL
Type IIa
boron < IDL
Tier 3 (H-defect > IDL)
example
Type IIa–H_{3387}
N_sVH^0 (3107 cm^{-1}) > IDL

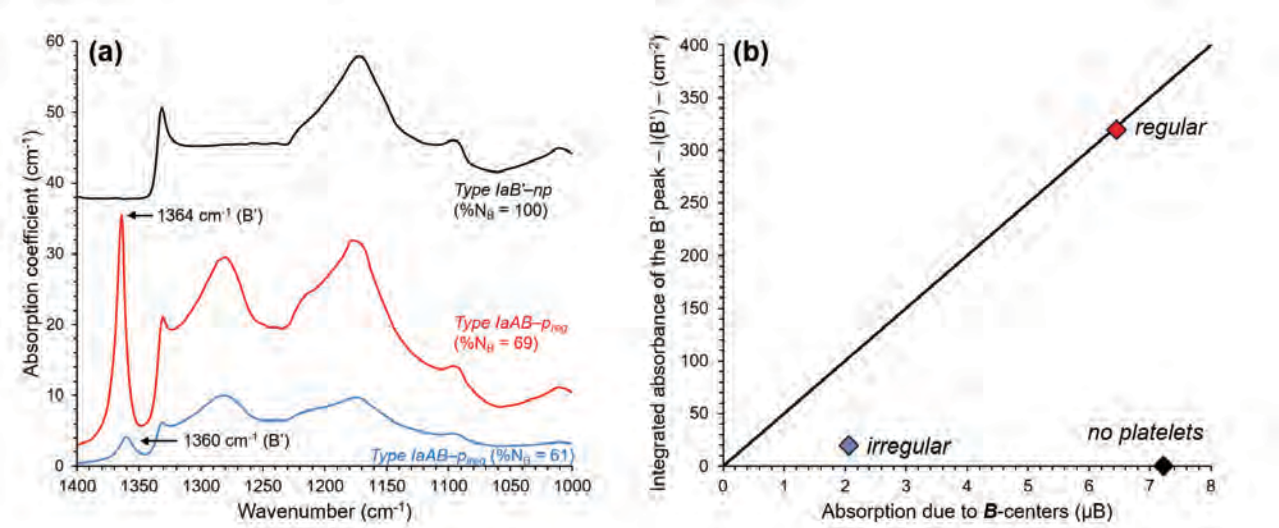

(a)
Type IaB'
%N_B = 100
N_B = 9.5 at.ppm
PQL_{Ia} = 7.9 at.ppm
S_C = 0.2676
Data
Fit
Absorption coefficient (cm^{-1})
Wavenumber (cm^{-1})

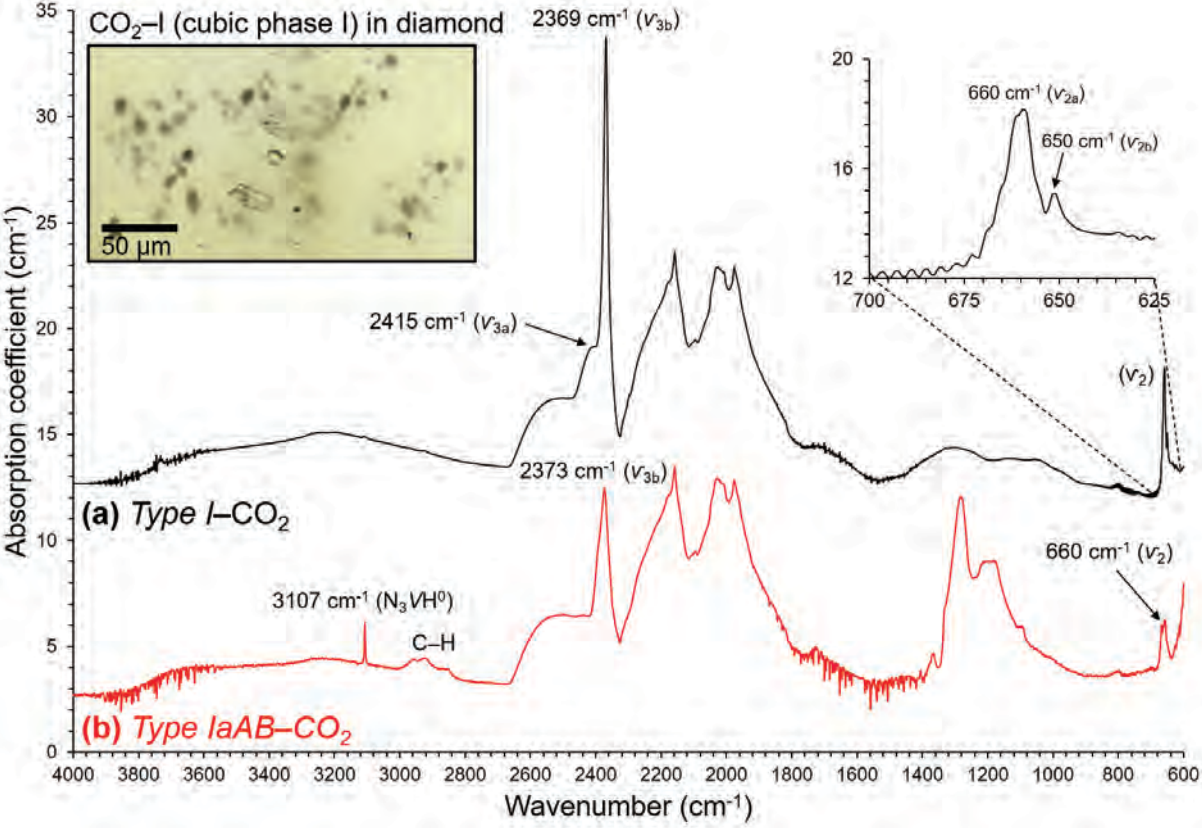

(b)
Type Ia
%N_B = ≤100
N_B = ~4.0 at.ppm
PQL_{Ia} = ≤7.9 at.ppm
S_C = 2.2215
Data
Fit
Absorption coefficient (cm^{-1})
Wavenumber (cm^{-1})

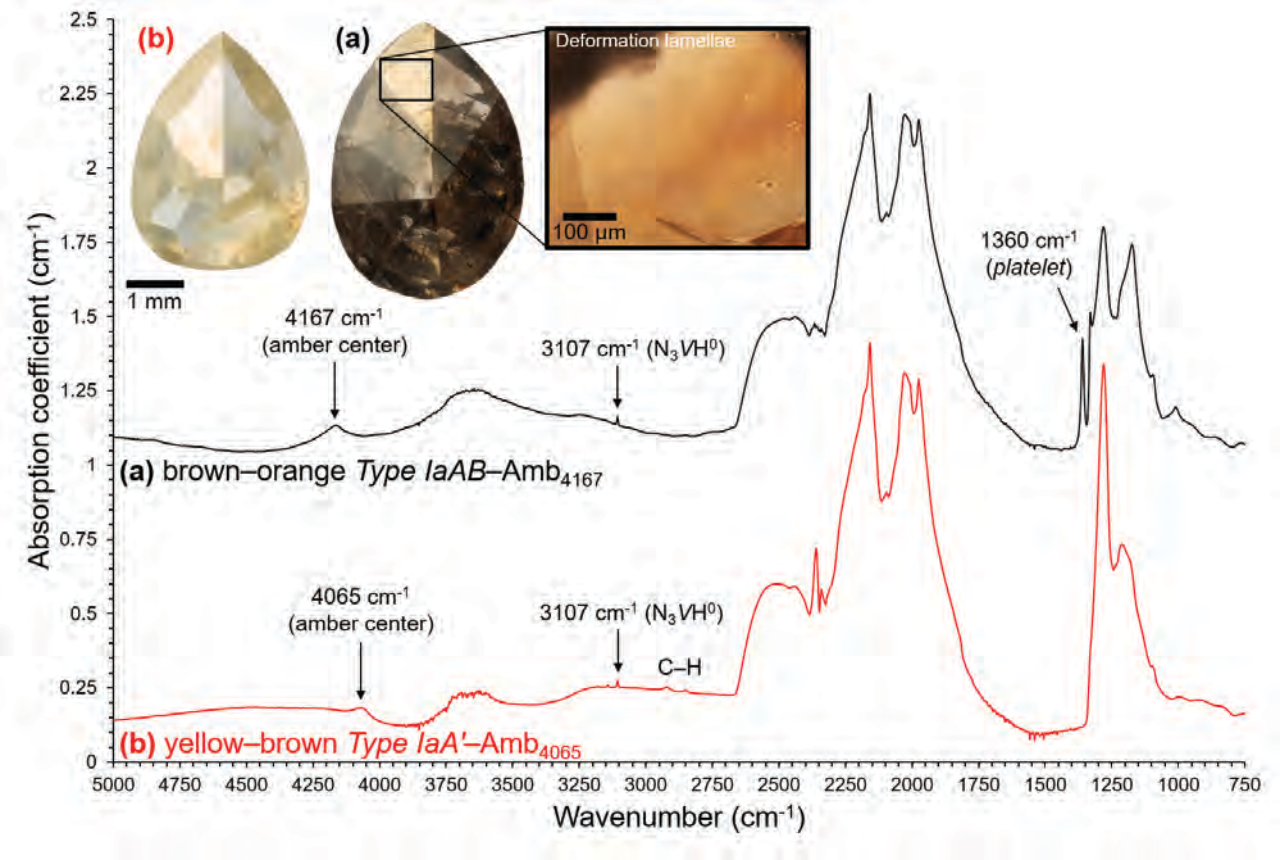

(c)
Type II
A-center
B-center
Absorption coefficient (cm^{-1})
Wavenumber (cm^{-1})

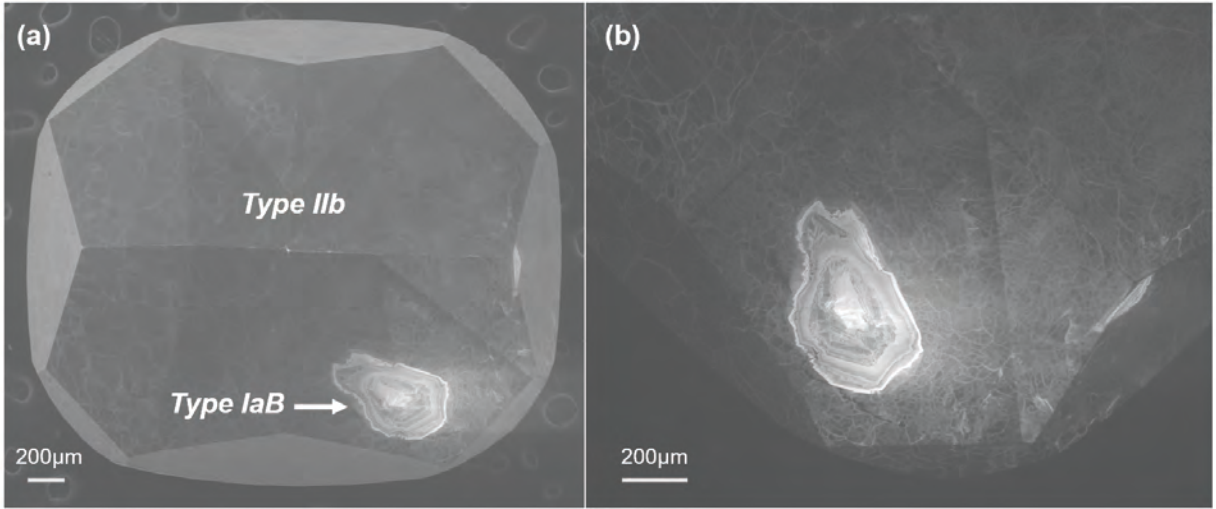

Type IaABC
N_C = 11.3
(%N_C = 17.5)
N_A = 18.6
(%N_A = 29.1)
N_B = 34.2
(%N_B = 53.4)
N_tot = 64.1
S_C = 0.046
C-center
1344 cm-1
data
fit
C comp
A comp
B comp
Absorption coefficient (cm-1)
Wavenumber (cm-1)
2
1.8
1.6
1.4
1.2
1
0.8
0.6
0.4
0.2
0
1400
1350
1300
1250
1200
1150
1100
1050
1000


(a) Type IbY–X
N_Y = 19.9
(%N_Y = 52.7)
N_X = 1.2
(%N_X = 3.1)
N_C = 13.6
(%N_C = 36.1)
(%N_TS = 91.9)
N_A = 3.0
(%N_A = 8.1)
N_tot = 37.7
S_C = 0.203
data
fit
C comp
A comp
X comp
Y comp
Absorption coefficient (cm⁻¹)
Wavenumber (cm⁻¹)
(b) Type IbCA–XY
N_Y = 26.2
(%N_Y = 14.8)
N_X = 4.8
(%N_X = 2.7)
N_C = 24.4
(%N_C = 13.8)
(%N_TS = 31.3)
N_A = 121.5
(%N_A = 68.7)
N_tot = 176.9
S_C = 0.027
data
fit
C comp
A comp
X comp
Y comp
Absorption coefficient (cm⁻¹)
Wavenumber (cm⁻¹)


(a)
Absorption coefficient (cm⁻¹)
Wavenumber (cm⁻¹)
Type IaB'–np
(%N_B = 100)
1364 cm⁻¹ (B')
Type IaAB–p_reg
(%N_B = 69)
1360 cm⁻¹ (B')
Type IaAB–p_irreg (%N_B = 61)
(b)
Integrated absorbance of the B' peak – I(B') – (cm⁻²)
Absorption due to B-centers (μB)
regular
irregular
no platelets


CO2–I (cubic phase I) in diamond
50 μm
2369 cm-1 (ν3b)
2415 cm-1 (ν3a)
660 cm-1 (ν2a)
650 cm-1 (ν2b)
(ν2)
(a) Type I–CO2
2373 cm-1 (ν3b)
3107 cm-1 (N3VH0)
C–H
660 cm-1 (ν2)
(b) Type IaAB–CO2
Absorption coefficient (cm-1)
Wavenumber (cm-1)


(b)
(a)
Deformation lamellae
100 µm
1 mm
4167 cm-1
(amber center)
3107 cm-1 (N3VH0)
1360 cm-1
(platelet)
(a) brown–orange Type IaAB–Amb4167
4065 cm-1
(amber center)
3107 cm-1 (N3VH0)
C–H
(b) yellow–brown Type IaA'–Amb4065
Absorption coefficient (cm-1)
Wavenumber (cm-1)
2.5
2.25
2
1.75
1.5
1.25
1
0.75
0.5
0.25
0
5000 4750 4500 4250 4000 3750 3500 3250 3000 2750 2500 2250 2000 1750 1500 1250 1000 750


(a)
Type IIb
Type IaB
200μm
(b)
200μm